

Polyphenolic and polydendritic molecules as modulators of glioblastoma multiforme and its microenvironment



Natali Joma

Department of Pharmacology & Therapeutics
Faculty of Medicine and Health Sciences
McGill University, Montréal, Quebec, Canada

December 2024

*A thesis submitted to McGill University
in a partial fulfilment of the requirements of the
degree of Master of Science (MSc).*

© Natali Joma, 2024

TABLE OF CONTENTS

| | |
|---|-----------|
| ABSTRACT..... | 3 |
| RÉSUMÉ..... | 5 |
| ACKNOWLEDGEMENTS..... | 7 |
| CONTRIBUTION OF AUTHORS..... | 8 |
| LIST OF FIGURES AND TABLES..... | 9 |
| LIST OF ABBREVIATIONS..... | 10 |
| CHAPTER 1 – LITERATURE REVIEW..... | 12 |
| 1.1 – Glioblastoma Multiforme Overview..... | 12 |
| 1.2 – Current Treatment Options..... | 12 |
| 1.2.1 – Recurrent GBM. | 15 |
| 1.2.2 – Emerging Therapies for GBM. | 15 |
| 1.3 – Tumor Microenvironment (TME)..... | 16 |
| 1.3.1 –Microglia and Tumor-Associated Macrophages (TAMs)..... | 17 |
| 1.3.2 – Tumor Acidosis..... | 19 |
| 1.4 – Redox Imbalance in GBM..... | 20 |
| 1.4.1 – High Mobility Group Box 1 (HMGB1)..... | 20 |
| 1.4.1.1 – HMGB1 in Cancer..... | 21 |
| 1.4.2 – Transcription Factor EB (TFEB)..... | 22 |
| 1.5 – Modulation of Redox Imbalance in TME..... | 25 |
| 1.5.1 – Fisetin..... | 25 |
| 1.5.2 – Dendrimers..... | 27 |
| 1.5.2.1 – Dendrimers as anti-inflammatory agents..... | 27 |
| 1.6 – Objectives..... | 29 |
| CHAPTER 2 – MATERIALS AND METHODS..... | 30 |
| CHAPTER 3 – EXPERIMENTAL RESULTS..... | 40 |
| CHAPTER 4 – DISCUSSION..... | 69 |
| CHAPTER 5 – CONCLUSION..... | 90 |
| CHAPTER 6 – REFERENCES (ALPHABETICAL) | 92 |

ABSTRACT

Glioblastoma multiforme (GBM) is a highly aggressive brain cancer, characterized by rapid progression, robust invasiveness, and resistance to conventional therapies. These attributes contribute to a dismal median survival rate of approximately 14-15 months. GBM reprograms its microenvironment to facilitate rapid proliferation and treatment resistance through elevated reactive oxygen species (ROS) production and dysregulation of redox-responsive transcription factors, including high mobility group box 1 (HMGB1) and transcription factor EB (TFEB). Post-translationally modified HMGB1 (e.g., AcHMGB1) can activate immune cells, such as microglia, in the tumor microenvironment (TME). Microglia accumulate near the hypoxic core of the tumor and release high levels of pro-inflammatory cytokines, contributing to neuroinflammation and redox imbalance.

This study explores the therapeutic potential of polyphenolic and polydendritic molecules with antioxidant and anti-inflammatory properties. Notably, flavonoids such as fisetin and quercetin can protect non-cancerous cells while eliminating cancerous cells in both 2D cultures and 3D tumoroids. Utilizing a series of *in vitro* assays, including MTT and LDH release assays, we show the dose-dependent cytotoxic effects of these compounds on human U251N GBM cells and human HMC3 microglia. Fisetin and quercetin significantly reduce GBM cell viability and metabolic activity with increasing concentrations, while microglial cells exhibit minimal cytotoxic responses. This suggests a differential cytotoxicity that selectively targets cancerous cells, sparing non-cancerous cells within the TME. Next, we evaluated the synergistic potential of fisetin with temozolomide (TMZ), a standard chemotherapeutic for GBM. The combination therapy significantly enhanced the reduction in GBM cell viability compared to individual treatments. Moreover, our study extended to the effects of fisetin on oxidative stress parameters and redox-sensitive transcription factors. Notably, fisetin treatment significantly mitigated spike protein-induced oxidative stress in both GBM cells and microglia, normalizing intracellular ROS levels, and selectively reducing the abundance of AcHMGB1 in microglia. Moreover, fisetin enhanced the nuclear translocation of TFEB in microglia, promoting lysosomal biogenesis and function—an essential cellular mechanism for maintaining cellular cleanup and homeostasis.

Exploring beyond natural compounds, we assessed the effects of synthetic dendritic polyglycerols (dPGs). These dendritic nanostructures not only possess inherent anti-inflammatory properties but also serve as efficient nanocarriers for drug delivery. Specifically, we tested dendritic polyglycerol amine (dPGA), structurally similar but oppositely charged from previously studied sulfated analogs (dPGS), on microglia and GBM cells. We hypothesized that dPGA is more cytotoxic to GBM cells than to microglia. We assessed MTT, LDH, and cell loss in both cell types, and analyzed lysosomal abundance and lysosomal activity (cathepsin B), due to its crucial role in cell survival. Unexpectedly, dPGA significantly increased lysosomal activity, attributed to its alkaline amino groups, contributing to its cytotoxic effects in GBM cells. The high lysosomal activity correlates with low abundance of TFEB and low lipid droplet abundance in GBM.

The approach of employing both natural and synthetic compounds underscores a strategic pivot in GBM treatment paradigms, targeting both the cancer cells and the supportive TME. The findings of this study illuminate the complex interplay between cell type-specific responses to therapeutic agents within the TME and advance the understanding of how modulation of biochemical pathways can potentially enhance GBM treatment efficacy.

RÉSUMÉ

Le glioblastome multiforme (GBM) est un cancer du cerveau très agressif, caractérisé par une progression rapide et une résistance aux traitements conventionnels qui contribuent à un taux de survie médiane faible d'environ 15 mois. Le GBM reprogramme son microenvironnement tumoral pour faciliter la prolifération rapide et la résistance au traitement par la production d'espèces d'oxygène réactives (ERO) élevées et la dérégulation des facteurs de transcription réactifs aux réactions redox, y compris le « high-mobility group box protein 1 » (HMGB1) et le facteur de transcription EB (TFEB). Les HMGB1 modifiées post-traductionnellement (par exemple, le HMGB acétylé; AcHMGB1) peuvent activer des cellules immunitaires, telles que la microglie, dans le microenvironnement tumoral (TME). Les microglies s'accumulent près du noyau hypoxique de la tumeur et libèrent des niveaux élevés de cytokines pro-inflammatoires, contribuant à la neuroinflammation et au déséquilibre redox.

Cette étude explore le potentiel thérapeutique des molécules polyphénoliques et polydendritiques aux propriétés antioxydantes et anti-inflammatoires. Les flavonoïdes tels que la fisétine et la quercétine peuvent notamment protéger les cellules non-cancéreuses tout en éliminant les cellules cancéreuses dans les cultures 2D et les tumeurs 3D. En utilisant une série d'essais *in vitro*, y compris des essais de libération de MTT et de LDH, nous montrons les effets cytotoxiques dose-dépendants de ces composés sur les cellules humaines U251N glioblastoma et microglia HMC3. La fisétine et la quercétine réduisent significativement la viabilité des cellules GBM et l'activité métabolique avec des concentrations croissantes, tandis que les cellules microgliales présentent des réponses cytotoxiques minimales. Cela suggère une cytotoxicité différentielle qui cible sélectivement les cellules cancéreuses, en épargnant les cellules non-cancéreuses dans la TME. Ensuite, nous avons évalué le potentiel synergique de la fisétine avec le témozolomide (TMZ), un chimiothérapeute standard pour le GBM. La thérapie combinée a significativement amélioré la réduction de la viabilité cellulaire du GBM par rapport aux traitements individuels. De plus, notre étude s'est étendue aux effets de la fisétine sur les paramètres du stress oxydatif et les facteurs de transcription redox-sensibles. Le traitement par la fisétine a considérablement atténué le stress oxydatif induit par les péplomère dans les cellules GBM et les microglies, normalisant les niveaux intracellulaires de ERO et réduisant sélectivement l'abondance d'AcHMGB1 dans les microglies, un indicateur de réduction de la réponse inflammatoire. De plus, la fisétine a amélioré la translocation nucléaire du TFEB dans les microglies, favorisant la biogenèse et la fonction lysosomales — un mécanisme cellulaire essentiel pour maintenir le nettoyage cellulaire et l'homéostasie.

En explorant au-delà des composés naturels, nous avons évalué les effets des polyglycérols dendritiques synthétiques (dPGs). Ces nanostructures dendritiques possèdent non seulement des propriétés anti-inflammatoires, mais servent également comme nano-transporteurs efficaces pour la livraison du médicament. Plus précisément, nous avons testé des amines de polyglycérol dendritique (dPGA), structurellement similaires mais chargées à l'opposé d'analogues sulfatés (dPGS) précédemment étudiés, sur des cellules microgliales et GBM. Nous avons émis l'hypothèse que le dPGA est plus

cytotoxique pour les cellules GBM que pour la microglie. Nous avons évalué le MTT, le LDH et la perte cellulaire dans les deux types de cellules et avons analysé l'abondance et l'activité lysosomale (cathepsine B), en raison de son rôle crucial dans la survie cellulaire. De façon inattendue, dPGA a significativement augmenté l'activité lysosomale, attribuée à ses groupes d'acides aminés alcalins, contribuant ainsi à ses effets cytotoxiques sur les cellules GBM. La forte activité lysosomale est corrélée à une faible abondance de TFEB et à une faible abondance de gouttelettes lipidiques.

L'approche consistant à utiliser des composés naturels et synthétiques souligne un pivot stratégique dans les paradigmes de traitement du GBM, ciblant à la fois les cellules cancéreuses et le TME de soutien. Les résultats de cette étude mettent en lumière l'interaction complexe entre les réponses spécifiques au type cellulaire aux agents thérapeutiques dans le TME et permettent de mieux comprendre comment la modulation des voies biochimiques peut potentiellement améliorer l'efficacité du traitement par GBM.

ACKNOWLEDGEMENTS

I would like to extend my deepest gratitude to my supervisor, Dr. Dusica Maysinger, for her invaluable guidance and unwavering support throughout my research journey. Her expertise and keen insights have not only shaped this project but also greatly enhanced my understanding in the field. I am profoundly grateful for the opportunities to grow as a researcher under her mentorship. Her unwavering passion for science and belief in my potential have shaped me as both a person and a scientist. I will fondly remember our conversations about our shared love for dark chocolate-covered ginger, exploring new cafes, and our walks near Mount Royal.

Thank you to the Nanofamily: Jocelyn Fang, Mahdi Jamoussi, Sabrina Kerbalaeva, Audrey Yu, Anaïs Berlinger-Lavoie, Patrick-Brian Bielawski, Marten Kagelmacher and especially Dr. Issan Zhang. I am deeply grateful for Dr. Zhang's unwavering support, encouragement, and assistance whenever needed.

My deepest appreciation goes to my thesis advisor, Dr. Lisa Münter, who made time for our meetings and fostered a trusting environment where I could confide. I am also grateful to my committee members, Dr. Anne McKinney and Dr. Ashok Kakkar, for their invaluable expertise and constructive feedback after my committee meetings. Thank you to the administration team of the Pharmacology & Therapeutics department. Their prompt assistance and willingness to help at every turn have been instrumental in my academic journey.

Thank you to Dr. Ashok Kakkar and Laura McKay from the Department of Chemistry at McGill University for providing the fisetin-loaded nanoparticles and pH-sensitive probes. I would also like to thank Dr. Ehsan Mohammadifar from the Institute of Chemistry and Biochemistry (Freie Universität Berlin) for providing the dPGS and dPGA.

Thank you to the Natural Sciences and Engineering Research Council of Canada (NSERC; RGPIN2020-07011) and the Fonds de Recherche du Québec – Santé (EuroNanoMed III - PLATMED) (FRQ-S #294233) for their financial support throughout this project. Additionally, I am thankful for the scholarships provided by the NSERC Canada Graduate Scholarship-Master's program and the CITF-IRTG.

Finally, my heartfelt thanks go to my parents, siblings, and friends for their constant love and support.

CONTRIBUTION OF AUTHORS

This thesis adheres to the traditional format specified in the McGill University Graduate and Postdoctoral Studies Office's Guidelines for Thesis Preparation. All experiments were conceptualized and planned by Dr. Dusica Maysinger, Dr. Issan Zhang, and Natali Joma. The experiments in Section 3 (Flavonoids) were conducted by both Dr. Issan Zhang and Natali Joma. The work involving dPGS and dPGA was carried out by Anaïs Berlinger-Lavoie, Dr. Issan Zhang, and Natali Joma. Molecular modeling was performed by Dr. Germanna L. Righetto. The pH-sensitive probes and fisetin-loaded nanoparticles were prepared and characterized by Laura McKay from the Department of Chemistry at McGill University.

Unless otherwise specified, all work presented in this thesis was completed by Natali Joma. The thesis was written entirely by Natali Joma and edited by Dr. Dusica Maysinger.

LIST OF FIGURES AND TABLES

CHAPTER 1 – LITERATURE REVIEW

Figure 1.1: Conventional and Non-Conventional Glioblastoma Treatments

Figure 1.2: Tumor Microenvironment

Figure 1.3: TFEB Signaling Cascade

Figure 1.4: Modulation of Redox-Responsive Transcription Factors

Figure 1.5: Structures of dPGS and dPGA

CHAPTER 2 – MATERIALS AND METHODS

Figure 2.1: Overview of Immunocytochemistry Protocol

Figure 2.2: Overview of GBM Tumoroid Preparation

Figure 2.3: Overview of Proximity Ligation Assay

Table 2.1: List of Materials

CHAPTER 3 – EXPERIMENTAL RESULTS

Figure 3.1: Dose-dependent lactate dehydrogenase (LDH) release and mitochondrial metabolic activity (MTT) in response to fisetin and quercetin

Figure 3.2: Dose-dependent effect in response to fisetin and TMZ

Figure 3.3: Oxidative stress in human microglia and GBM cells treated with fisetin +/- spike

Figure 3.4: AcHMGB1 in human GBM cells and microglia treated with fisetin +/- spike

Figure 3.5: TFEB in human GBM cells and microglia treated with fisetin +/- spike

Figure 3.6: Lysosome abundance and activity in human glioblastoma and microglia

Figure 3.7: Lipid droplets in human microglia and GBM cells

Figure 3.8: Cell viability of microglia in response to treatment with increasing concentrations of dPGS or dPGA

Figure 3.9: Cell viability of GBM cells in response to treatment with increasing concentrations of dPGS or dPGA

Figure 3.10: LAMP-2 abundance and cathepsin B activity in GBM cells after 24h

Figure 3.11: dPGA decreases LD abundance in GBM cells after 24h

Figure 3.12: Detection of encapsulated SNAFL in GBM cells treated with dPGA or dPGS (100 nM)

Figure 3.13: LysoTracker and cathepsin B activity in microglia treated with dPGS or dPGA

Figure 3.14: dPGS, but not dPGA, increases TFEB abundance in human microglia

CHAPTER 4 – DISCUSSION

Figure 4.1: A simplified presentation of the mechanisms of action of fisetin

Figure 4.2: Interactions between HMGB1/HSP72 in microglia and glioblastoma treated with fisetin (25 μ M) or quercetin (25 μ M) for 24 h in serum-deprived media

Figure 4.3: Docking analyses of fisetin binding to target proteins

Figure 4.4: Nanocarriers developed for the delivery of flavonoids

Figure 4.5: Fisetin-loaded nanoparticles

Figure 4.6: Overview of dPGS and dPGA treatments on cell viability, lysosomal activity, and lipid droplet abundance in GBM cells and microglia

LIST OF ABBREVIATIONS

| | |
|---------------------------------|--|
| AcHMGB1 | Acetylated High-Mobility Group Box 1 |
| AP-1 | Activator Protein 1 |
| ATG5 | Autophagy Related 5 |
| BCL-2 | B-cell CLL/lymphoma 2 |
| BBB | Blood-Brain Barrier |
| CD39 | Cluster of Differentiation 39 |
| CDK4/6 | Cyclin-Dependent Kinase 4/6 |
| CNS | Central Nervous System |
| DAMPs | Damage-Associated Molecular Patterns |
| DPG | Dendritic polyglycerol |
| DPGA | Dendritic polyglycerol amines |
| DPGS | Dendritic polyglycerol sulfates |
| DCVAX®-L | Dendritic Cell Vaccine |
| DRD2 | Dopamine Receptor D2 |
| EGFR | Epidermal Growth Factor Receptor |
| EGF | Epidermal Growth Factor |
| FDA | Food and Drug Administration |
| GAMs | Glioma-Associated Macrophages |
| GBM | Glioblastoma Multiforme |
| GSCs | Glioma Stem Cells |
| GSH | Glutathione |
| GSSG | Glutathione Disulfide |
| HIF-1α | Hypoxia-Inducible Factor 1- α |
| HMGB1 | High-Mobility Group Box 1 |
| HDAC | Histone Deacetylase |
| HER2 | Human Epidermal Growth Factor Receptor 2 |
| HSP72 | Heat Shock Protein 72 |
| IGF-1 | Insulin-like Growth Factor 1 |
| IL-4, IL-6, IL-10 | Interleukin 4, 6, 10 |
| KEAP1 | Kelch-like ECH-associated protein 1 |
| LAMP2 | Lysosome-Associated Membrane Protein 2 |
| LPS | Lipopolysaccharide |
| MGMT | O-6-methylguanine-DNA methyltransferase |
| MDSCs | Myeloid-Derived Suppressor Cells |
| MMPs | Matrix Metalloproteinases |
| NF-κB | Nuclear Factor kappa-light-chain-enhancer of activated B cells |
| NRF2 | Nuclear Factor Erythroid 2-Related Factor 2 |
| NTRK | Neurotrophic Tyrosine Receptor Kinase |
| PD-1 | Programmed Cell Death Protein 1 |
| PDGF | Platelet-Derived Growth Factor |
| PD-L1 | Programmed Death-Ligand 1 |
| PHD2 | Prolyl Hydroxylase Domain-containing Protein 2 |
| RAGE | Receptor for Advanced Glycation Endproducts |
| ROS | Reactive Oxygen Species |

| | |
|---------------------------------|--|
| TAMs | Tumor-Associated Macrophages |
| TFEB | Transcription Factor EB |
| TGF-β | Transforming Growth Factor Beta |
| TMZ | Temozolomide |
| TME | Tumor Microenvironment |
| TNF-α | Tumor Necrosis Factor Alpha |
| TLR | Toll-Like Receptor |
| TRK | Tropomyosin receptor kinase |
| Tregs | Regulatory T cells |
| VEGF-α | Vascular Endothelial Growth Factor Alpha |
| VEGF | Vascular Endothelial Growth Factor |

Chapter 1 – LITERATURE REVIEW

1.1 – Glioblastoma Multiforme Overview

Glioblastoma multiforme (GBM) is the most prevalent and aggressive primary brain tumor, classified as a grade IV glioma. It has one of the lowest five-year survival rates among all cancers, with a median survival of only 15 months (Tamimi & Juweid, 2017). GBM incidence increases with age and is greater in men than women. Moreover, GBM is more prevalent in Caucasians than other ethnicities (Davis, 2016). Although the exact pathogenesis of GBM remains largely unknown, lower-grade gliomas, such as astrocytomas, can recur, mutate, or transform into GBM (Yalamarty et al., 2023).

GBM tumors are aggressive, growing rapidly and typically occurring in the temporal and frontal lobes. This growth exerts pressure on the brain, causing symptoms such as progressive focal neurological deficits, vomiting, drowsiness, headaches, nausea and, in severe cases, seizures and hemiparesis (Kanderi & Gupta, 2024). Tumor spreading beyond the CNS is rare. The most common sites of extra-cranial metastasis are the lungs and pleura (Kurdi et al., 2023).

The primary causes of glioblastomas are not well understood. These tumors appear sporadically without any genetic predisposition, but in most cases, involve gene mutations, insertions, and deletions that affect cellular growth signaling pathways (Bleeker et al., 2012). GBM lethality arises from uncontrolled cellular proliferation, angiogenesis, genetic instability, intratumoral heterogeneity, and resistance to apoptosis (Balça-Silva et al., 2019). Although various treatment strategies are available, GBM remains highly aggressive, with most recurrences (75-90%) occurring within 2-3 cm of the initial tumor site (Davis, 2016).

1.2 – Current Treatment Options

The treatment of brain tumors encounters unique challenges, primarily due to the presence of the blood-brain barrier (BBB), a highly selective semipermeable membrane that separates the bloodstream from the brain (Mo et al., 2021). The BBB is composed of capillary endothelial cells, astrocytes surrounding the capillaries, and pericytes

embedded in the capillary basal lamina. Factors including molecular weight, lipophilicity, and charge determine a molecule's ability to cross the BBB (Thomsen et al., 2017). The BBB prevents nearly all large molecules (greater than 400 Da) and about 98% of small molecules from entering the central nervous system (CNS) (Pardridge, 2005).

Conventional treatments for GBM include surgical resection, radiotherapy, and chemotherapy, with surgery being the primary intervention for initial tumors (Fernandes et al., 2017). Surgery aims to remove most of the tumor while preserving surrounding healthy tissue, minimizing recurrence, and maintaining neurological function. However, due to the invasive nature of GBM, complete tumor removal is rarely possible, requiring additional treatments such as radiotherapy and chemotherapy (Hatoum et al., 2019).

Currently approved chemotherapeutic agents for GBM include temozolomide (TMZ) and bevacizumab (Avastin®) (Hatoum et al., 2019). TMZ, a DNA alkylating agent, is administered at 150–200 mg/m²/day for 5 days in a 28-day cycle (Stupp et al., 2009). Once administered, it is transformed into its active form, monomethyl triazene 5-(3-methyl-1-triazeno) imidazole-4-carboxamide (Tanaka et al., 2023). The primary mechanism of TMZ involves methylation at the O6 position of guanine, causing mutations that bypass the mismatch repair system (MMR) (C.-H. Fan et al., 2013). This process activates a series of signals that trigger cell cycle checkpoints, ultimately causing the cell to arrest in the G2-M phase and undergo apoptosis due to damage in both single and double strands of DNA. A subset of patients respond better to TMZ due to the presence of methylated promoters in the O-6-methylguanine-DNA methyltransferase (MGMT) gene, which is associated with higher survival rates. MGMT repairs DNA damage caused by TMZ, and its methylation status is a crucial biomarker for GBM prognosis (Kitange et al., 2009; I. Zhang et al., 2018).

TMZ monotherapy is effective in only 5.4% of patients. However, TMZ combined with radiotherapy showed an increase in survival rate from 1.9% (radiotherapy alone) to 9.8% (McDuff et al., 2019). Another approved treatment for GBM is bevacizumab. Bevacizumab is an anti-angiogenic humanized monoclonal antibody that targets vascular endothelial growth factor alpha (VEGF- α) (Hatoum et al., 2019). Despite these

treatments, tumor progression and recurrence are common due to the development of TMZ resistance (Yalamarty et al., 2023).

Although TMZ is a standard treatment, it has significant toxicity and does not cure the disease. Consequently, targeted therapies are being explored to reduce toxicity and more effectively inhibit tumor growth. Tumor complexity and problematic treatment outcome are being recognized and tackled with new approaches. **Figure 1.1** highlights conventional and non-conventional treatments of GBM, including surgery, radiotherapy, cytotoxic chemotherapy, gene therapy, immunotherapy, and nanotherapy.

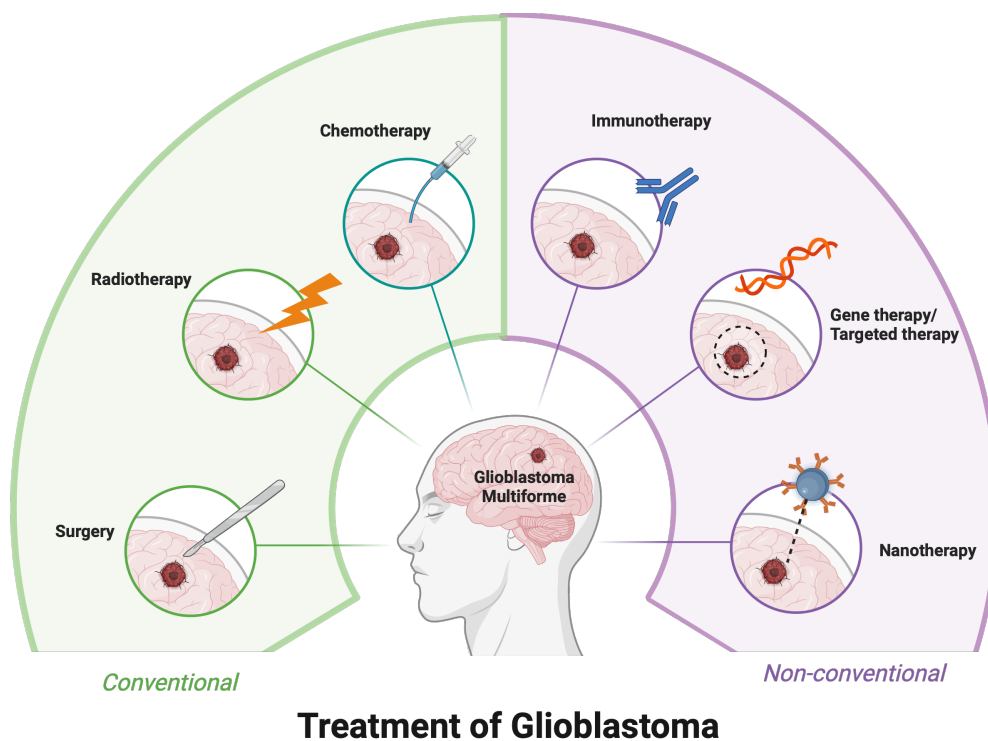


Figure 1.1 – Conventional and Non-Conventional Glioblastoma Treatments. Overview of the diverse treatment strategies for glioblastoma, emphasizing the combination of conventional methods—such as surgery, radiation, and chemotherapy—with innovative non-conventional approaches, including nanotherapy, targeted therapy, immunotherapy, and gene therapy. The integration of these therapies aims to improve therapeutic outcomes by addressing the complexity and resilience of glioblastoma, highlighting the need for multi-modal treatment strategies in combating this aggressive brain tumor. Created with ©BioRender ([biorender.com](https://www.biorender.com)).

1.2.1 – Recurrent GBM

Once GBM recurs, treatment options become limited and depend on factors such as patient age, disease stage, and overall health. In such cases, patients may be enrolled in clinical trials for new therapies. Treatment options include a second surgical resection to remove most of the tumor, reirradiation to target any remaining cancer cells, and re-treatment with chemotherapeutic agents such as nitrosoureas and TMZ. Bevacizumab is also commonly used, and tyrosine kinase inhibitors, which target specific enzymes involved in cancer cell growth pathways, are considered part of the treatment strategy (Tosoni et al., 2016).

Despite these available treatments, the prognosis for patients with recurrent GBM remains poor, with a median overall survival of just 6.2 months following recurrence (Gorlia et al., 2013). Researchers have investigated several combination therapies to improve outcomes. For instance, a Phase II study showed that the combination of bevacizumab and irinotecan provided the longest median progression-free survival at 5.6 months (Friedman et al., 2009). Another study reported that the longest overall survival of 12 months was achieved with a combination of lomustine and bevacizumab (Taal et al., 2014).

1.2.2 – Emerging Therapies for GBM

Ongoing research is crucial for finding more successful treatments for GBM, as current options offer limited hope for long-term survival. Current clinical trials are investigating small molecules and other innovative approaches to improve GBM prognosis (Ghosh et al., 2024; Shikalov et al., 2024; Valerius et al., 2024). These trials aim to identify treatments that can effectively target tumor cells while minimizing toxicity and adverse effects.

Clinical trials have shown improvements in overall long-term survival for patients with primary or recurrent GBM (Mittal et al., 2018; Stupp et al., 2015). Emerging therapies include targeted therapies that focus on specific biomarkers within tumors, and immunotherapies such as CAR-T cells and immune checkpoint inhibitors. Personalized

medicine and genomics tailor treatments to individual patients. Moreover, novel drug delivery methods, such as convection-enhanced delivery, aim to improve drug pharmacokinetics (Rodríguez-Camacho et al., 2022). These diverse approaches indicate a shift toward more precise, personalized, and potentially less toxic treatments, although further research and clinical trials are required to establish their efficacy and safety. Recent reviews discuss current and emerging approaches to treating GBM (Nelson & Dietrich, 2023; Rodríguez-Camacho et al., 2022; Smolarska et al., 2023).

1.3 – Tumor Microenvironment (TME)

A tumor is not merely a collection of cancer cells but a heterogeneous assembly of infiltrating resident host cells, secreted factors, and extracellular matrix components (Anderson & Simon, 2020). Tumor cells undergo significant molecular, cellular, and physical alterations within their host tissues to facilitate tumor growth and progression. The TME is a complex and continuously evolving entity. Due to its diverse components and dynamic nature, the TME is crucial in supporting cancer cell survival and influencing their response to therapy.

Recent studies have highlighted the critical roles of different cell types within the GBM microenvironment, including tumor-associated macrophages (TAMs), microglia, astrocytes, endothelial cells, and immune cells (**Figure 1.2**) (Anderson & Simon, 2020; Geribaldi-Doldán et al., 2021; Klemm et al., 2020; Le et al., 2003; Matias et al., 2018; G. Wang et al., 2022). Understanding the interactions between these cell types and GBM cells is essential for developing effective treatments. Communication between tumor and surrounding cells is facilitated by soluble factors such as cytokines, chemokines, matrix remodeling enzymes, and growth factors. Additionally, tumor cells use exosomes, gap junctions, cell-free DNA, and horizontal DNA transfer to interact with each other and/or non-cancerous cells. Recognizing the complex communication network between tumors and normal cells for GBM development and progression has led to a renewed focus on therapeutic targeting of GBM (P. Sharma et al., 2023).

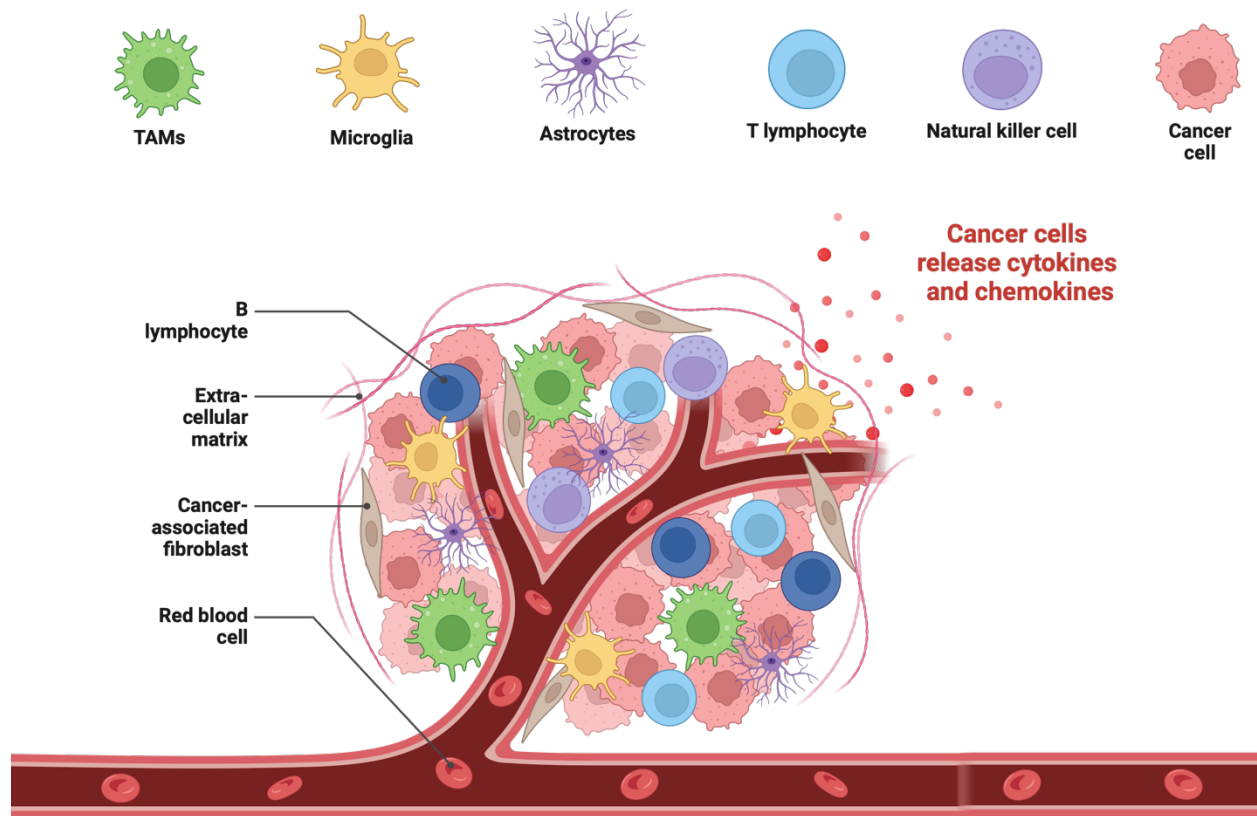


Figure 1.2 – Tumor Microenvironment. The TME is a complex network of cellular and non-cellular components. These include endothelial cells, neurons, astrocytes, oligodendrocytes, and resident immune cells such as microglia. It also contains tumor-infiltrating circulating immune cells, including tumor-associated macrophages (TAMs) and tumor-infiltrating lymphocytes (TILs). Non-cellular components include apocrine and paracrine signaling molecules, exosomes, extracellular matrix (ECM) components, and ECM-remodeling enzymes. The diversity and dynamic interplay within the TME are essential for cancer cell survival and greatly influence their response to therapeutic interventions. Created with ©BioRender ([biorender.com](https://www.biorender.com)).

1.3.1 – Microglia and Tumor-Associated Macrophages (TAMs)

The cells central to this thesis are microglia, as they constitute 30-40% of the tumor mass (G. Wang et al., 2022). Microglia and tumor-associated macrophages (TAMs) are the most abundant immune cells in the microenvironment of most primary gliomas (Deng et al., 2019). These myeloid cell lineages exhibit remarkable diversity in their origin, phenotype, and function. Microglia and some macrophages originate from embryonic progenitors in the yolk sac, while others arise from bone marrow-derived macrophages.

The glioma microenvironment significantly impacts microglia and TAMs, which are highly dynamic cell populations (Klemm et al., 2020). Macrophages can undergo either M1 or M2 polarization in response to various cytokines and chemokines. M1 macrophages are immune-supportive and inhibit cancer functions, whereas M2 macrophages generally support tumor growth. Although conventional phenotyping may not fully capture the functional complexity of TAMs, these cells are generally immunosuppressive in the glioma microenvironment (Lin et al., 2024). Despite the underlying mechanisms not being fully understood, TAMs produce anti-inflammatory cytokines (IL-4, IL-10, and TGF- β) and tumor-promoting factors (IGF-1, EGF, and PDGF), promote angiogenesis (via VEGF and IL-8), disrupt metabolism, and activate immune checkpoints by expressing PD-L1 and CD39 (Lin et al., 2024).

TAMs play an important role in cellular homeostasis via phagocytosis and antigen presentation. Developing therapies that harness these cells is promising. Glioma cells produce cytokines such as CSF1 and IL34, which stimulate TAMs via colony-stimulating factor 1 receptor (CSF1R). One effective approach is to target CSF1R. Several CSF1R inhibitors, notably effective in reprogramming TAMs toward an anti-tumor phenotype, have shown reduced M2 polarization, hindered tumor growth, and increased survival in murine GBM models across various preclinical models (Akkari et al., 2020; Pyonteck et al., 2013). However, a Phase II study of a CSF1R inhibitor (PLX3397), did not meet therapeutic efficacy expectations despite good tolerance and target engagement in recurrent GBM patients (Butowski et al., 2016). Additional studies have explored other CSF1R inhibitors, such as BLZ945, pexidartinib, and various blocking antibodies, both as monotherapies and in combination with radiotherapy or immune checkpoint inhibitors (Falchook et al., 2021; Przystal et al., 2021; Rao et al., 2022; Weiss et al., 2021). Notably, in brain cancer models, tumors often recur despite initial benefits from CSF1R inhibition, possibly due to increased levels of macrophage-derived insulin-like growth factor 1 (IGF-1) and other mechanisms (Quail & Joyce, 2017; Yan et al., 2017).

Gliomas are also associated with reactive astrocytes (Le et al., 2003), which enhance glioma invasiveness through releasing neurotrophic factors and upregulating

matrix metalloproteases production (Charles et al., 2012). Furthermore, astrocytes may connect with glioma cells via gap junctions facilitating the transfer of molecules across a broad network, promoting cell health and homeostasis (Y. Yang et al., 2022).

1.3.2 – Tumor Acidosis

GBM is also influenced by its chemical environment. More specifically, the emergence of tumor acidosis, which progressively affects intrinsic cellular processes (P. Sharma et al., 2023). This acidic TME can lead to an immunosuppressive environment and confer treatment resistance (Corbet & Feron, 2017). Key factors leading to acidosis include metabolic shifts in GBM cells toward aerobic glycolysis, known as the Warburg effect. This metabolic adaptation allows cancer cells to consume large amounts of metabolic intermediates, reducing extracellular glucose in the TME, and increasing lactic acid and hydrogen ion (H^+) production and secretion. These changes also affect the tumor's energy metabolism. Cancer cells have enhanced secretion mechanisms, including upregulated monocarboxylate transporter-4 (MCT-4) and Na^+ - H^+ transporters. This adaptation allows them to avoid programmed cell death associated with reduced intracellular pH by increasing their capacity to export metabolites into the extracellular space (Abdel-Hakeem et al., 2021; Estrella et al., 2013; Pavlova & Thompson, 2016; Riemann et al., 2016; Webb et al., 2021), effectively lowering the TME's pH (Vaupel & Mayer, 2014; Wiedmann et al., 2012).

Malignant cells trigger protective mechanisms to enhance their survival under acidic conditions. For instance, they upregulate proteins like LAMP2, which safeguards lysosomal and plasma membrane integrity against acid proteolysis. Additionally, they boost the expression of autophagy-related proteins such as ATG5 and anti-apoptotic proteins like BCL-2 when chronically exposed to low pH conditions. These adaptive defense mechanisms associated with tumor-related acidosis further enhance the cells' ability to withstand extreme environmental stress (Hulikova & Swietach, 2014; Vaupel & Mayer, 2014). Targeting acidosis with inhibitors that regulate pH balance in the TME, in conjunction with standard-of-care therapy (Duraj et al., 2021), is becoming a promising

therapeutic strategy against GBMs. This approach is currently being evaluated in ongoing clinical trials (NCT03011671).

1.4 – Redox Imbalance in GBM

One of the key factors contributing to the malignancy and treatment resistance of GBM is dysregulated redox homeostasis within the tumor cells. The redox environment plays a critical role in regulating cellular functions. Various factors are central to maintaining this balance, including glutathione, NF- κ B, Nrf2, HMGB1, and TFEB. This thesis will primarily focus on HMGB1 and TFEB.

Cancer cells show high basal levels of reactive oxygen species (ROS), necessary for their increased proliferative rate (Szatrowski & Nathan, 1991). Oxidative stress enhances cancer cell invasiveness but also supports glioblastoma stem cell (GSC) maintenance, ultimately contributing to treatment resistance and tumor recurrence. Moreover, ROS in the TME can influence the quantity and quality of surrounding non-cancer cells by releasing pro-tumorigenic and pro-inflammatory signals. Oxidative stress can be triggered by environmental stressors, such as chemicals, pollutants, and radiation. Microglia can be activated by lipopolysaccharide (LPS), a component of gram-negative bacterial cell walls. In this study, we used viral stressor (SARS-CoV-2 Spike protein) to induce oxidative stress in non-neoplastic (microglia) and neoplastic (GBM) cells.

1.4.1 – High Mobility Group Box 1 (HMGB1)

Oxidative stress triggers the release of damage-associated molecular patterns (DAMPs), such as high-mobility group box protein 1 (HMGB1), which plays a critical role in both inflammation and tumor cell proliferation (Kang et al., 2013). HMGB1, a nuclear and secreted protein, is overexpressed in various solid tumors and drives tumor progression (S. Wang & Zhang, 2020).

HMGB1 is a highly conserved nucleoprotein and a member of the non-histone chromatin-associated proteins. HMGB1 can translocate from the nucleus to the cytoplasm after undergoing post-translational modifications like acetylation,

phosphorylation, and methylation. Following chemoradiotherapy or hypoxia, HMGB1 can translocate to the extracellular space either through active secretion from immune cells or passive release from cells undergoing apoptosis or necrosis. Once outside, HMGB1 acts as an alarmin binding to receptors like the receptor for advanced glycation end products (RAGE) and Toll-like receptors 2/4/9 (TLR-2/4/9) (Paudel et al., 2019).

Nuclear HMGB1 is important for DNA replication, transcription, and chromatin remodeling, aiding in DNA damage repair and genomic stability. Cytoplasmic HMGB1 supports immune responses by promoting autophagy, inhibiting apoptosis, and regulating mitochondrial function (Huebener et al., 2014). As a DAMP, extracellular HMGB1 enhances immune responses, aiding in immune cell maturation, activation, and cytokine production (Rivera Vargas & Apetoh, 2017). It can also interact with chemokines like CXCL11 to amplify immune responses (Q. Gao et al., 2019). Due to its multifunctionality, HMGB1's dysregulation is linked to various diseases, particularly inflammatory disorders and cancers.

1.4.1.1 – HMGB1 in Cancer

HMGB1 has been linked to tumor progression, invasion, and metastasis, with abundant expression in various tumors and undifferentiated cells (Fukami et al., 2009). HMGB1, a classic DAMP, is released by necrotic cells and secreted by monocytes, macrophages, and dendritic cells (DCs) (Andersson & Tracey, 2011; H. Wang et al., 1999). It serves as a sensor of intracellular oxidative status, released following the oxidation of cysteine residues, and it promotes genomic instability in neoplastic cells through ROS-induced DNA damage (Kang et al., 2013; Stros, 2010; Y. Tang et al., 2016). TLR2, TLR4, TLR9, and RAGE receptors, expressed in macrophages, interact with HMGB1, triggering NF- κ B signaling and the release of pro-inflammatory molecules (Galdiero et al., 2013). These tumor-resident macrophages sustain the inflammatory tumor environment, alongside neutrophils, enhancing the oxidative state through high ROS amounts and NOX2 activation in response to various DAMPs (Galdiero et al., 2013). Tumor cells exploit this inflammatory milieu to proliferate, produce new tumor endothelial cells to support angiogenesis, and release cytokines, growth factors, extracellular matrix-

degrading enzymes, and angiogenic factors such as vascular endothelial growth factor (VEGF), Bv8, and MMP9 (Christiansen & Detmar, 2011).

Accumulating evidence has demonstrated that hypoxia causes tumor cells to actively secrete HMGB1 into the extracellular matrix. Extracellular HMGB1 subsequently functions as a paracrine/autocrine factor, activating signaling cascades through binding to its receptors. Importantly, HMGB1 is highly expressed in GBM tissue and is associated with poor prognosis (Ye et al., 2022).

The interaction between HMGB1 and RAGE contributes to the accelerated growth of gliomas in diabetic mice (I. Y. Zhang et al., 2020). HMGB1 promotes the phenotype of cancer stem-like cells in several types of cancer, including lung, colon, and pancreatic cancer (Qian et al., 2019; L. Zhang et al., 2019; X.-L. Zhao et al., 2017). Temozolomide treatment induces the upregulation of HMGB1 in biopsy-derived GBM cells, promoting the formation of glioma stem cells (GSCs) via TLR2 (X.-Y. Gao et al., 2021). Additionally, hypoxia upregulates the expression of DAMP receptors (Rider et al., 2012; Russo et al., 2015). It has been reported that RAGE expression increases with the upregulation of HIF-1 α expression in both GBM tumor tissues and cell lines. Hence, it is speculated that HMGB1 might be linked with GBM progression by promoting GSC growth under hypoxic conditions (Tafani et al., 2011).

1.4.2 – Transcription Factor EB (TFEB)

Transcription factor EB (TFEB), a member of the MiT/TFE family of transcription factors, is the master regulator of lysosomal biogenesis and autophagy. It exerts its effects by directly binding to the promoter of lysosomal and autophagic genes (Martina & Puertollano, 2016a). By binding to the Coordinated Lysosomal Expression and Regulation (CLEAR) motif, TFEB enhances the expression of associated genes, activating lysosomal protein production and influencing multiple steps in autophagy. Given the critical role of autophagy in tumor progression and its increased activity in various cancers, TFEB's function as a regulatory factor has received significant attention (Napolitano & Ballabio, 2016; Sardiello et al., 2009). Additionally, TFEB contributes to

cancer onset and progression by regulating the autophagolysosomal system and is involved in acquiring pro-tumor phenotypes (He et al., 2019; J. H. Kim et al., 2021).

TFEB is primarily regulated post-translationally, predominantly through phosphorylation at Ser142 and Ser211, which determines its activity (Napolitano & Ballabio, 2016). In nutrient-rich conditions, Ser142 and Ser211 are both phosphorylated, keeping TFEB in the cytosol in an inactive state. Conversely, nutrient scarcity or lysosomal dysfunction prompts TFEB's translocation to the nucleus, where it is activated (**Figure 1.3**) (M. Chen et al., 2021; Napolitano & Ballabio, 2016; Perera & Zoncu, 2016). The heightened demand for energy and synthetic components in rapidly proliferating cancer cells underlines the autophagolysosomal system's increased activity, making TFEB a notable research target in oncology. TFEB overexpression has been observed in various cancers, including melanoma, renal cell carcinoma, pancreatic adenocarcinoma, non-small cell lung cancer, and colorectal cancer. Conversely, TFEB knockdown inhibits tumor growth and reduces malignant phenotypes, highlighting its oncogenic role in a broad spectrum of cancers (Y. Fan et al., 2018; Kuiper et al., 2003; Y. Li et al., 2020; Perera et al., 2015; Zhou et al., 2021).

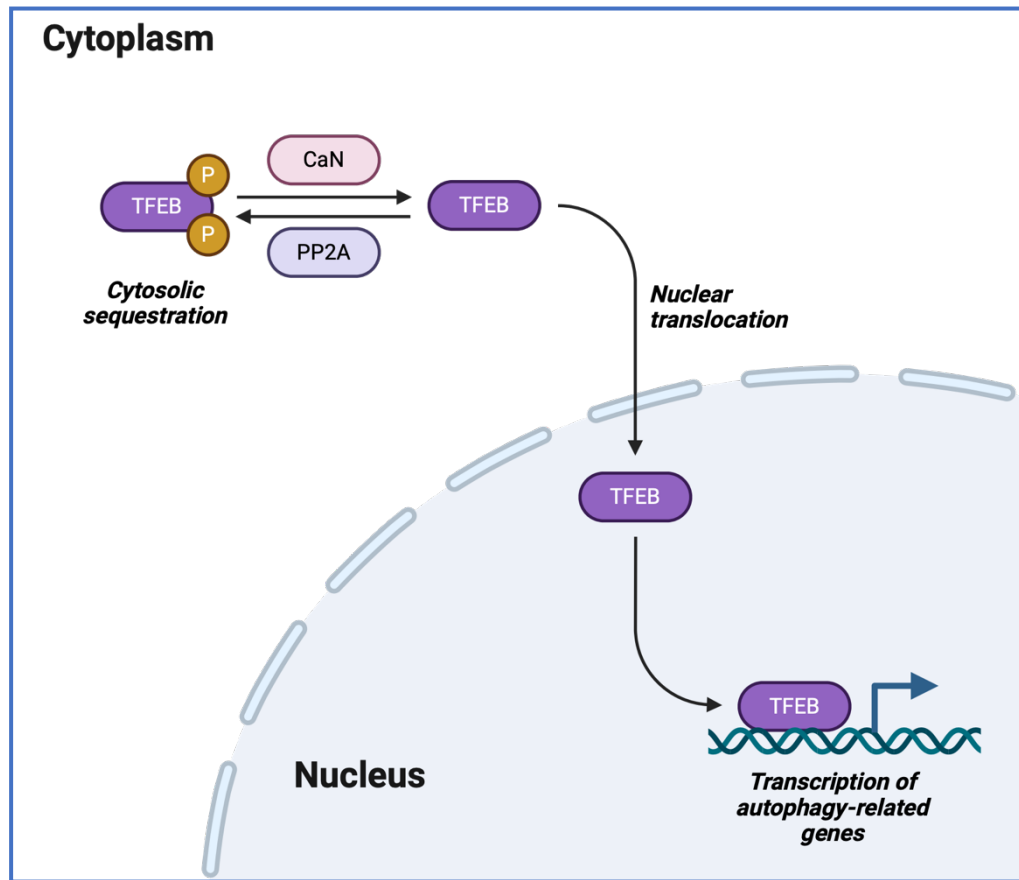


Figure 1.3. TFEB Signaling Cascade. In the inactive state, TFEB is phosphorylated and sequestered in the cytoplasm. Under these conditions, lysosomal biogenesis is minimal. Upon cellular stress or nutrient deprivation, TFEB is dephosphorylated by the phosphatase calcineurin. Dephosphorylation triggers the translocation of TFEB from the cytoplasm to the nucleus. Once in the nucleus, TFEB binds to the CLEAR elements in the promoters of target genes, leading to the transcriptional activation of a network of genes involved in lysosomal biogenesis and function. Created with ©BioRender (biorender.com).

1.5 – Modulation of Redox Imbalance in TME

1.5.1 – Fisetin

The flavonol fisetin (7,3',4'-flavon-3-ol) is a yellow coloring agent found in various plants including onions, strawberries, apples, and persimmons, first isolated from Venetian sumac (Gryniewicz & Demchuk, 2019). Fisetin plays a role in various biological processes that may contribute to its therapeutic effects. Its hydrophobic properties allow it to permeate and accumulate in the cell membrane, leading to antioxidant and anti-inflammatory effects. The therapeutic effects of fisetin are believed to arise from the modulation of NF- κ B and Nrf2 redox-responsive transcription factors (Sandireddy et al., 2016). Multiple ongoing clinical trials are studying the effects of fisetin in various age-related diseases, including osteoarthritis, frail elderly syndrome, and femoroacetabular impingement, suggesting the potential clinical benefits of fisetin in terms of practicality, safety, and tolerability.

Flavonoids are natural polyphenolic compounds commonly found in many fruits and vegetables. Their structure is characterized by a 2-phenyl-benzo-pyrane backbone, consisting of two benzene rings attached to a 3-carbon unit heterocyclic pyran ring (C6–C3–C6), which is crucial for their classification (Mbara et al., 2022). Flavonoids are known for their therapeutic activity against a range of diseases, including cancer, cardiovascular disease, and neurodegenerative disorders (Batra & Sharma, 2013). They exhibit varying effects on cells and organs, which can be partly attributed to the complexity of human tissues and the diversity of cellular responses, particularly in the brain (Atanasov et al., 2015; Forman & Zhang, 2021; Harvey et al., 2015). These differences are especially noticeable when comparing cancer cells with non-transformed cells (Newman & Cragg, 2020).

Due to the limitations of TMZ as monotherapy for GBM, we explored combination therapy with TMZ, fisetin, and other compounds. The rationale for combination therapy is that GBM is a heterogeneous disease, with genetic and epigenetic differences not only between single cancer cells but also between different niches of the tumor tissue (e.g., hypoxic, necrotic, semi-vascularized). Thus, drug combinations and drugs with multiple mechanisms of action are proposed to have lower risks of encountering significant drug

resistance in GBM compared to drugs with a single mode of action (e.g., TMZ). Several natural compounds have multiple anti-cancer mechanisms of action. Phenolic compounds isolated from natural sources, such as quercetin and fisetin, are particularly interesting due to their tumor-killing properties and low toxicity to normal cells (**Figure 1.4**).

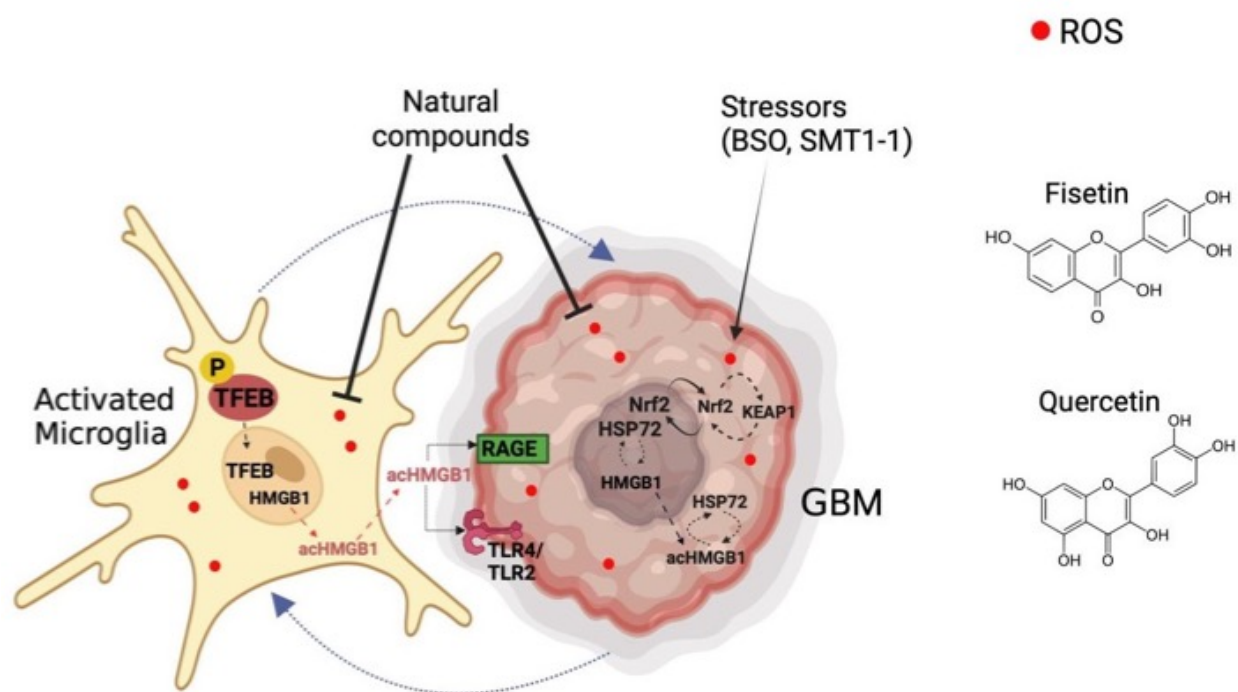


Figure 1.4. Modulation of Redox-Responsive Transcription Factors by Fisetin and Quercetin in GBM and TME. Fisetin and quercetin, natural polyphenols, play a crucial role in the elimination of ROS within GBM and the TME. These compounds effectively modulate redox-responsive transcription factors, specifically HMGB1 and TFEB, which are key players in cellular redox balance and inflammatory responses. By influencing these factors, fisetin and quercetin contribute to the reduction of oxidative stress and promote anti-inflammatory mechanisms, potentially impairing tumor progression and improving therapeutic outcomes in GBM. Created with ©BioRender (biorender.com). Figure adapted from (Joma et al., 2023).

1.5.2 – Dendrimers

1.5.2.1 – Dendrimers as anti-inflammatory agents

Nanostructures have been introduced in oncology primarily as drug nanocarriers. Numerous candidate nanostructures are currently at various stages of clinical trials. In tumors exhibiting the enhanced permeability and retention (EPR) effect, nanostructures can preferentially accumulate at the tumor site. A significant advantage of nanostructures is their ability to be tailored for specific tasks by modifying their size, shape, or functional groups. Additionally, many nanostructures not only serve as drug carriers but also possess inherent therapeutic effects.

Dendritic polyglycerol sulfate (dPGS) is a hyperbranched polyglycerol scaffold functionalized with peripheral sulfate groups, renowned for its intrinsic anti-inflammatory activity. The structure of dPGS can be found in **Figure 1.5**. Darnedde et al. showed the inhibition of cell adhesion molecules, specifically leukocytic L-selectin and endothelial P-selectin by dPGS. Results from that study highlight the decrease in leukocyte extravasation and alleviation of chronic inflammation in a contact dermatitis mouse model (Darnedde et al., 2010). Furthermore, dPGS interacts with complement factors C3 and C5, reducing the anaphylatoxin C5a levels *in vivo*. The anionic sulfate groups of dPGS target and bind selectins at positively charged protein motifs. The binding affinity is influenced by the size and degree of sulfation of dPGS.

Our group has studied the role of dPGS in modulating neuroinflammation, particularly focusing on its effects on glial cells. dPGS has significantly reduced proinflammatory cytokines and nitrites from lipopolysaccharide (LPS)-activated microglia, preventing the hyperactivation of microglia in response to inflammatory stimuli (Maysinger et al., 2015). Additionally, dPGS normalized the LPS-induced morphological changes of hippocampal dendritic spines and restored the functionality of CA1 pyramidal neurons. In established Alzheimer's disease models exposed to the neurotoxic 42 amino acid amyloid-beta ($A\beta_{42}$) peptide, dPGS was found to prevent $A\beta$ fibril formation through direct binding after being internalized by glial cells and hippocampal slice cultures (Maysinger et al., 2018). Moreover, dPGS attenuated $A\beta_{42}$ -induced glial hyperactivation

by reducing lipocalin-2 (LCN-2) production primarily in astrocytes. These results highlight the potential of dPGS in treating inflammation-associated neurological disorders.

Extending our *in silico* investigations, we hypothesized that structurally similar dendritic polyglycerol (dPG) but oppositely charged dendritic polyglycerol amine (dPGA) could act as a cytotoxic agent for GBM. Considering the challenges posed by pH and acidity in TME, we proposed that the positively charged dPGA might increase the pH, thereby assisting in the eradication of cancer cells, especially when used in conjunction with other therapeutic drugs. dPGA have emerged as a promising class of nanostructures for cancer therapy, noted for their highly branched architecture and positively charged surface. These properties enhance their interaction with cellular membranes and their ability to penetrate tumor tissues. The structure of dPGA can be found in **Figure 1.5**.

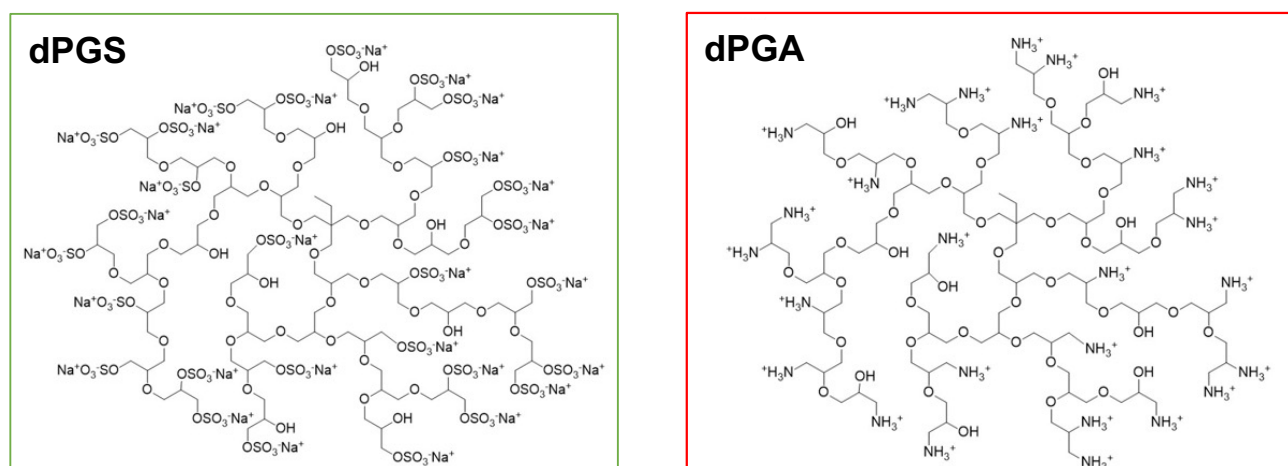


Figure 1.5. Structures of Dendritic Polyglycerol Sulfate (dPGS) and Dendritic Polyglycerol Amine (dPGA). Structures of two dendritic polyglycerol derivatives: dPGS and dPGA. dPGS is characterized by its highly branched polyglycerol scaffold with peripheral sulfate groups, imparting a negative charge. Conversely, dPGA features a similar branched structure but is functionalized with amine groups, resulting in a positively charged surface.

1.6 – Objectives

In our study, we investigated the effects of pharmacological intervention using fisetin, both alone and in combination with TMZ, a standard chemotherapy for GBM. Additionally, we explored the application of nanostructures, specifically dendrimers, on the TME, with a particular focus on the responsiveness of microglia. Fisetin, a small natural compound, was selected for its polyphenolic properties, which are known to exhibit anti-inflammatory effects. In contrast, dendrimers are completely synthetic entities characterized by their larger molecular mass and high biocompatibility. These dendritic nanostructures not only possess inherent anti-inflammatory properties but also serve as efficient nanocarriers for drug delivery. By leveraging the distinct advantages of fisetin and dendrimers, our research aims to enhance therapeutic outcomes in GBM by modulating the TME and improving microglial response.

CHAPTER 2 – MATERIALS AND METHODS

2.1 – Cell Culture

Human microglia clone 3 (HMC3) cells and human U251N glioblastoma cells were sourced from the American Tissue Culture Collection (ATCC). Cells were routinely cultured in Dulbecco's Modified Eagle Medium (DMEM; Gibco, #11995-065) supplemented with 5% fetal bovine serum (FBS; Wisent #080-450) and 1% Penicillin-Streptomycin (P-S; Invitrogen, #15140-122). Both cell types were maintained at 37°C in a humidified atmosphere containing 5% CO₂. Cells were used for experiments within 35 passages. The use of human cell lines was authorized by the McGill University Institutional Review Board under IRB Study Number A05-M37-20A (20-05-013).

2.2 – Cell Treatment

Cells grown to 70-80% confluency were detached using 0.05% trypsin-EDTA (Invitrogen, #25300062) and seeded on 12 mm glass coverslips (Karl Hecht™; #41001112) or 96-well cell culture plates (Sarstedt; #83.3924) at a density of 7,000 cells per well. After 24 hours, cells were treated as specified for each experiment, in serum-free media for either 24 or 72 hours.

2.3 – Cell Counting

Confluent monolayer cell cultures of 70–80% were detached using 0.05% trypsin–EDTA (Invitrogen, #25300062), seeded in 96-well cell culture plates (Sarstedt; #83.3924) at 2,500 cells per well, and cultured for 24 hours. Cells were then treated with increasing concentrations of temozolomide (TMZ; Sigma-Aldrich; #85622-93-1) and/or fisetin (Cayman Chemical; #528-48-3) for 72 hours. Nuclei were stained with 10 µM Hoechst 33342 (Molecular Probes, #H-1399) for 30 minutes, and cells were counted using the Cell Counter plugin in FIJI (ImageJ). Following this, the combination index (CI) was calculated using the formula (L. Zhao et al., 2010):

$$CI = \frac{IC_{50}(A+B)}{IC_{50}(A)} + \frac{IC_{50}(A+B)}{IC_{50}(B)}$$

Where IC_{50} (A) and IC_{50} (B) represent the IC_{50} values of each individual drug, while IC_{50} (A+B) represents the IC_{50} value of both drugs in combination.

2.4 – Lipid Droplet Labeling

Cells seeded on glass coverslips at a density of 7,000 cells per coverslip were cultured for 24 hours. Following treatment in serum-containing media, cells were washed with PBS and fixed in 4% paraformaldehyde (BDH; #29447) for 10 minutes. After washing, cells were incubated with 10 μ M BODIPY 493/503 (Invitrogen; #D3922) and Hoechst 33342 (Molecular Probes; #H-1399) for 20 minutes. The cells were then washed four times with PBS and mounted on microscope slides using EverBrite (Biotium; #23001). Samples were imaged using a fluorescence microscope (Leica DMI4000 B) with the UV and GFP filters at 63x magnification.

2.5 – Mitochondrial Metabolic Activity (MTT)

HMC3 or U251N cells were seeded in 96-well plates (Sarstedt; #83.3924) at 7,000 cells/well for 24h treatment and 2,500 cells/well for 72h treatment, and cultured for 24h before treatment. Cells were washed twice with phosphate-buffered saline (PBS) before treatment with increasing concentrations of fisetin (5, 15, 25, 50, 100 μ M; Cayman Chemical; #528-48-3), quercetin (5, 15, 25, 50, 100 μ M; Cayman Chemical; #849061-97-8), or dPGS/dPGA (0, 1, 10, 100, 500, and 1000 nM) in serum-deprived DMEM for 24 h or 72 h. dPGS and dPGA were provided by Dr. Ehsan Mohammadifar from the Institute of Chemistry and Biochemistry (Freie Universität Berlin). Following treatment, cells were incubated with 0.5 mg/ml MTT (Millipore-Sigma; #12352207) at 37°C for 30 minutes. The medium was removed, and cells were lysed with dimethyl sulfoxide (DMSO; Millipore-Sigma; #83730-53-4). Colorimetric measurements were taken at 595 nm (Spark 10M, Tecan, Männedorf, Switzerland).

2.6 – Lactose Dehydrogenase (LDH) Release Assay

HMC3 and U251N cells used for the MTT assay were also utilized for the LDH assay. After treatment, the medium was collected in a separate 96-well plate (Sarstedt;

#83.3924) and incubated with the reagent from the Cytotoxicity Detection Kit (Roche; #11644793001) for 30 minutes, protected from light, at room temperature. Colorimetric measurements were taken at 492 nm (Spark 10M, Tecan, Männedorf, Switzerland).

2.7 – Resazurin Assay

U251N cells were seeded and treated as described for the MTT assay. After treatment, the medium was removed and replaced with phenol-free DMEM (Nutrient Mixture F-12, Gibco, #21041-025). Alamar Blue (10%, v/v, Invitrogen, Lot #2142779) was added before incubating at 37°C until the medium became pink (4h). Colorimetric measurements were then taken at 570 nm (Spark 10M, Tecan, Männedorf, Switzerland).

2.8 – CellROX Assay

Cells were seeded at 7,000 cells per glass coverslip and cultured for 24 h. Cells were washed twice with PBS before treatment with fisetin (25 µM; Cayman Chemical; #528-48-3) or quercetin (25 µM; Cayman Chemical; #849061-97-8) with or without SARS-CoV-2 spike protein (SMT1-1, 5 µM, National Research Council Canada, Ottawa, ON, Canada). After treatment, cells were incubated for 30 min at 37°C with CellROX Deep Red (5 µM; Thermo Fisher Scientific; #C10422) to detect intracellular oxidative stress. Cell nuclei were labeled with Hoechst 33342 (10 µM; Molecular Probes; #H-1399). Cells were rinsed in phenol-free DMEM once and imaged using a fluorescence microscope with the CY5 filter at 20x magnification (Leica DMI 4000B).

2.9 – Immunocytochemistry (ICC)

Cells were seeded at 7,000 cells/coverslip on 12 mm circular glass coverslips (Karl Hecht™, #41001112) and cultured for 24 h before treatment. Following treatment, cells were fixed in 4% PFA (10 min; BDH; #29447), permeabilized with 0.1% Triton X-100 (v/v, 10 min, Sigma-Aldrich, #9036-19-5), and blocked in 10% goat serum (v/v, 1 h, Thermo Fisher Scientific; #50197Z) in PBS. Cells were incubated with primary antibodies overnight at 4°C, namely rabbit anti-TFEB (1:500, Sigma-Aldrich, SAB4503154-100UG), rabbit anti-HMGB1 acetyl-Lys12 (1:500, MyBioSource, MBS9404216), rabbit anti-

HMGB1 (1:500, Abcam, #ab18256), or rat anti-LAMP2 (1:500, Abcam, ABFG0786233). Cells were washed in PBS three times and incubated with secondary antibodies for 1 h at room temperature: goat anti-rabbit Alexa Fluor 647 (1:500, Invitrogen, A-21245) or goat anti-rat Alexa Fluor 647 (1:500, Life Technologies, A21247). Cells were washed with PBS; nuclei and F-actin were labeled with Hoechst 33342 (10 μ M; Molecular Probes, #H-1399) and F-actin with 1:400 Alexa Fluor® 488 Phalloidin (1:400, Invitrogen, A-12379) for 20 min, respectively. After three more washings with PBS, coverslips were mounted on Fisherbrand microscope slides (Fisher Scientific, #12-550-143) using Aqua-Poly/Mount (Polysciences, #18606-20). Samples were imaged using a fluorescence microscope (Leica DMI4000B, Leica), and intracellular fluorescence was analyzed in ImageJ at 63x magnification using the CY5, UV, and GFP filters. The nuclear and/or cytoplasmic fluorescence of TFEB, LAMP2, HMGB1, or acetylated HMGB1 for each cell was measured and normalized to the nuclear or cytoplasmic area. The background fluorescence was subtracted from the mean background fluorescence value. Schematic found in **Figure 2.1**.

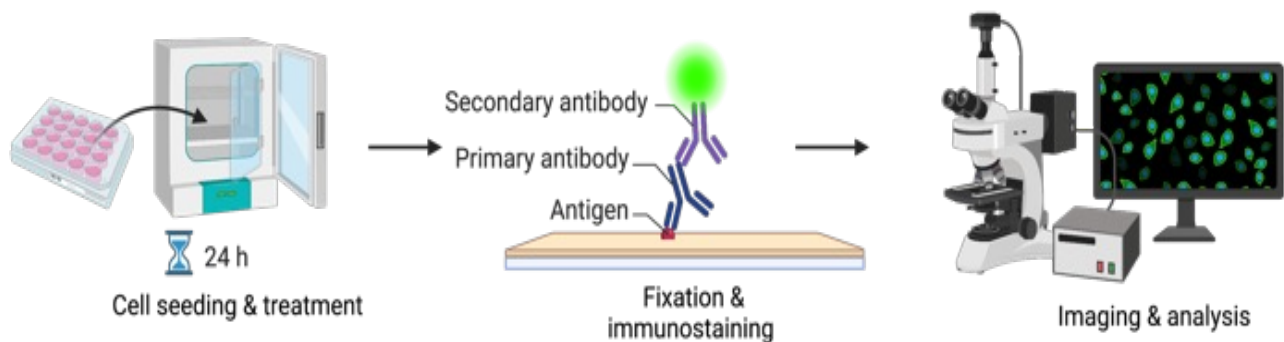


Figure 2.1. Overview of Immunocytochemistry Protocol. Human microglia and GBM cells were seeded at 7,000 cells/coverslip and cultured for 24 h. After treatment, cells were fixed and permeabilized. Cells were incubated with primary antibody overnight, followed by a one-hour incubation with the secondary antibody at room temperature. Nuclei and F- actin were labeled with Hoechst 33342 (10 μ M) and Phalloidin (1:400), respectively. Samples were then imaged using a fluorescence microscope. Created with ©BioRender (biorender.com).

2.10 – Measurement of Cathepsin B Activity (Magic Red)

U251N and HMC3 cells were seeded and treated as previously described in section 2.2. Cells were seeded at 7,000 cells/coverslip on glass coverslips and cultured for 24 h before treatment. 30 min prior to the end of treatment, the fluorogenic substrate Magic Red (1:260, ImmunoChemistry Technologies; #937) and Hoechst 33342 (10 μ M; Molecular Probes, #H-1399) in phenol-free media were directly added to cells. Cells were then incubated for 30 min at 37°C, protected from light. Cells were washed twice with PBS and rinsed twice in phenol-free DMEM. Cells were then imaged using a fluorescent microscope (Leica DMI 4000B) at 20x magnification using the CY3 and UV filters. Fluorescence intensity was analyzed using ImageJ.

2.11 – LysoTracker

Cells were seeded and treated as previously described in section 2.2. Cells were seeded at 7,000 cells/coverslip on glass coverslips and cultured for 24h before treatment. 30 min prior to the end of treatment, LysoTracker Red DND-99 (50 nM; Molecular Probes; #L7528) and Hoechst 33342 (10 μ M; Molecular Probes, #H-1399) in phenol-free media were directly added to cells. Cells were then incubated for 30 min at 37°C, protected from light. Cells were washed twice with PBS and rinsed twice in phenol-free DMEM. They were then imaged using a fluorescent microscope (Leica DMI 4000B) at 63x magnification using the CY3 and UV filters. Fluorescence intensity was analyzed using ImageJ.

2.12 – GBM Tumoroid Preparation

U251N tumoroids were prepared using the hanging drop method (Del Duca et al., 2004). Drops of 5000 cells in 20 μ L medium were pipetted onto the inner side of the lid of a 100 mm Petri dish (Thermo Fisher Scientific; #263991). The lid was quickly flipped 180° to cover the Petri dish filled with 20 mL PBS. Hanging drops were cultured at 37°C for 48 h to allow tumoroids to form. Tumoroids were then gently scooped into a medium-filled Petri dish coated with 2% agarose and cultured for 48 h. Tumoroids were implanted in agarose gel. The gels were covered with 100 μ L DMEM with or without treatment. Tumoroids were

imaged using light microscopy immediately after implantation on day 0 and day 12. Tumor size (area) was measured using ImageJ. Schematic found in **Figure 2.2**.

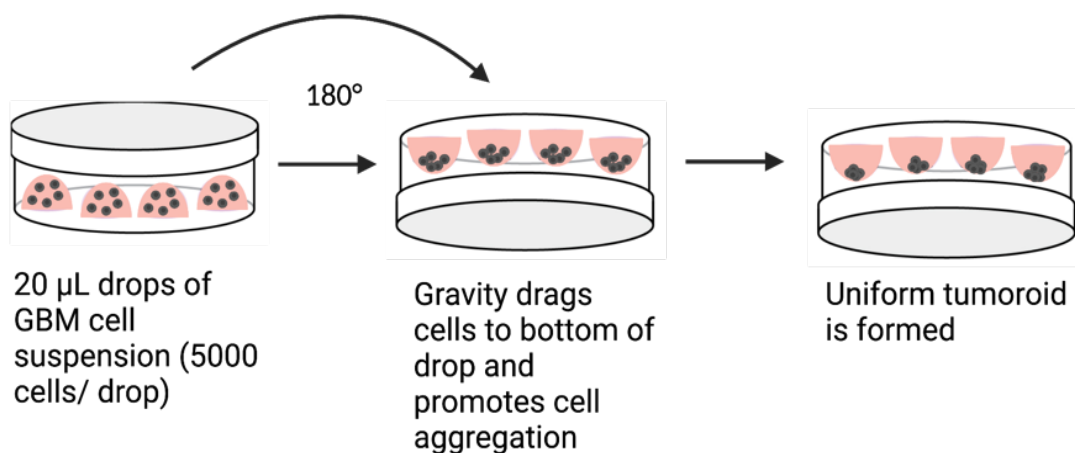


Figure 2.2. Overview of GBM Tumoroid Preparation. GBM tumoroids were prepared using the hanging drop method. 20 μ L drops of GBM cell suspension (5,000 cells/ drop) were pipetted onto the lid of a 10 cm Petri dish, which was then flipped 180 °. The hanging drops were cultured at 37 °C for 48 h to allow tumoroids to form. Created with ©BioRender ([biorender.com](https://www.biorender.com)).

2.13 – Molecular Docking

Modeling was done by Dr. Germanna L. Righetto from the Structural Genomics Consortium at the University of Toronto. The crystal structures of HMGB1 (PDB: 1AAB) and HSP72 bound to ADP (PDB ID: 5BN9) were selected for docking analysis because of their high resolution and overall high-quality scores among the proteins deposited in the Protein Data Bank for each target. Prior to the docking, PyMOL (The PyMOL Molecular Graphics System, Version 1.2r3pre, Schrödinger, LLC) was used to edit the protein structures and delete any undesired ligands or binding partners. The SwissDock web server was used for molecular docking, and well-characterized binding pockets were defined as regions of interest. In the case of HSP72, the docking was restricted to the binding region of the compound co-crystallized with the protein. For the apo HMGB1 structure, previous docking and NMR information of protein binding to glycyrrhizin and salicylic acid was used to define the likely binding region for the natural compounds. The software UCSF Chimera (version 1.14.0) was used to analyze the docking results and curate the most promising binding modes for each molecule. Binding modes with the most

favorable energy (low DG) and making more contact with the protein binding region were chosen for further analysis. The software LigPlot+ (version 2.2.8) was used to investigate the characteristics of protein-ligand binding, such as contacting amino acids and interaction strengths. PyMOL software (version 2.4.0) was used to create 3D representations of the results observed on LigPlot+ for the binding modes with a higher number of contacting amino acids and a higher number of hydrogen bonds and hydrophobic contacts for each natural compound analyzed.

2.14 – Proximity Ligation Assay

Experiments were done in collaboration with Dr. Issan Zhang. Cells were seeded at 7,000 cells per glass coverslip and cultured for 24 h before treatment. At the end of treatment, cells were washed twice with PBS, fixed with 4% paraformaldehyde (10 min, Millipore-Sigma, Oakville, ON, Canada), and then permeabilized with 0.1% Triton X-100 (v/v), 10 min (Millipore-Sigma, Oakville, ON, Canada). Blocking was performed for 1 h following instructions from the Duolink kit (Thermo Fisher Scientific, Oakville, ON, Canada). Samples were incubated with primary antibodies (rabbit anti-HMGB1, Abcam, Toronto, ON, Canada, 1/500; mouse anti-HSP70, Abcam, Toronto, ON, Canada, 1/500) overnight at 4°C in a humidified chamber. Samples were then washed and processed for proximity ligation following the manufacturer's recommendations. Nuclei were labeled for 10 min with Hoechst 33342 (10 µM), and actin was labeled for 20 min with Phalloidin Alexa Fluor 488 (1/400, Thermo Fisher Scientific, Oakville, ON, Canada). Samples were imaged using a fluorescence microscope (Leica DMI 4000B). Schematic found in **Figure 2.3**.

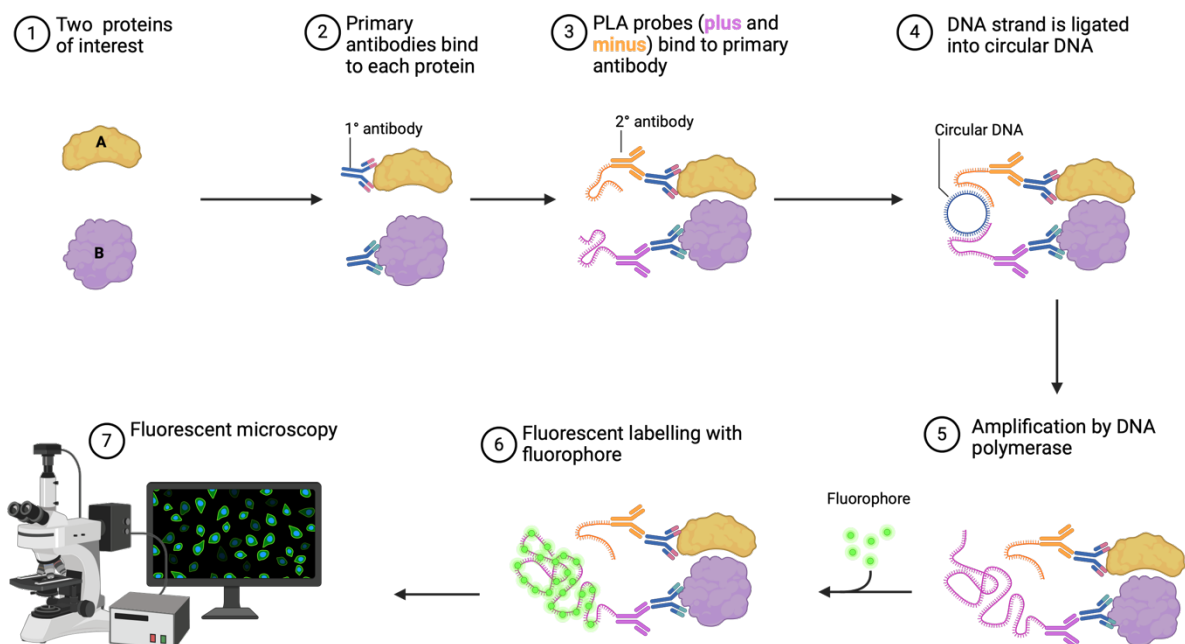


Figure 2.3. Overview of Proximity Ligation Assay. Cells were first seeded on glass coverslips within a 6-well plate. After treatment, the cells are fixed and permeabilized. Two primary antibodies, each from different species, are applied to target specific proteins. Corresponding PLA probes that recognize the species of the primary antibodies then bind to them. Following this, a PLA ligase generates a circular DNA template, which is amplified by a DNA polymerase. Fluorescently labeled oligonucleotide Duolink probes attach to the amplified DNA, emitting fluorescence that is detectable and quantifiable using a fluorescence microscope. Created with ©BioRender ([biorender.com](https://www.biorender.com)).

2.15 – Preparation of Fisetin Nanoparticles

Fisetin nanoparticles were prepared and characterized by Laura McKay from the Department of Chemistry at McGill University using the co-solvent evaporation method, as described previously (Soliman et al., 2010). A fisetin feed ratio of 10% was optimized to maximize encapsulation efficiency. The solutions were protected from light and stirred for 18 hours to completely remove the organic solvent and promote micelle formation. The aqueous solutions were then passed twice through 0.22 μm polyvinylidene fluoride (PVDF) syringe filters to eliminate any residual free fisetin. Aliquots were analyzed for hydrodynamic diameters and polydispersity index using dynamic light scattering (DLS), and micelle structure was assessed through transmission electron microscopy (TEM). In a typical TEM procedure, 15 μL of the micellar solution was placed on a carbon-coated copper grid, excess solution was removed after five minutes with Whatman filter paper,

and the sample was stained with 2% uranyl acetate for one minute. The grid was then dried for 30 minutes before imaging. For micelle drug content analysis by UV-Vis spectroscopy, 20 μ L aliquots were dissolved in 480 μ L of methanol. Encapsulation efficiency (EE) and loading capacity (LC) were calculated using the following formulas:

$$\text{Fisetin encapsulation efficiency (EE) \%} = 100 \cdot \left(\frac{\text{Loaded fisetin}}{\text{Total added fisetin}} \right)$$

$$\text{Fisetin loading capacity (LC) \%} = 100 \cdot \left(\frac{\text{Loaded fisetin}}{\text{Loaded fisetin} + \text{Polymer}} \right)$$

2.16 – Drug Release

Fisetin release from fisetin-loaded micelles was evaluated using the dynamic dialysis method (Lotocki et al., 2021). For this, 2.0 mL of sample was placed into dialysis membranes (3.5 kDa MWCO) and dialyzed against 140 mL of phosphate buffered saline (PBS) containing 1% Tween® 80 by volume. The system was stirred at 400 rpm and protected from light. At specific intervals, the samples were homogenized by several inversions, and 20 μ L aliquots were diluted in 480 μ L of methanol for immediate UV-Vis spectroscopy measurement. Free drug release was conducted similarly using 0.50 mg of fisetin solubilized in a 2 mL solution of MQ water/dimethylacetamide/PEG750 in a 45/40/15 ratio for comparison.

2.17 – Statistical Analysis

Data are presented as mean and standard deviation (SD) (mean \pm SD). Statistical significance was determined using a two-way analysis of variance (ANOVA), followed by Tukey's multiple comparison test. A Bonferroni correction was applied for multiple comparisons. p-values less than 0.05 were considered significant. Experiments were repeated independently at least three times. Statistical analysis and graph representations were performed using GraphPad Prism (version 10.0.0).

| REAGENT | SOURCE | IDENTIFIER |
|--|--|------------------------|
| ANTIBODIES | | |
| Rabbit anti-TFEB | Sigma-Aldrich | SAB4503154-100UG |
| Rabbit anti-acetylated-HMGB1 | MyBioSource | MBS9404216 |
| Goat anti-rabbit Alexa Fluor 647 | Invitrogen | A-21245 |
| Goat anti-rat Alexa Fluor 647 | Life Technologies | A21247 |
| Mouse anti-KEAP1 | Proteintech | 10503-2-AP |
| Rabbit anti-HMGB1 | Abcam | ab18256 |
| Mouse anti- HSP70 | Abcam | ab2787 |
| Rat anti-LAMP2 | Abcam | ABFG0786233 |
| CELLS | | |
| HMC3 human microglia | ATCC | CRL-3304 |
| U251N human glioblastoma | ATCC | - |
| CHEMICALS | | |
| Dulbecco's modified eagle medium (DMEM) | Gibco | 11995-065 |
| Fetal bovine serum (FBS) | Wisent | 080-450 |
| Penicillin–streptomycin | Invitrogen | 15140-122 |
| Trypsin-EDTA | Invitrogen | 25300062 |
| SARS-CoV-2 spike protein (SMT1-1) | National Research Council Canada | - |
| Fisetin | Cayman Chemical | 528-48-3 |
| Temozolomide | Sigma-Aldrich | 85622-93-1 |
| Hoechst 33342 | Molecular Probes | H-1399 |
| Alexa Fluor® 488 phalloidin | Invitrogen | A-12379 |
| Quercetin | Cayman Chemical | 849061-97-8 |
| Dendritic polyglycerol sulfate (dPGS) | Institute of Chemistry and Biochemistry (Freie Universität Berlin) | Dr. Ehsan Mohammadifar |
| Dendritic polyglycerol amine (dPGA) | Institute of Chemistry and Biochemistry (Freie Universität Berlin) | Dr. Ehsan Mohammadifar |
| 4% Paraformaldehyde | BDH | 29447 |
| BODIPY 493/503 | Invitrogen | D3922 |
| EverBrite | Biotium | 23001 |
| Aqua-poly/mount | Polysciences | 18606-20 |
| Mitochondrial metabolic activity kit (MTT) | Millipore-Sigma | 12352207 |
| Dimethylsulfoxide (DMSO) | Millipore-Sigma | 67-68-5 |
| CellROX deep red | Thermo Fisher Scientific | C10422 |
| Triton X-100 | Sigma-Aldrich | 9036-19-5 |
| 10% goat serum | Thermo Fisher Scientific | 50197Z |
| Magic red® fluorescent cathepsin b assay kit | ImmunoChemistry Technologies | 937 |
| MATERIALS | | |
| 12 mm circular glass coverslips | Karl Hecht TM | 41001112 |
| 96-well cell plates | Sarstedt | 83.3924 |
| 24-well plates | Sarstedt | 83.3922 |
| Cytotoxicity detection kit (LDH) | Roche | 11644793001 |
| Fisherbrand TM microscope slides | Fisher Scientific | 12-550-143 |
| Duolink PLA control kit | Thermo Fisher Scientific | DUO92202 |
| 100 mm petri dish | Thermo Fisher Scientific | 263991 |

Table 2.1. List of Materials. This table provides a comprehensive list of all antibodies, chemicals, and materials utilized in this thesis, organized by reagent type, source, and identifier number.

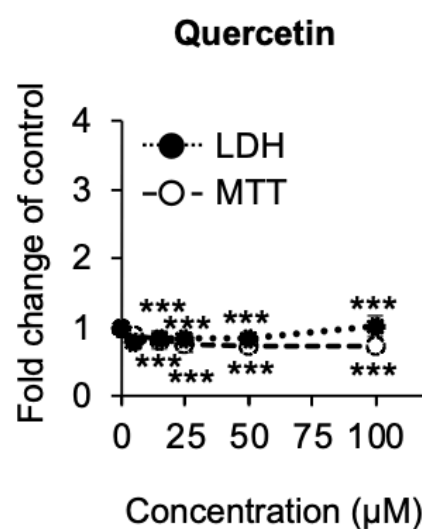
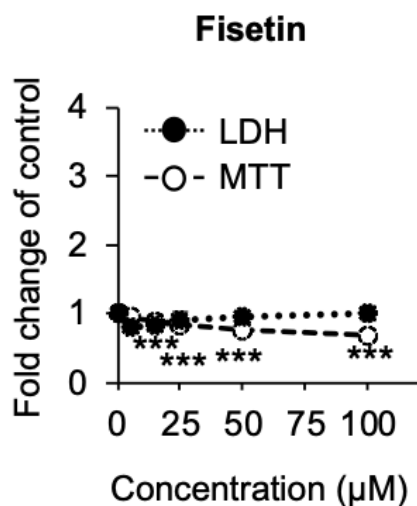
CHAPTER 3 – EXPERIMENTAL RESULTS

3.1 – *Flavonoids Exhibit Differential Cytotoxicity in GBM Cells and Microglia*

The first aim of this study was to evaluate the cytotoxic effects of the flavonoids fisetin and quercetin (positive control) in human U251N glioblastoma (GBM) cells and human HMC3 microglia, as a component of the tumor microenvironment. Both compounds have previously been tested in various cell types both *in vitro* and *in vivo* models. We assessed the cytotoxicity of these flavonoids on mitochondrial metabolic activity using the MTT assay and lactate dehydrogenase (LDH) release in microglia and GBM cells. Concentration-dependent and time-dependent effects were evaluated. Cell viability and cytotoxicity were tested across a range of flavonoid concentrations from 0 to 100 μM . Assessments were done both by cell counting and fluorescent microscopy to visualize changes in cell morphology.

The results show a minimal impact of fisetin and quercetin on microglia viability (**Figure 3.1A**), while both compounds significantly reduced GBM cell viability in a dose-dependent manner (**Figure 3.1B**). This indicates differential cytotoxicity between these cell types. Despite the relative simplicity of these experiments, they provide an important initial insight into the potential detrimental effects of flavonoids on two key cellular components in GBM and the tumor microenvironment.

A Microglia



B Glioblastoma

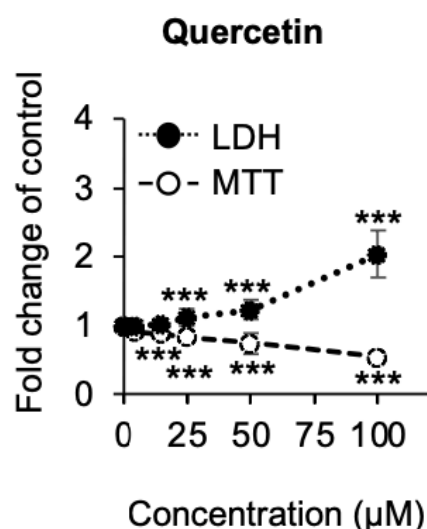
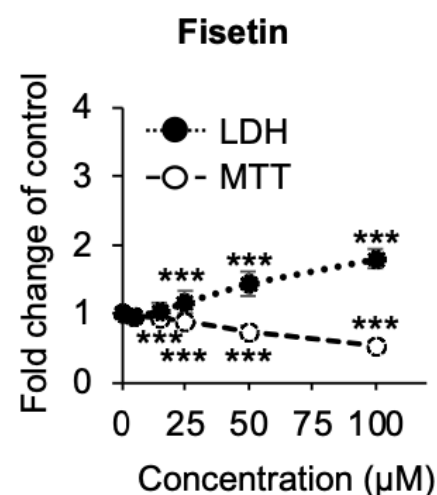


Figure 3.1. Dose-dependent lactate dehydrogenase (LDH) release and mitochondrial metabolic activity (MTT) in response to fisetin and quercetin. (A) Human microglia and (B) GBM cells were treated with increasing concentrations of selected compounds (0, 5, 15, 25, 50, 100 µM for fisetin and quercetin) for 24 h in serum-deprived conditions. Culture medium was used to assess LDH release, and cellular mitochondrial metabolic activity was measured using the MTT assay. Shown are the average fold change in LDH or MTT

compared to the mean of the untreated control (set to 1) \pm SD from at least 3 independent experiments. (***) $p < 0.001$). Figure adapted from (Joma et al., 2023).

3.2 – Combination of Fisetin and Temozolomide Synergistically Inhibit GBM Survival

Natural compounds may not directly induce cancer cell death but can enhance the efficacy of anti-cancer drugs such as TMZ. We evaluated the impact of combining fisetin and TMZ on GBM cells using cell counting and MTT assays, followed by calculating the combination index (CI). The combination of fisetin and TMZ at their respective IC₅₀ concentrations was more effective than either compound alone. When 10 μ M fisetin was combined with 30 μ M TMZ, a 70% reduction in GBM cell viability was observed after 72 hours (**Figure 3.2A**). The CI value for the fisetin-TMZ combination was 0.00013 (CI < 1), indicating a synergistic effect.

Further testing was conducted on GBM tumoroids, which serve as a more relevant *in vivo* model. Since tumoroids are more drug-resistant than monolayer cultures, a higher concentration of fisetin (25 μ M) was used. Consistent with results from monolayer cultures, the combination of fisetin and TMZ resulted in a reduction in tumoroid size, whereas individual treatments did not significantly impact tumor size (**Figure 3.2B**).

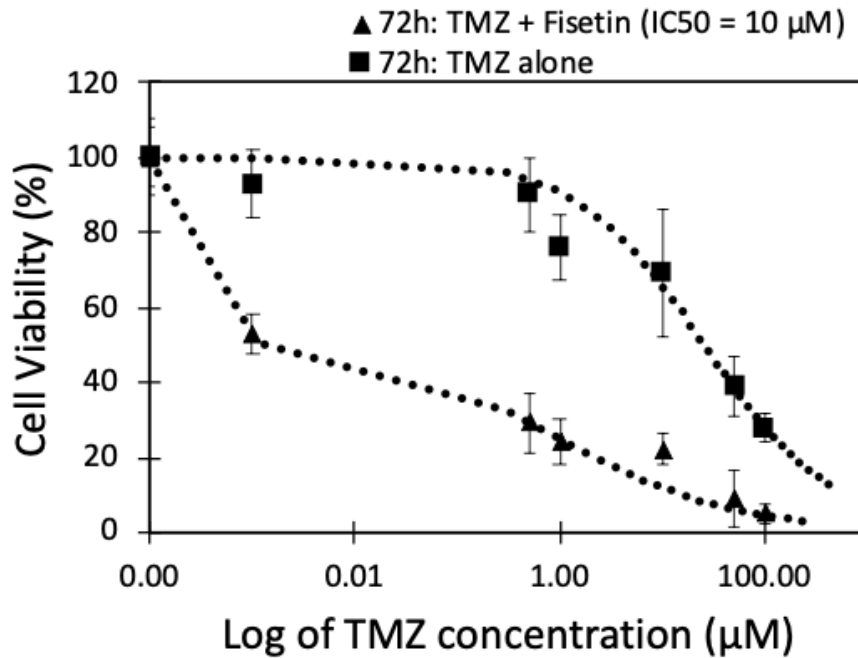
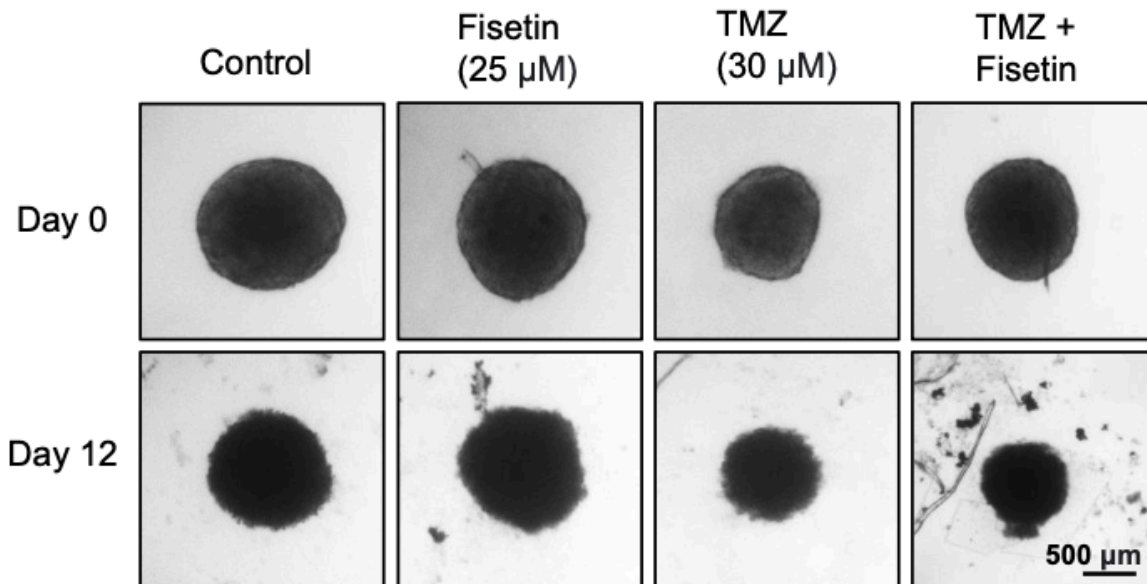
A**B**

Figure 3.2. Dose-dependent effect in response to fisetin and TMZ. **(A)** Dose-dependent decrease in cell viability (72 h) with the combination of a fixed concentration of fisetin (10 μM) and increasing concentration of TMZ (0.001, 0.5, 1, 10, 50, and 100 μM). Each point represents the mean from three independent experiments normalized to the untreated control. Cell viability was measured by counting Hoechst 33342-labeled nuclei imaged using a fluorescence microscope. **(B)** Representative micrographs of GBM tumoroids treated with TMZ (30 μM) +/- fisetin (25 μM) on day 0 and day 12. Tumor size (area) was calculated using ImageJ. Figure adapted from (Joma et al., 2023).

3.3 – Fisetin Reduces Oxidative Stress in GBM and Microglia

Many natural compounds have been shown to modulate oxidative stress, which is sustained differently in normal and transformed cells. Oxidative stress enhances cancer cell invasiveness and supports glioblastoma stem cell maintenance, contributing to treatment resistance and tumor recurrence. Environmental stressors such as chemicals, pollutants, and radiation are known triggers for oxidative stress. Previously, we established that microglia could be activated by lipopolysaccharide (LPS), a component of Gram-negative bacterial cell walls (Maysinger et al., 2023). We investigated the antioxidant effects of fisetin on both microglia and GBM cells when subjected to an exogenous stressor (SARS-CoV-2 spike protein), which has been shown to induce oxidative stress (**Figure 3.3**).

To confirm the effects on ROS status, we detected changes in intracellular ROS using the fluorescent probe CellROX. We found that spike protein increased ROS production in both microglia (**Figure 3.3A, B**) and GBM cells (**Figure 3.3C**). However, spike-mediated oxidative stress was significantly attenuated after treating microglia and GBM cells with fisetin. These results show that fisetin treatment normalized ROS levels back to control and suppressed spike-induced oxidative stress in both cell types, indicating a lack of cell type-specific effects of fisetin on ROS modulation.

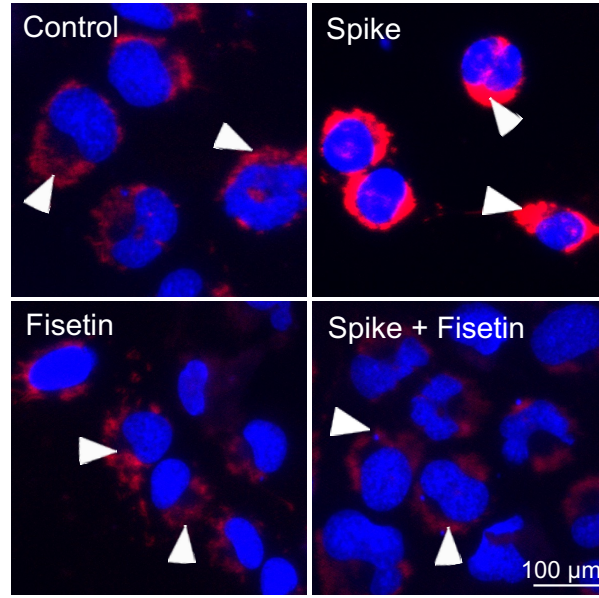
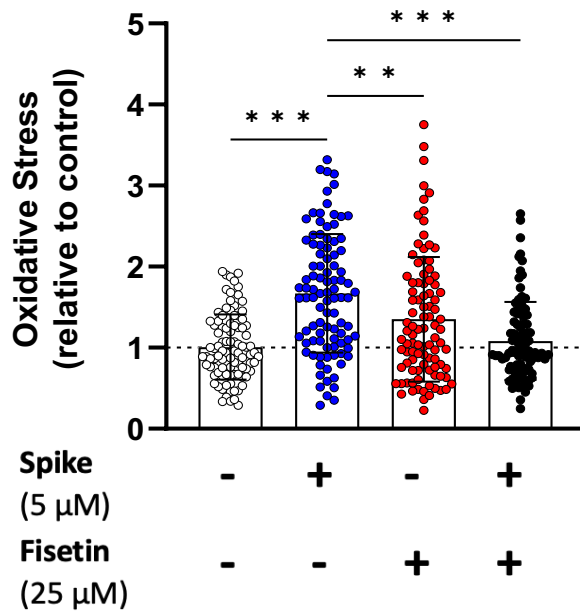
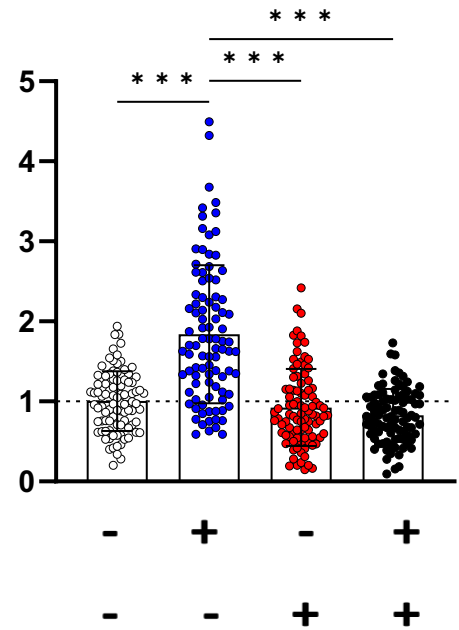
A**B****Microglia****C****Glioblastoma**

Figure 3.3. Oxidative stress in human microglia and GBM cells treated with fisetin +/- spike. Microglia and GBM cells were treated with spike (5 μ M), fisetin (25 μ M), or a combination of spike and fisetin for 24 h in serum-free media. **(A)** Representative fluorescence micrographs of microglia loaded with CellROX Deep Red (red) and imaged using a fluorescence microscope. Nuclei (blue) were labeled with Hoechst 33342. The arrowheads represent intracellular ROS. Scale bar = 100 μ m. Shown are the normalized intracellular fluorescence values to the mean of the untreated control (set to 1) for **(B)** microglia and **(C)** GBM cells. Dotted lines represent the mean of the control group

normalized to 1. Statistical analysis was assessed using two-way ANOVA, followed by Tukey's multiple comparison test. At least 90 cells from three independent experiments were analyzed. Mean \pm SD. (** $p \leq 0.01$, *** $p \leq 0.001$). Figure adapted from (Joma et al., 2023).

3.4 – Fisetin Decreases Cytosolic AcHMGB1 Abundance in Microglia, but Not in GBM

An important redox-sensitive transcription factor affected by oxidative stress is high mobility group box 1 (HMGB1). HMGB1 typically localizes to the nucleus, where it can undergo post-translational modifications, including acetylation (**Figure 3.4A**). In response to oxidative stress, HMGB1 translocates to the cytoplasm and is released into the extracellular space as an alarmin. We used immunocytochemistry (ICC) to assess the levels of nuclear and cytosolic acetylated HMGB1 (AcHMGB1) in microglia and GBM cells treated with fisetin, spike, or their combination. Fisetin, with or without spike, significantly reduced cytosolic AcHMGB1 in microglia (**Figure 3.4B, C**). Interestingly, fisetin did not affect the abundance of cytosolic AcHMGB1 in GBM cells (**Figure 3.4D**).

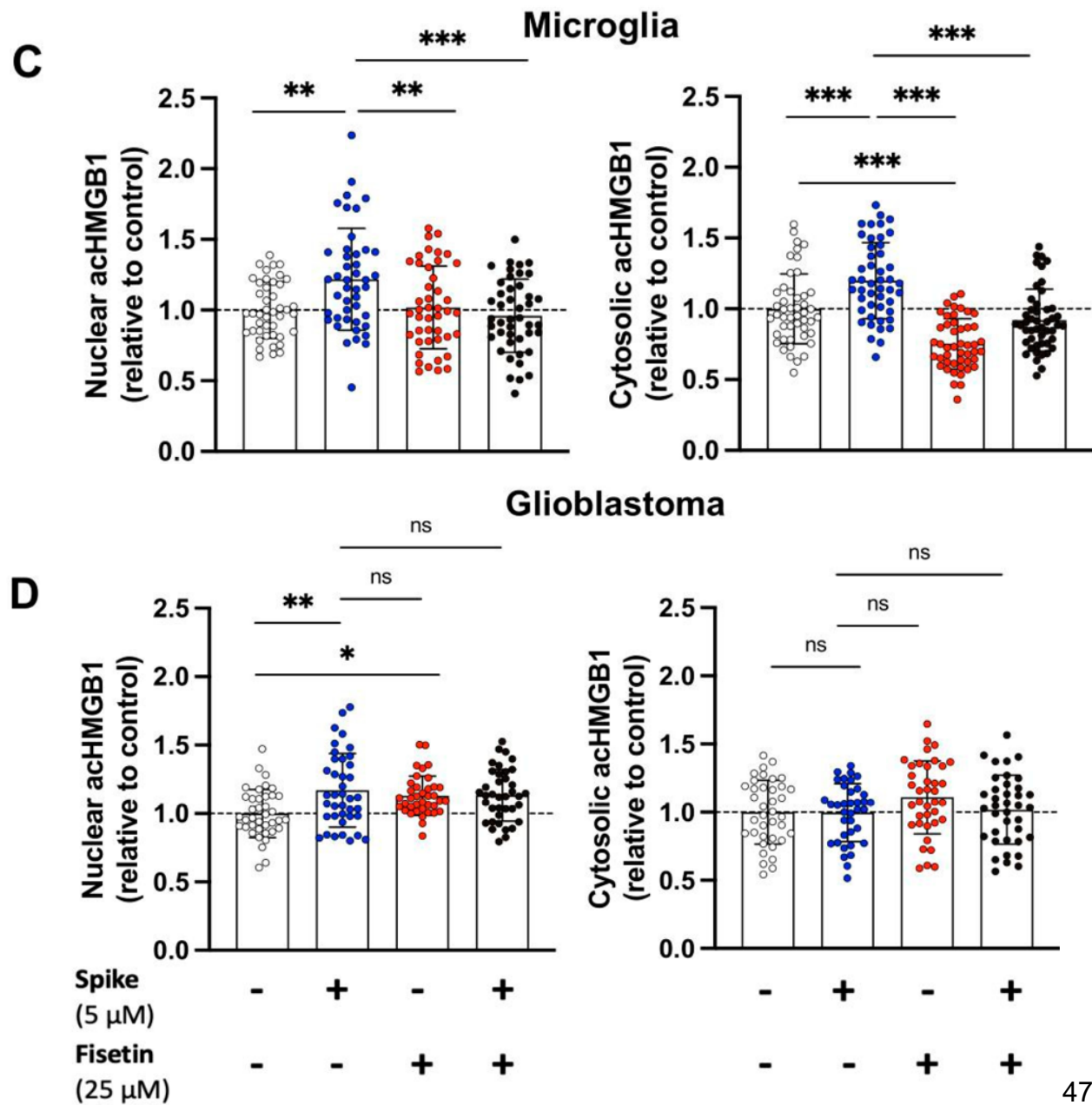
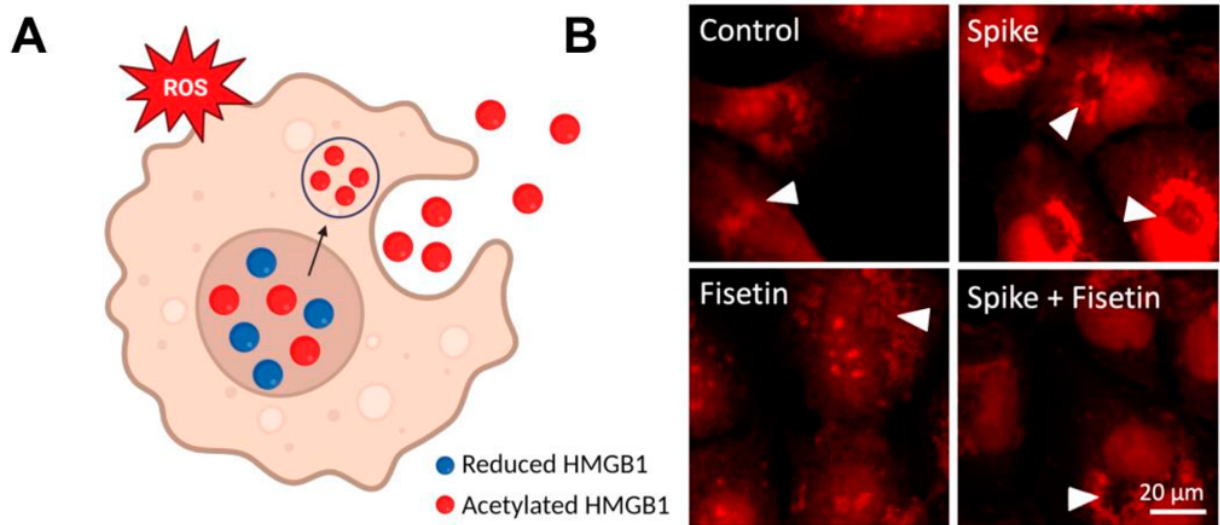


Figure 3.4. AcHMGB1 in human GBM cells and microglia treated with fisetin +/- spike. GBM cells and microglia were treated with spike (5 μ M), fisetin (25 μ M), or a combination of spike and fisetin for 24 h in serum-free media. **(A)** Under stress, AcHMGB1 translocates to the cytoplasm and can be released into the extracellular space as an alarmin. **(B)** Microglia were labeled for AcHMGB1 (red) and imaged using a fluorescence microscope. Scale bar = 20 μ m. The arrowheads represent cytosolic AcHMGB1. Shown are the normalized intracellular fluorescence values to the mean of the untreated control (set to 1) in **(C)** human microglia and **(D)** GBM cells. Dotted lines represent the mean of the control group normalized to 1. Statistical analysis was assessed using two-way ANOVA, followed by Tukey's multiple comparison test. At least 40 cells from three independent experiments were analyzed. Mean \pm SD. (ns—nonsignificant, * $p \leq 0.05$, ** $p \leq 0.01$, *** $p \leq 0.001$). Figure adapted from (Joma et al., 2023).

3.5 – Fisetin Increases TFEB Abundance in Stressed Microglia

Another key redox-responsive transcription factor is transcription factor EB (TFEB). TFEB regulates the expression of genes essential for lysosomal biogenesis and enzymatic activities, including the protease cathepsin B. Typically, TFEB is primarily located in the cytosol; however, under stress conditions, TFEB translocates to the nucleus, promoting the expression of multiple target genes involved in autophagy (**Figure 3.5A**). We used ICC to evaluate the abundance of nuclear and cytosolic TFEB in microglia and GBM cells treated with fisetin, spike, or their combination. Fisetin increased the abundance of TFEB in both the nucleus and cytosol of stressed microglia (**Figure 3.5B, C**). Notably, the increase in TFEB levels was less pronounced in GBM cells (**Figure 3.5D**).

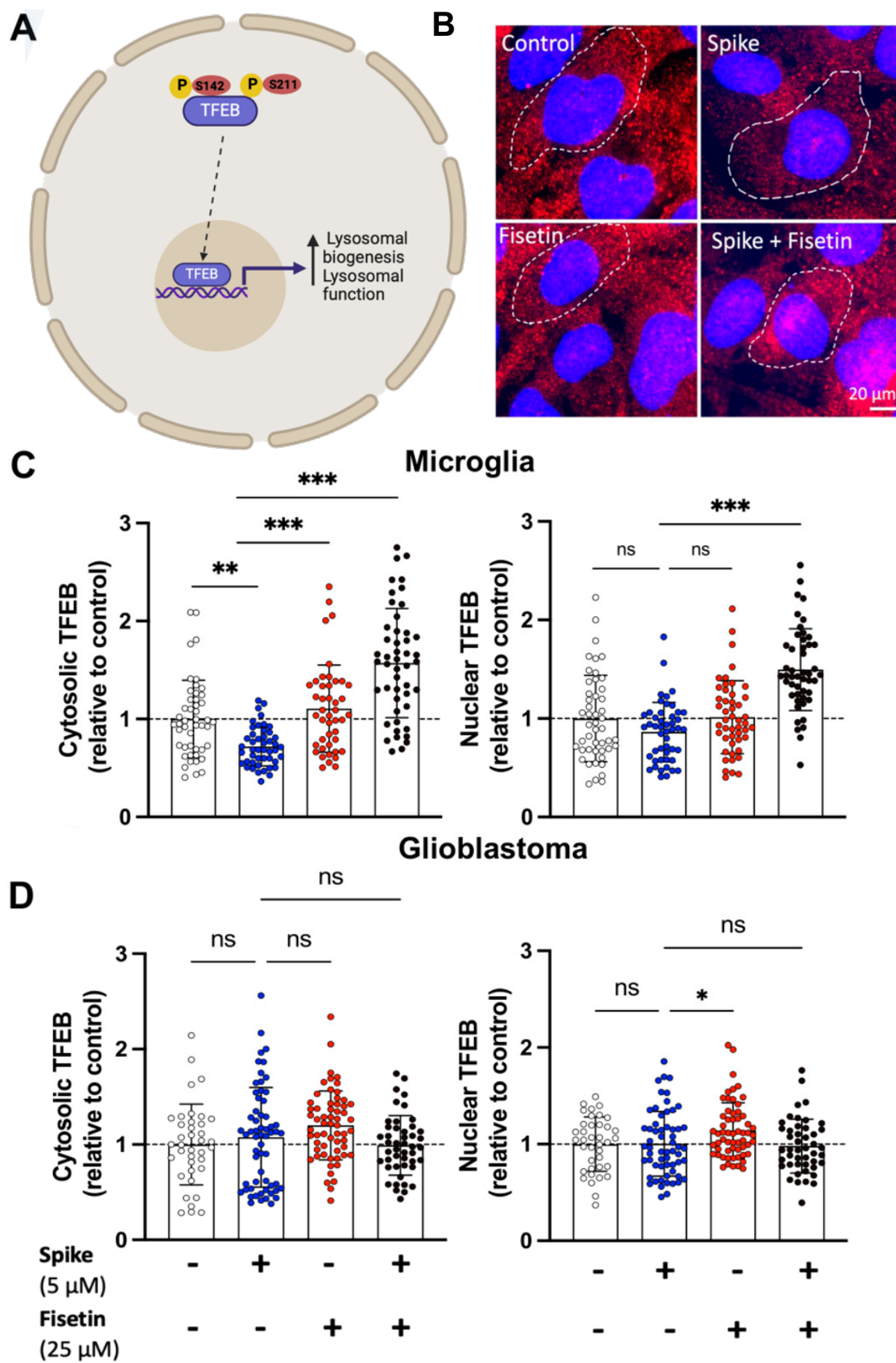


Figure 3.5. TFEB in human GBM cells and microglia treated with fisetin +/- spike. GBM cells and microglia were treated with spike (5 μ M), fisetin (25 μ M), or a combination of spike and fisetin for 24 h in serum-free media. **(A)** TFEB undergoes dephosphorylation under conditions of stress, where it is free to translocate to the nucleus and upregulate transcription of lysosomal biogenesis and function. **(B)** Microglia were labeled for TFEB (red) using rabbit anti-TFEB (1:500) and imaged using a fluorescence microscope. Nuclei were labeled with Hoechst 33342 (blue). Scale bar = 20 μ m. Shown are the normalized intracellular fluorescence values to the mean of the untreated control (set to 1) in **(C)** human microglia and **(D)** GBM cells. Dotted lines represent the mean of the control group normalized to 1. Statistical analysis was assessed using two-way ANOVA, followed by Tukey's multiple comparison test. At least 40 cells from three independent experiments were analyzed. Mean \pm SD. (ns—nonsignificant, * $p \leq 0.05$, ** $p \leq 0.01$, *** $p \leq 0.001$). Figure adapted from (Joma et al., 2023).

3.6 – Fisetin Increases Lysosomal Abundance and Activity in Microglia

The transient nuclear accumulation of TFEB could lead to enhanced lysosomal biogenesis and lysosomal enzyme activities. To test this, we monitored the abundance of lysosomes using the membrane protein LAMP-2, a marker for lysosomes and late endosomes (**Figure 3.6A**). While LAMP-2 serves as an indicator of lysosome abundance, it does not reflect their functional capacity. Therefore, we measured the activity of cathepsin B, a lysosomal protease, to evaluate lysosomal function (**Figure 3.6B**). Our findings indicate that fisetin treatment resulted in increased LAMP-2 levels in microglia, which correlated with an increase in cathepsin B activity (**Figure 3.6C**). This aligns with the observed nuclear accumulation of TFEB, suggesting an overall enhancement in lysosomal function and possibly an increase in their number or size. In contrast, while fisetin also increased LAMP-2 levels in GBM cells, cathepsin B activity remained unchanged (**Figure 3.6D**).

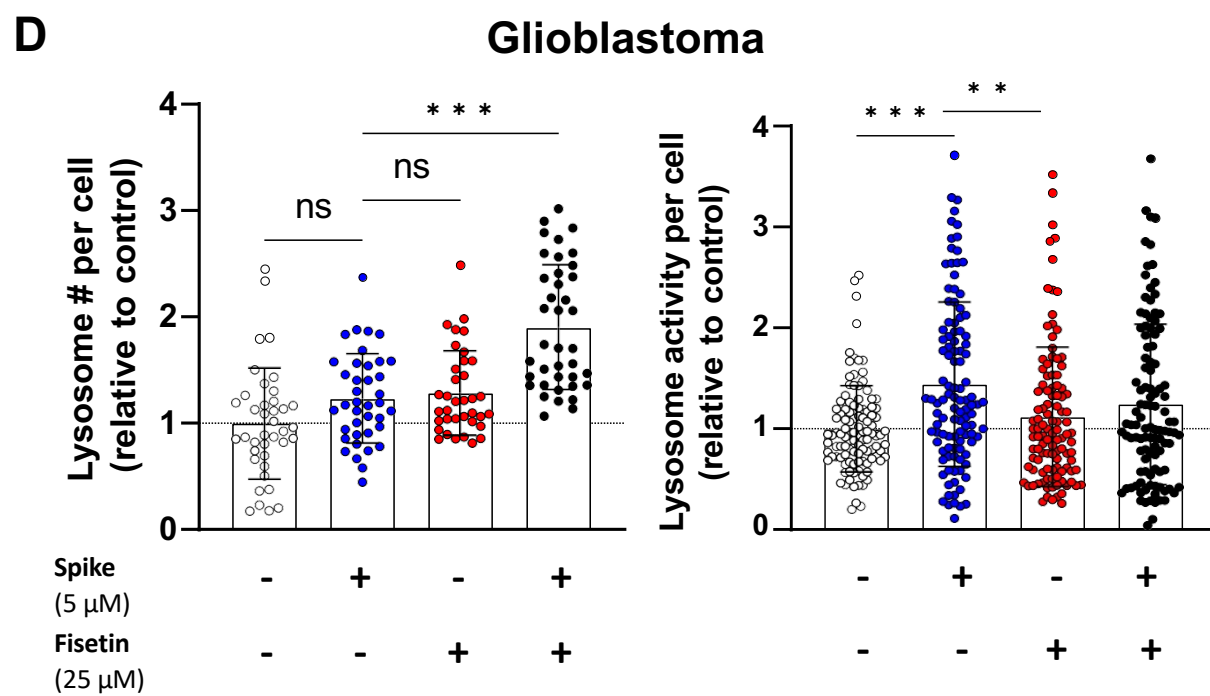
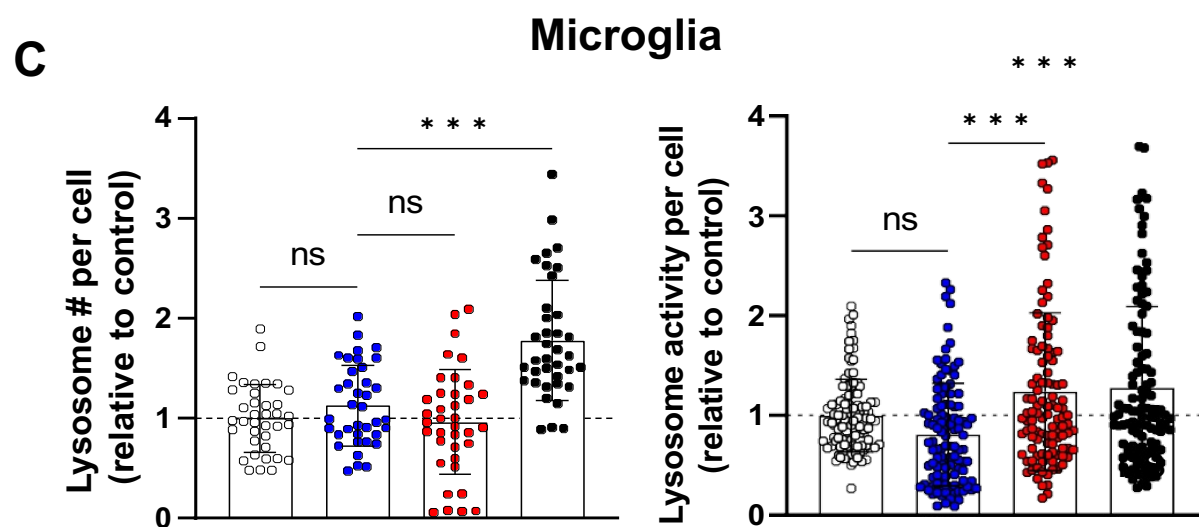
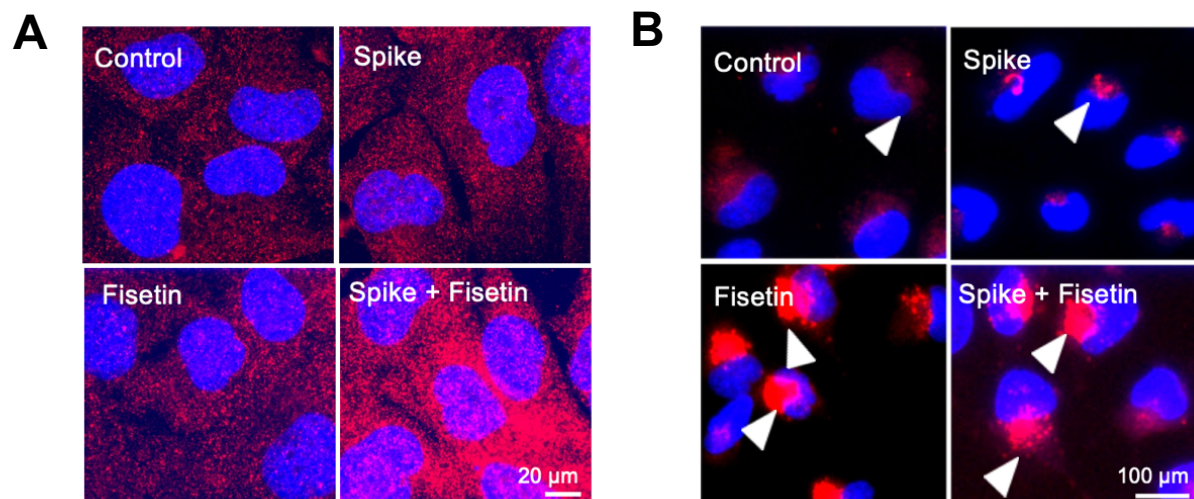


Figure 3.6. Lysosome abundance and activity in human glioblastoma and microglia. Cells were treated with Fisetin (25 μ M) for 24 h in the presence and absence of Spike (5 μ M). **(A)** LAMP-2 was detected in microglia with fluorescent microscope (red); nuclei were labelled with Hoechst 33342 (10 μ M) (blue). **(B)** Magic red was detected in live microglia with fluorescent microscope (red); nuclei were labelled with Hoechst 33342 (10 μ M) (blue). **(C) (D)** Shown are the normalized intracellular fluorescence values to the untreated control (set to 1) from three independent experiments. Mean \pm SD. * $P \leq 0.05$, ** $P \leq 0.01$, *** $P \leq 0.001$.

3.7 – Fisetin Increases Lipid Droplet Abundance in Microglia, but not in GBM

An increase in lysosomal abundance and catalytic activity is often accompanied by a decrease of lipid droplets (LDs). Serving as organelles that store energy and defend against oxidative stress, LDs play crucial roles in cellular dynamics. To investigate LD dynamics during oxidative stress, we examined changes in LD numbers in microglia and GBM cells treated with spike, with and without fisetin. Using fluorescence imaging, we monitored the abundance of LDs, visualized with the neutral lipid-selective fluorescent dye BODIPY 493/503. Fisetin treatment led to a significant increase in LD abundance in microglia after 24 hours, compared to untreated cells (**Figure 3.7A**). In contrast, fisetin did not affect LD abundance in GBM cells (**Figure 3.7B**). It is important to highlight that under baseline conditions, GBM cells already have a high count of LDs. This suggests that LDs may offer a protective advantage in microglia. Additionally, we observed that the lipid composition of LDs did not include a significant concentration of oxidized lipids, as the levels of lipotoxins did not increase. We are currently conducting a more detailed analysis of the lipid species within LDs using mass spectrometry (MS) and high-performance liquid chromatography (HPLC).

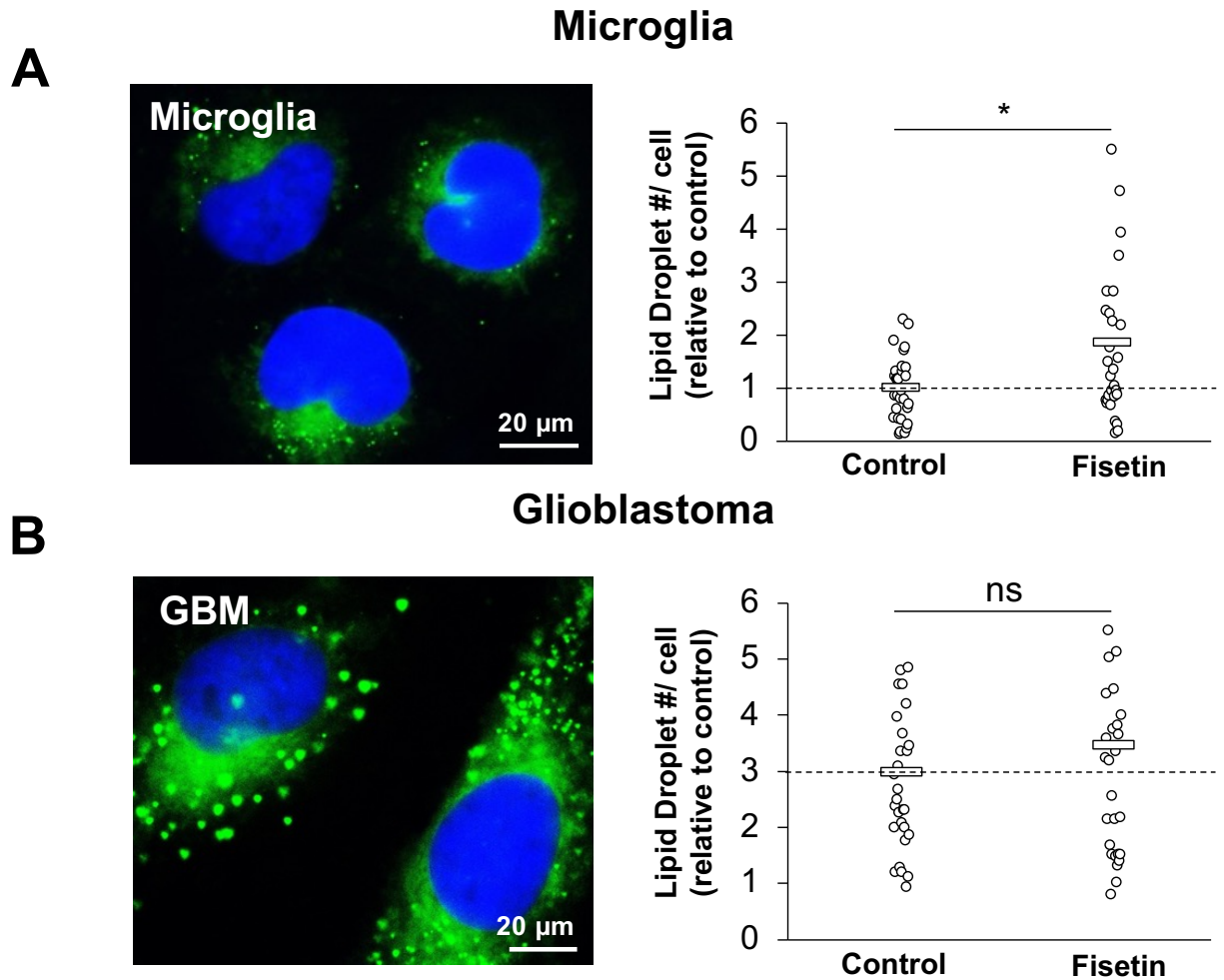


Figure 3.7. Lipid droplets in human microglia and GBM cells. Cells were treated with fisetin (25 μ M) for 24 h. BODIPY was detected in live cells with fluorescent microscope (green); nuclei were labelled with Hoechst 33342 (10 μ M) (blue). Shown are the normalized intracellular fluorescence values to the untreated control (set to 1) from three independent experiments in **(A)** microglia and **(B)** GBM cells. A total of 23 cells were analyzed for each condition. * $P \leq 0.05$.

3.8 – Cytotoxicity of dendrimers in microglia

In addition to natural polyphenols, we tested synthetic dendritic polyglycerols (dPG) in microglia and GBM. These structures, featuring a multi-branched polyglycerol core, combine a biocompatible polyether scaffold with a high potential for functionalization (Frey & Haag, 2002). One of the most promising modifications of dPGs is the addition of anionic sulfate groups (dPGS). Originally developed as a heparin analog, dPGS has demonstrated significant anticoagulant and anti-inflammatory properties (Dernedde et al., 2010; Silberreis et al., 2019; Türk et al., 2004). Conversely, large dPG functionalized with cationic amine groups (dPGA) has been found beneficial in supporting long-term neural cell cultures (Clément et al., 2022). We assessed the effects of dPGS and dPGA on the cell viability of microglia using MTT and LDH assays (**Figure 3.8**). Our findings indicate that dPGS neither reduced mitochondrial activity nor induced LDH release in microglia after 24 or 72 hours (**Figure 3.8A**). On the other hand, dPGA prompted LDH release in microglia at both time points (**Figure 3.8B**).

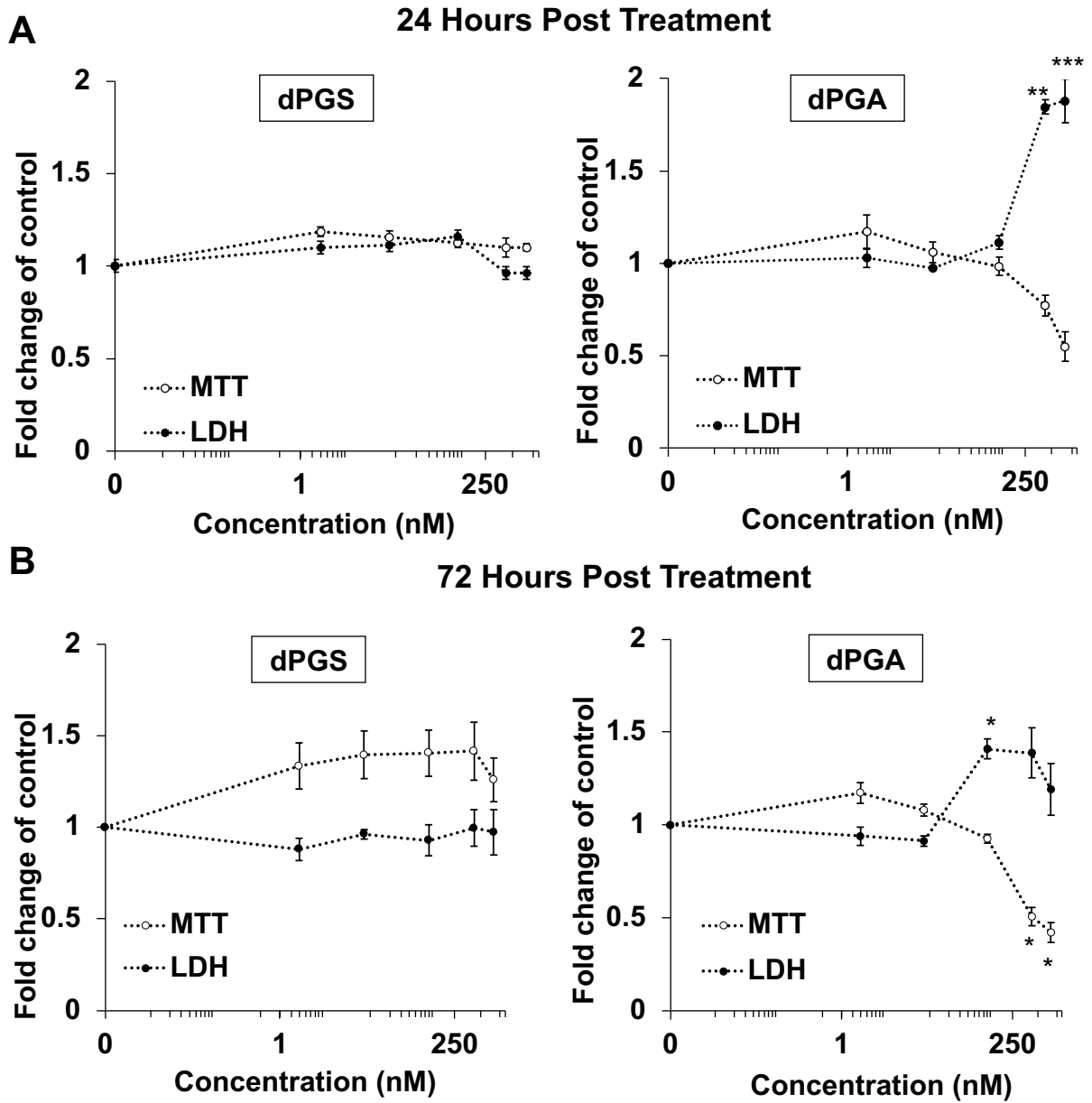


Figure 3.8. Cell viability of microglia in response to treatment with increasing concentrations of dPGS or dPGA (0, 1, 10, 100, 500, 1,000 nM) after **A**) 24h and **B**) 72h. Experiments were repeated three times, in triplicate. Mean \pm SEM. (* $p < 0.05$; ** $p < 0.01$; *** $p < 0.001$)

3.9 – Cytotoxicity of dendrimers in GBM

GBM cell viability was evaluated using the resazurin assay to measure metabolic activity as an indicator of cell health. Results revealed significant cell death in GBM cultures treated with 1 μ M of dPGA (**Figure 3.8A**), while dPGS did not affect cell viability. The toxicity of dPGA was further confirmed with continued observations over 72 hours, where even lower concentrations (100 nM) proved lethal to GBM cells (**Figure 3.9B**). Expanding on these findings, further tests were conducted on GBM tumoroids, a model that closely resembles *in vivo* conditions due to its three-dimensional structure and enhanced drug resistance compared to traditional monolayer cultures. dPGA treatment over a 10-day period resulted in a noticeable reduction in tumoroid size, consistent with the effects observed in monolayer cultures (**Figure 3.9C**). Moreover, significant sloughing from the peripheral and proliferative layers of the tumoroids indicated a profound impact on tumor integrity and cell viability in this complex model. However, the effect of dPGA on size reduction appears less dramatic compared to its early cytotoxicity, likely because the residual viable cells post-treatment may recover partially over time. This partial recovery could indicate a rebound phenomenon or an adaptive response of surviving cells to the treatment, which warrants further investigation. Interestingly, although dPGS was non-toxic in monolayer cultures after 72 hours, a decrease in GBM tumor size was observed after 10 days, suggesting some delayed effects on tumor dynamics. dPGS appears to impair pathways related to extracellular matrix interactions and cell motility, which could explain its delayed effect over the 10-day period. This behavior contrasts with dPGA's immediate cytotoxicity and suggests distinct mechanisms of action between the two dendrimers.

Glioblastoma Viability Post-dPG Treatment

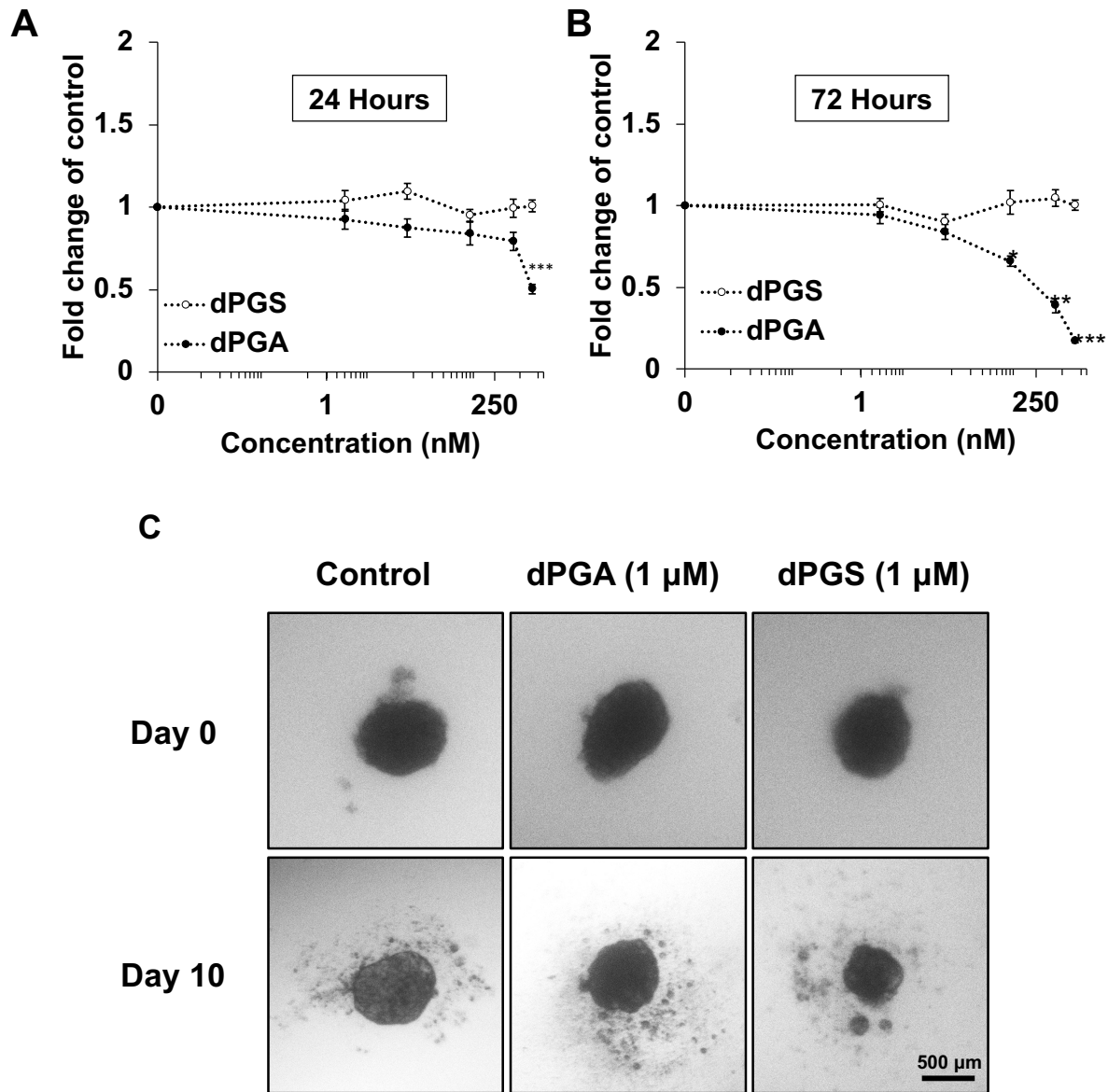


Figure 3.9. Cell viability of GBM cells in response to treatment with increasing concentrations of dPGS or dPGA (0, 1, 10, 100, 500, 1,000 nM). GBM cell viability measured with the resazurin assay after **A**) 24h and **B**) 72h. Experiments were repeated three times, in triplicate. Mean \pm SEM. (* $p < 0.05$; ** $p < 0.01$; *** $p < 0.001$). **C**) Representative micrographs of GBM tumoroids treated with dPGA or dPGS (1 μ M) on day 0 and day 10. Tumor size (area) was calculated using ImageJ.

3.10 – dPGA increases LAMP-2 abundance and lysosomal activity in GBM cells

Following the observed cytotoxic effects of dPGA on GBM cells, we sought to explore the underlying mechanisms of cell death, with a particular focus on the role of lysosomes. We used ICC to examine lysosomal abundance in GBM cells, using LAMP-2 as a marker after 24 hours of treatment with either dPGS or dPGA (1 μ M) (**Figure 3.10**). The cells treated with dPGA displayed pyknotic nuclei and signs of apoptosis, as evidenced by the morphological changes (**Figure 3.10B,C**). Moreover, many cells exhibited atypical morphologies, suggesting the activation of various cell death pathways. In depth cell death mechanisms are a part of ongoing studies. A marked increase in LAMP-2 fluorescence, alongside these distorted cellular forms, indicated that lysosomal dysfunction might be involved in the cytotoxic effects observed. To further evaluate lysosomal function, we analyzed cathepsin B activity, a key lysosomal protease. After 24 hours of treatment with either dPGS or dPGA, there were distinctive effects on cathepsin B activity. dPGS treatment resulted in decreased cathepsin B activity, whereas dPGA treatment significantly increased this activity by 85% compared to untreated control (**Figure 3.10D,E**). These results suggest that GBM cells attempt to rescue themselves from dPGA treatment by degrading proteins and lipids to provide energy for survival.

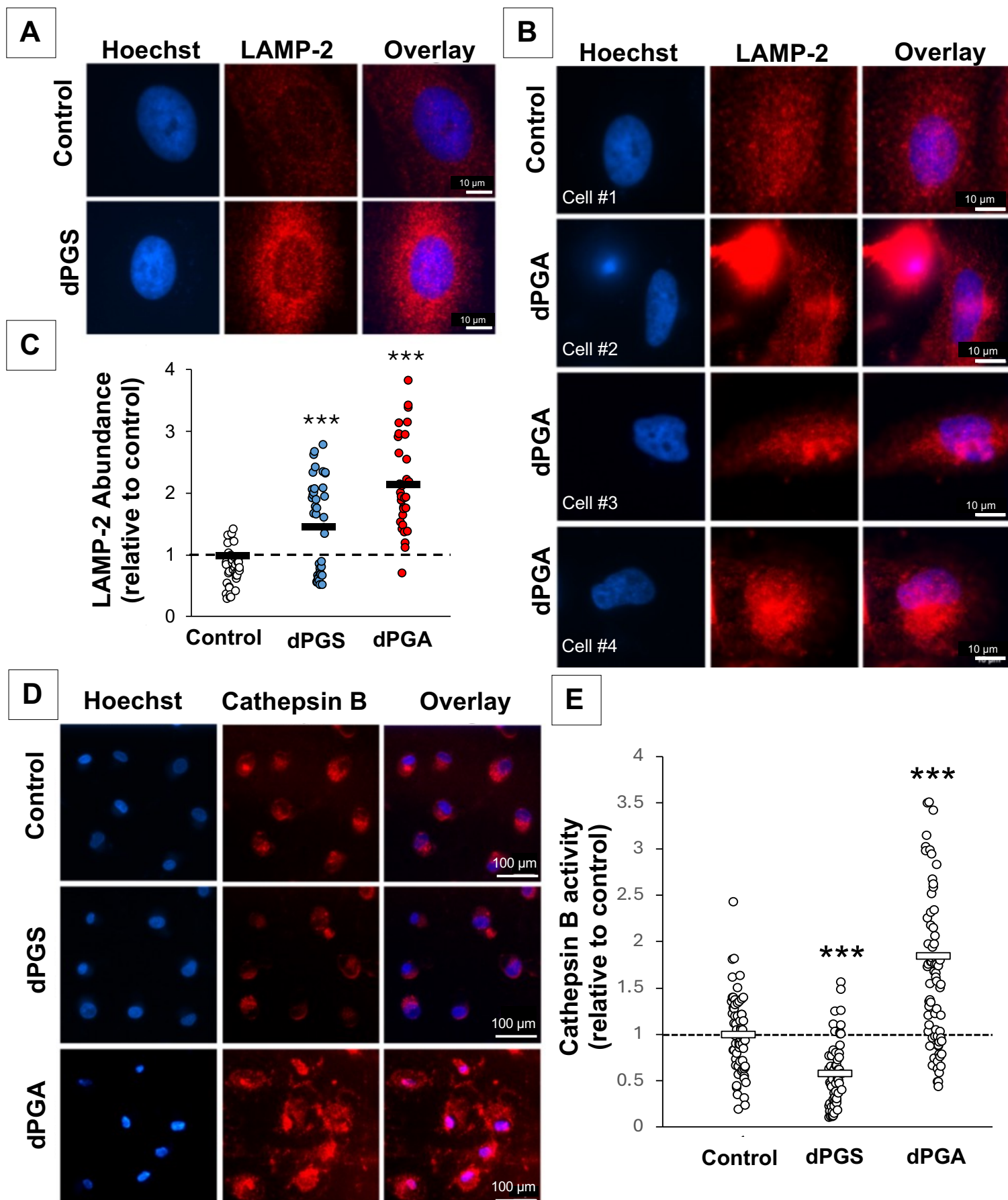


Figure 3.10. LAMP-2 abundance and cathepsin B activity in GBM cells after 24h. Lysosomal abundance in GBM cells after 24h treatment with **A)** 1 μ M dPGS or **B)** 1 μ M dPGA. Cells were labeled for LAMP-2 (red) with rat anti-LAMP2 (1/200) and imaged via fluorescence microscopy. Nuclei were labeled with Hoechst 33342 (blue). Scale bar: 10 μ m. **C)** Shown are the normalized fluorescence intensity values to the mean of the untreated control \pm SEM. At least 30 cells from three different experiments were analyzed. (** $p < 0.001$). **D)** GBM cells were treated with 1 μ M dPGS or dPGA for 24 hours, followed by measuring cathepsin B (red) with Magic Red™ and imaged via fluorescence microscopy. Nuclei were labeled with Hoechst 33342 (blue). Scale bar: 100 μ m. **E)** Shown are the normalized fluorescence intensity values to the mean of the untreated control \pm SEM. At least 77 cells from three different experiments were analyzed. (** $p < 0.001$).

3.11 – dPGA decreases lipid droplet abundance in GBM cells

Given that lysosomal abundance and activity were affected by dPGA, we examined the effect of dPGS and dPGA (1 μ M) on LD abundance in GBM cells using BODIPY 493/503 staining. Our findings showed that dPGA decreased LD abundance by 38% compared to the control, whereas dPGS showed no significant difference (**Figure 3.11**).

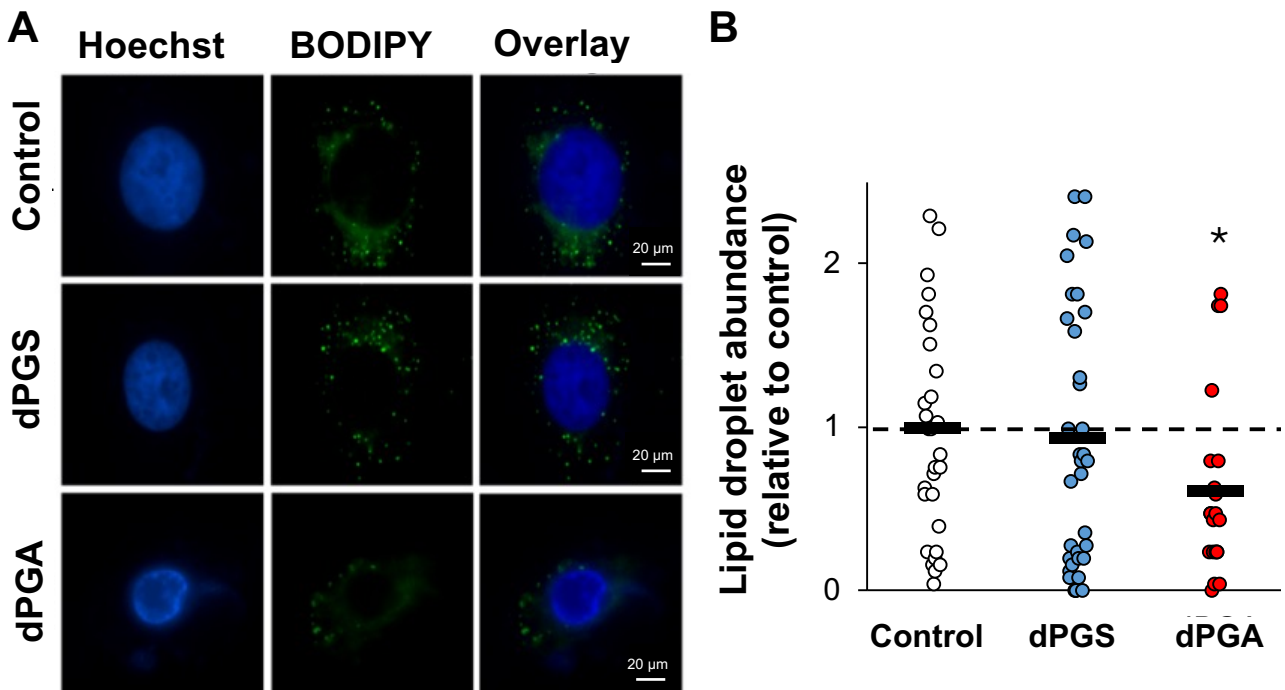


Figure 3.11. dPGA decreases LD abundance in GBM cells after 24h. Lipid droplet abundance in GBM cells after 24h treatment with 1 μ M dPGA or dPGA. **A)** Cells were stained with BODIPY 493/503 (green) and imaged via fluorescence microscopy. Nuclei were labeled with Hoechst 33342 (blue). Scale bar: 20 μ m. **B)** Shown are the normalized fluorescence intensity values to the mean of the untreated control \pm SEM. At least 21 cells from three individual experiments were analyzed. (* $p < 0.05$).

3.12 – dPGA increases lysosomal pH in GBM cells

Given the differing charges of dPGS and dPGA, with dPGS being negatively charged and dPGA being positively charged, potentially impacting lysosomal pH, we utilized a pH-sensitive probe called SNAFL to investigate these effects. The probe, which increases in green fluorescence as pH rises, allowed us to monitor pH changes within the cellular environment. Our results revealed an increase in green fluorescence in GBM treated with dPGA compared to both dPGS and the control, suggesting that dPGA causes an increase in lysosomal pH (**Figure 3.12**). Furthermore, colocalization studies verified that the pH-sensitive probe was localized within the lysosomes, confirming that the observed pH changes were specific to these organelles. While these findings appear contradictory to the lysosomal activity data—where an increase in cathepsin B activity was noted following dPGA treatment—it is crucial to recognize that we only tested one cathepsin. Other enzymes might be more responsive to the alkaline shift induced by dPGA.

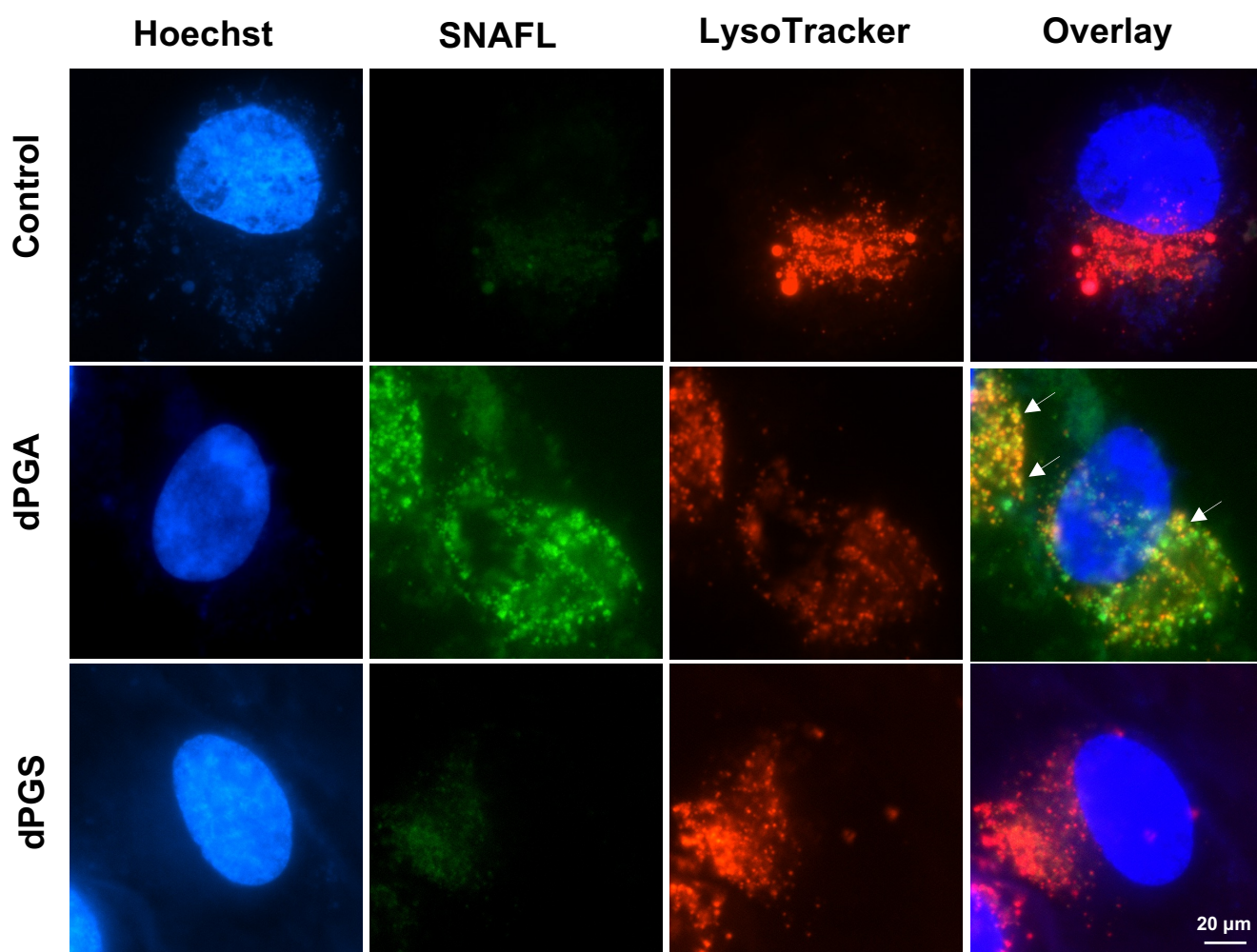


Figure 3.12. Detection of SNAFL in GBM cells treated with dPGA or dPGS (100 nM). SNAFL was prepared by Laura McKay from the Chemistry department at McGill University. SNAFL (1.5 μ M) and LysoTracker Red (50 nM) were added 30 minutes prior to imaging and was detected using fluorescent live imaging (GFP green and CY5 red); nuclei were labelled with Hoechst 33342 (blue). White arrows indicate co-localization of encapsulated SNAFL and lysosomes.

3.13 – dPGA decreases lysosomal biomarker (LysoTracker) in microglia, but does not affect lysosomal activity

Following our observations on lysosomal dynamics in GBM cells, we extended our investigation to microglia, which are the predominant macrophages of the CNS and constitute 30-40% of the cellular makeup in the TME. Utilizing LysoTracker dyes, which are specific for labeling acidic organelles in live cells, we assessed the impact of both dPGS and dPGA on lysosomal abundance in microglia (**Figure 3.13**). Our results indicated a noticeable decrease in LysoTracker staining, suggesting either a reduction in lysosomal activity or a decrease in the number of lysosomes (**Figure 3.13A,B**). This reduction in fluorescence could also imply changes in lysosomal pH or a compromise in lysosomal integrity, reflecting altered functional states of these critical organelles in the microglia. Interestingly, while LAMP-2 levels decreased, dPGS led to an increase in cathepsin B activity, unlike dPGA, which had no significant effect (**Figure 3.13C,D**). This response contrasts with what was observed in GBM cells, underscoring a possible cell type-specific reaction to these nanostructures.

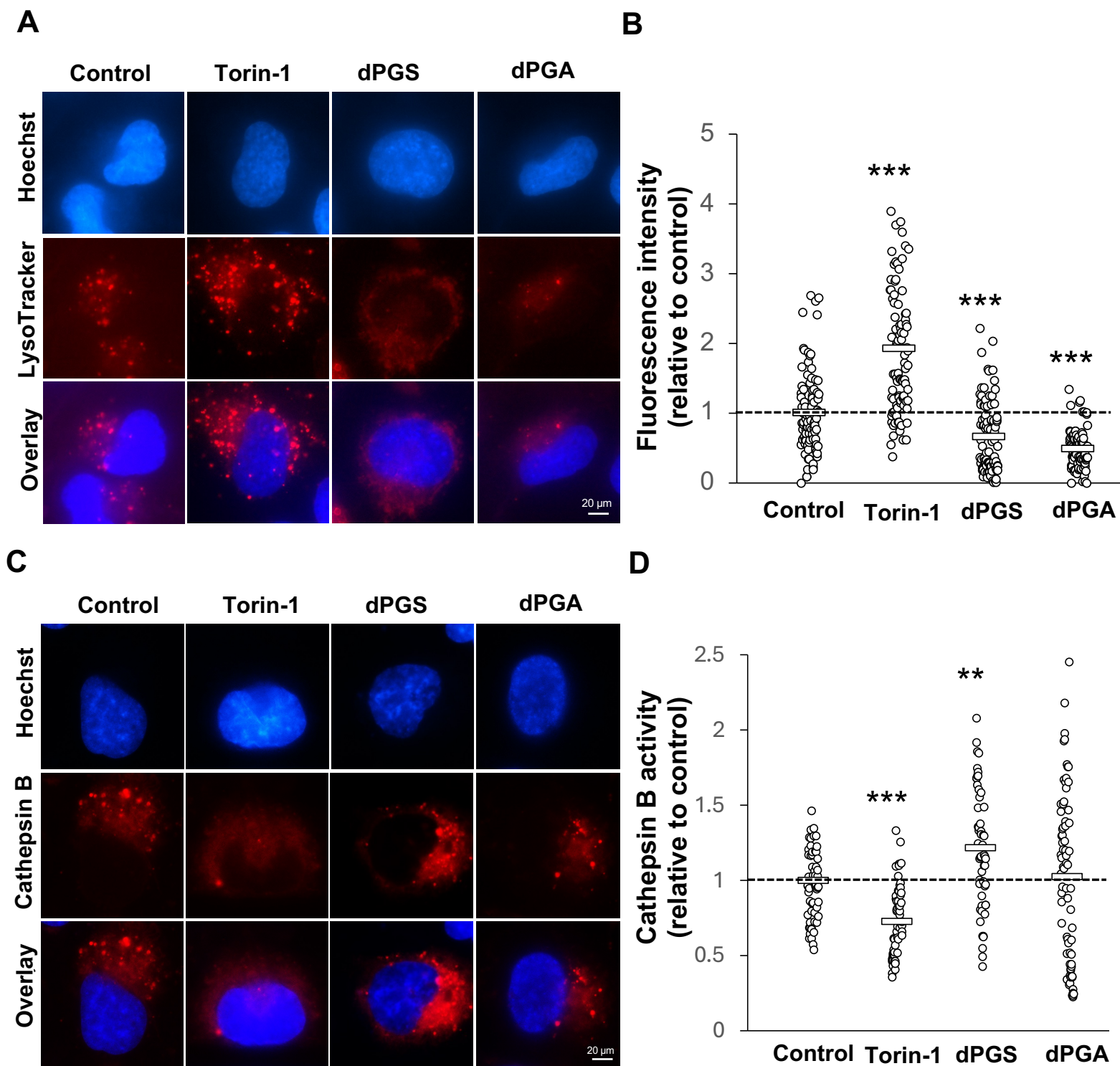


Figure 3.13. LysoTracker and cathepsin B activity in microglia treated with dPGS or dPGA. Microglia were treated with dPGS or dPGA (0.1 μ M) for 24h. Torin-1 (250 nM) served as positive control. LysoTracker Red (50 nM) was added 30 minutes prior to imaging and was detected using fluorescent live imaging (CY3 red); nuclei were labelled with Hoechst 33342 (blue). **A**) Shown are representative fluorescence micrographs of cells labelled for lysotracker (red) and nuclei (blue). **B**) Shown are dot plots of nuclear to

cytosolic TFEB ratio per cell, as fold change of the control (set to 1) from at least 50 cells. $**p < 0.01$. **C)** Cathepsin B (red) with Magic Red™ was measured in microglia via fluorescence microscopy. Nuclei were labeled with Hoechst 33342 (blue). Scale bar: 20 μ m. **D)** Shown are the normalized fluorescence intensity values to the mean of the untreated control \pm SEM. At least 77 cells from three different experiments were analyzed. ($***p < 0.001$).

3.14 – dPGS, but not dPGA, increases TFEB abundance in human microglia

Given that dPGS affects lysosomal activity, we next looked at TFEB, a critical transcription factor involved in regulating lysosomal biogenesis and autophagy. Our results demonstrated that dPGS, but not dPGA, significantly increases TFEB abundance in microglia (**Figure 3.14**). This observation correlates with the increase in cathepsin B activity in microglia following dPGS treatment. Moreover, dPGS may promote the shuttling of TFEB between the nucleus to the cytosol. Such translocation can indicate a shift in TFEB's activity, where it regulates lysosomal biogenesis and autophagy-related genes. This could imply a modulation of TFEB's transcriptional activity, potentially affecting the microglial response to stressful stimuli or inflammation.

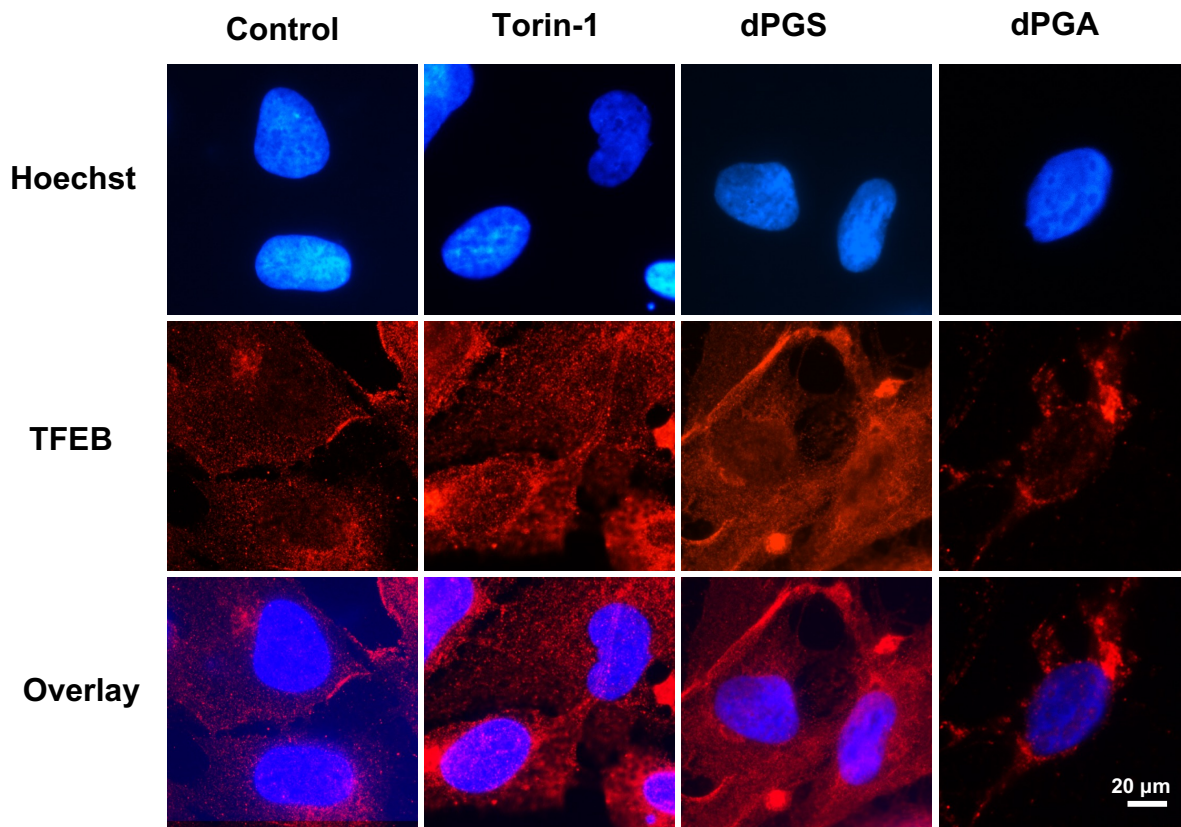
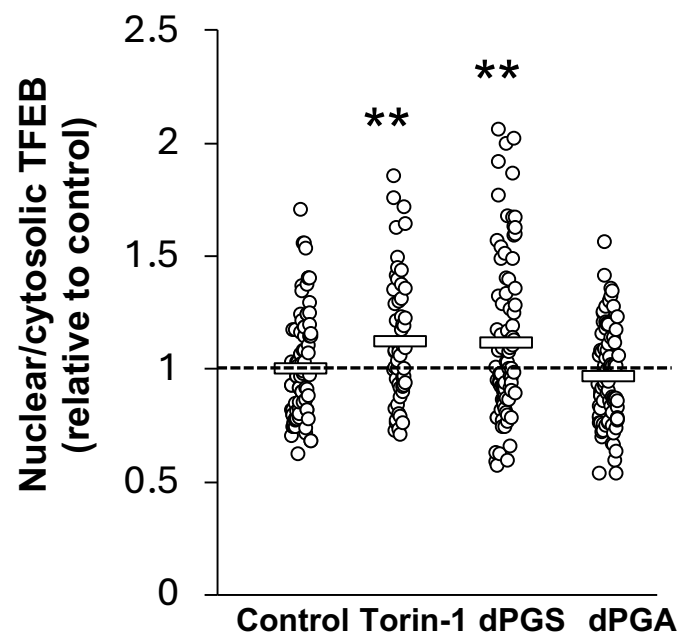
A**B**

Figure 3.14. dPGS, but not dPGA, increases TFEB abundance in human microglia. Microglia treated with dPGS or dPGA (0.1 μ M) for 24h were assessed by immunocytochemistry. Torin-1 (250 nM) served as positive control. **A)** Shown are representative fluorescence micrographs of cells labelled for TFEB (red) and nuclei (blue). **B)** Shown are dot plots of nuclear to cytosolic TFEB ratio per cell, as fold change of the control (set to 1) from at least 50 cells. **p<0.01

CHAPTER 4 – DISCUSSION

The goals of this thesis are as follows:

1. To present and interpret novel data on glioblastoma (GBM) treatment using polyphenols, starting from monolayer cultures, and progressing to 3D models (tumoroids). These models were employed to evaluate both single and combination therapies, highlighting the role of various signal transduction pathways. The study specifically focused on redox-sensitive transcription factors, including HMGB1, HSP72, and TFEB.
2. To demonstrate how cells within the GBM microenvironment, particularly microglia, can be modulated to reduce the harmful effects of neuroinflammation, emphasizing the roles of lysosomes and lipid droplets.
3. To investigate the use of nanostructures, especially dendrimers with sulfate and amino groups, within the tumor microenvironment (TME), focusing on the responsiveness of microglia.

4.1 – Polyphenols cytotoxicity and redox-imbalance in TME

The first step in evaluating the effectiveness of polyphenols as modulators of the TME was to establish the concentration and time-dependent effects on GBM cells and microglia.

GBM is a lethal brain tumor characterized by its aggressive growth and resistance to conventional treatments. A critical aspect of its malignancy is the redox imbalance within the TME (Olivier et al., 2021). This redox imbalance not only promotes tumor growth by causing DNA damage and genetic instability but also enhances the tumor's ability to invade surrounding tissues (Agrawal et al., 2023). The oxidative stress created by this imbalance contributes to the tumor's resilience against therapies, highlighting the need for innovative approaches to restore redox equilibrium as part of comprehensive cancer therapy.

Microglia, the resident immune cells of the central nervous system (CNS), play a complex and often paradoxical role in the TME (Muzio et al., 2021). Microglia can be activated by various cytokines and chemokines released by GBM cells, adopting a pro-

tumoral phenotype characterized by the release of growth factors, cytokines, and enzymes that facilitate tumor invasion and angiogenesis (Nusraty et al., 2024). For instance, microglia secrete matrix metalloproteinases (MMPs) that degrade the extracellular matrix, aiding tumor cell migration. Additionally, they produce pro-inflammatory cytokines like IL-6 and TNF- α , which can create a supportive niche for tumor growth and protect tumor cells from immune surveillance (Pallarés-Moratalla & Bergers, 2024).

To establish the concentration-dependent effect of fisetin, we used a human HMC3 microglia cell line and a human U251N GBM cell line. Cells were treated with increasing concentrations of fisetin or quercetin (as a positive control) (0-100 μ M for 24 h). Lactate dehydrogenase release (LDH) and mitochondrial metabolic activity were measured. Results suggested that neither fisetin nor quercetin displayed cytotoxic effects in microglia; however, GBM cells showed greater sensitivity to fisetin and quercetin, exhibiting pronounced concentration-dependent decreases in mitochondrial metabolic activity and significantly higher LDH release (**Figure 3.1**).

While temozolomide (TMZ) is commonly used to treat GBM and astrocytoma, patients often develop resistance to it. Combining TMZ with other therapeutic agents may help overcome this resistance. Therefore, we explored the potential synergistic effects of fisetin when combined with TMZ. Due to the lack of robust and representative *in vivo* models that accurately mimic the complexity and heterogeneity of GBM, we prepared tumoroids using the hanging drop method (Del Duca et al., 2004). These three-dimensional cultures offer a more physiologically relevant environment compared to traditional two-dimensional cell cultures, better replicating the cellular interactions and microenvironments of actual tumors. Numerous studies have employed various types of 3D cultures to model GBM. Notably, Tatla et al., 2021 reported a disease-relevant, vascularized tumoroid *in vitro* model with stem-like features and stromal surrounds. This model aims to recapitulate GBM's complex microenvironment, including elements such as hypoxia, vasculature-related stromal cells, and growth factors that support angiogenesis. An overview of 3D human GBM models has been summarized by Wang et al., 2023. Our results showed that the combination of fisetin and TMZ reduced tumoroid

area more effectively than either treatment alone (**Figure 3.2**), demonstrating a synergistic effect with a combination index (CI) of less than 1. TMZ is one of the few clinically approved drugs for GBM treatment, yet a substantial portion of both newly diagnosed and recurrent tumors are resistant to it (Singh et al., 2021; Teraiya et al., 2023). Given the limited effectiveness of monotherapies in GBM, we previously tested sahaquine, an HDAC inhibitor, in combination with TMZ in 3D tumoroids, which resulted in reduced cell migration and invasion compared to either treatment alone (I. Zhang et al., 2018).

4.2 – Polyphenols as modulators of oxidative stress

Polyphenols, known for their antioxidant properties, are particularly intriguing in the context of GBM treatment. Polyphenols can modulate redox imbalance by directly scavenging free radicals and enhancing the body's own antioxidant defense mechanisms (Rudrapal et al., 2022). Their ability to influence key molecules involved in the oxidative stress response, such as Nrf2, makes them potent agents in restoring redox homeostasis (Sharifi-Rad et al., 2023). Fisetin, a dietary flavonoid commonly found in various fruits and vegetables, has gained attention for its antioxidant properties and its potential to mitigate a wide range of serious diseases, including cancer, neurodegeneration, and age-related disease (Y. Chen et al., 2015; Gryniewicz & Demchuk, 2019; Jia et al., 2019; Kumar et al., 2023; Mahoney et al., 2023; Nabizadeh et al., 2023; Sandireddy et al., 2016).

The anticancer properties of fisetin are mediated by its ability to affect different signaling pathways in various cellular types, as summarized in **Figure 4.1**. For example, Murtaza et al. showed that fisetin inhibits the growth of pancreatic cancer AsPC-1 cells by downregulating NF- κ B signaling (Murtaza et al., 2009). In prostate and colon cancer, fisetin activates distinct pathways to promote apoptosis (Khan et al., 2008; J. A. Kim et al., 2015). A recent study by Wang et al. developed a microenvironment-responsive nano-drug delivery system that sensitizes glioma to doxorubicin with fisetin (W. Wang et al., 2024). Our study showed that fisetin reduced oxidative stress in both non-cancerous (microglia) and cancerous (GBM) cells (**Figure 3.3**). Due to its hydrophobic nature, fisetin can penetrate and accumulate within cell membranes, where it exhibits antioxidant and anti-

inflammatory properties (W. Wang et al., 2024). Currently, fisetin is being investigated in multiple clinical trials for various cancers and age-related conditions, including osteoarthritis, coronavirus infections, frail elderly syndrome, and chronic kidney diseases (Chaib et al., 2022).

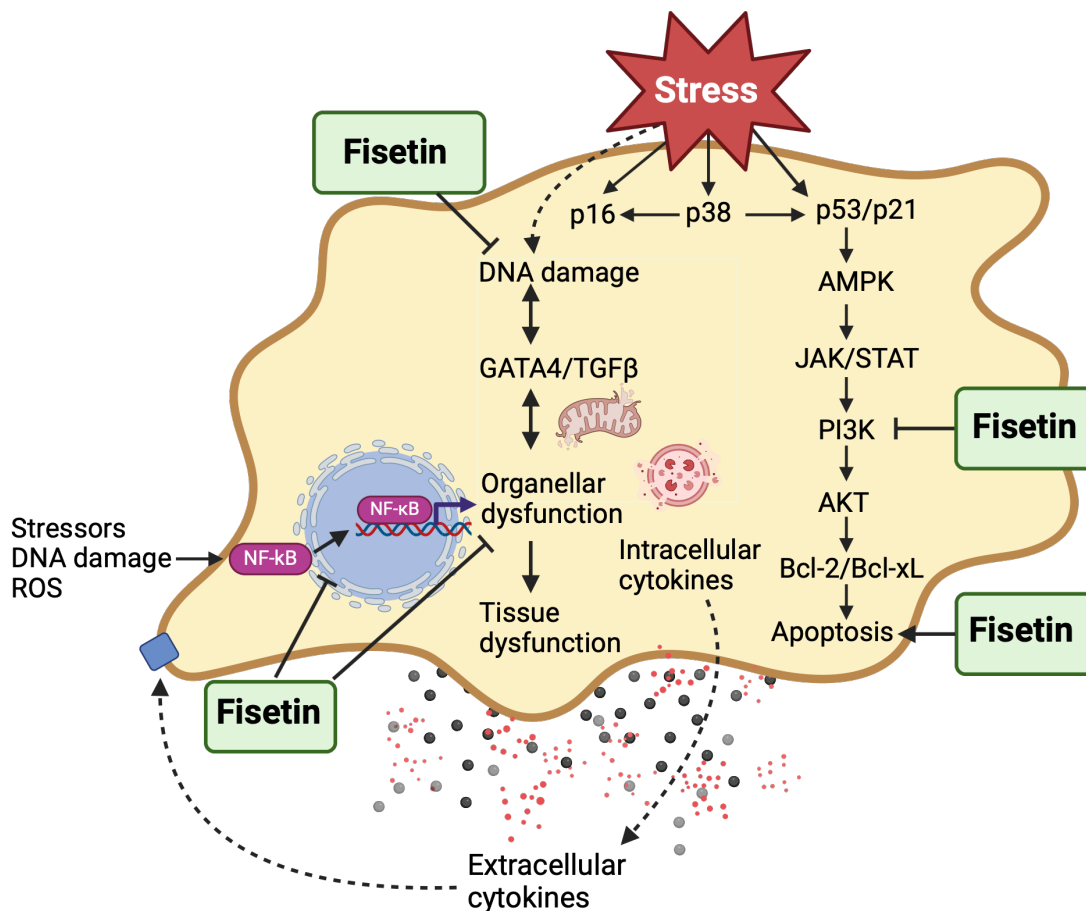


Figure 4.1. A simplified presentation of the mechanisms of action of fisetin. Created with ©BioRender (biorender.com). Figure adapted from (Joma et al., 2024).

4.3 – Modulation of AcHMGB1 and its interactions with binding partner HSP72

Central to the disruption of antioxidant mechanisms in GBM are key redox-responsive transcription factors, including TFEB, HSP72, and HMGB1 (F. Chen et al., 2024). HMGB1, a redox-sensitive protein, is released by GBM cells in response to cellular stress and damage. HMGB1 can be secreted to the extracellular space via active secretion or passive release by necrotic cells (Lv et al., 2024). Once outside, it can act as a paracrine factor and interact with receptors, particularly RAGE, thereby activating signaling pathways that regulate cell growth, differentiation, motility, and death (R. Chen et al., 2022). The interaction between HMGB1 and RAGE has been suggested to promote the proliferation and invasion of various tumor cells (A. Fan et al., 2024; Lai et al., 2021).

Post-translational modifications (PTMs), including acetylation, oxidation, and methylation, significantly influence HMGB1 function. Acetylation of HMGB1 (AcHMGB1), restricts its nuclear re-entry, facilitating its accumulation in the cytosol and eventual secretion (Andersson et al., 2021; Kwak et al., 2020). Interestingly, we found that fisetin did not affect AcHMGB1 abundance and translocation in GBM. However, fisetin reduced cytosolic AcHMGB1 levels in microglia (**Figure 3.4**). This suggests that fisetin modulates the release of AcHMGB1 in immune cells and, in turn, reduces the exacerbated inflammation in the TME. Bassi et al. showed that glioma cells contain HMGB1 predominantly in the nucleus and cannot secrete it constitutively or upon stimulation. However, necrotic glioma cells can release HMGB1 after it has translocated from the nucleus to the cytosol (Bassi et al., 2008). These findings suggest that HMGB1 is acting as an autocrine factor that promotes the growth and migration of tumor cells.

Several studies have suggested a potential interaction between HMGB1 and heat shock protein 72 (HSP72), a chaperone crucial for mitigating effects of oxidation, inflammation, and other stressors (Bassi et al., 2008; Bielawski et al., 2024; Campisi et al., 2003; Fujii et al., 2021). Using proximity ligation assays (PLA), we examined the interactions between HMGB1 and HSP72 in microglia and GBM cells. Fisetin significantly enhanced the interaction between HMGB1-HSP72 in GBM, but not in microglia (**Figure 4.2**). Enhanced HMGB1-HSP72 interactions by fisetin could increase HSP72's protective role and reduce HMGB1 release in GBM. Nevertheless, confirming these effects would require further experimental validation.

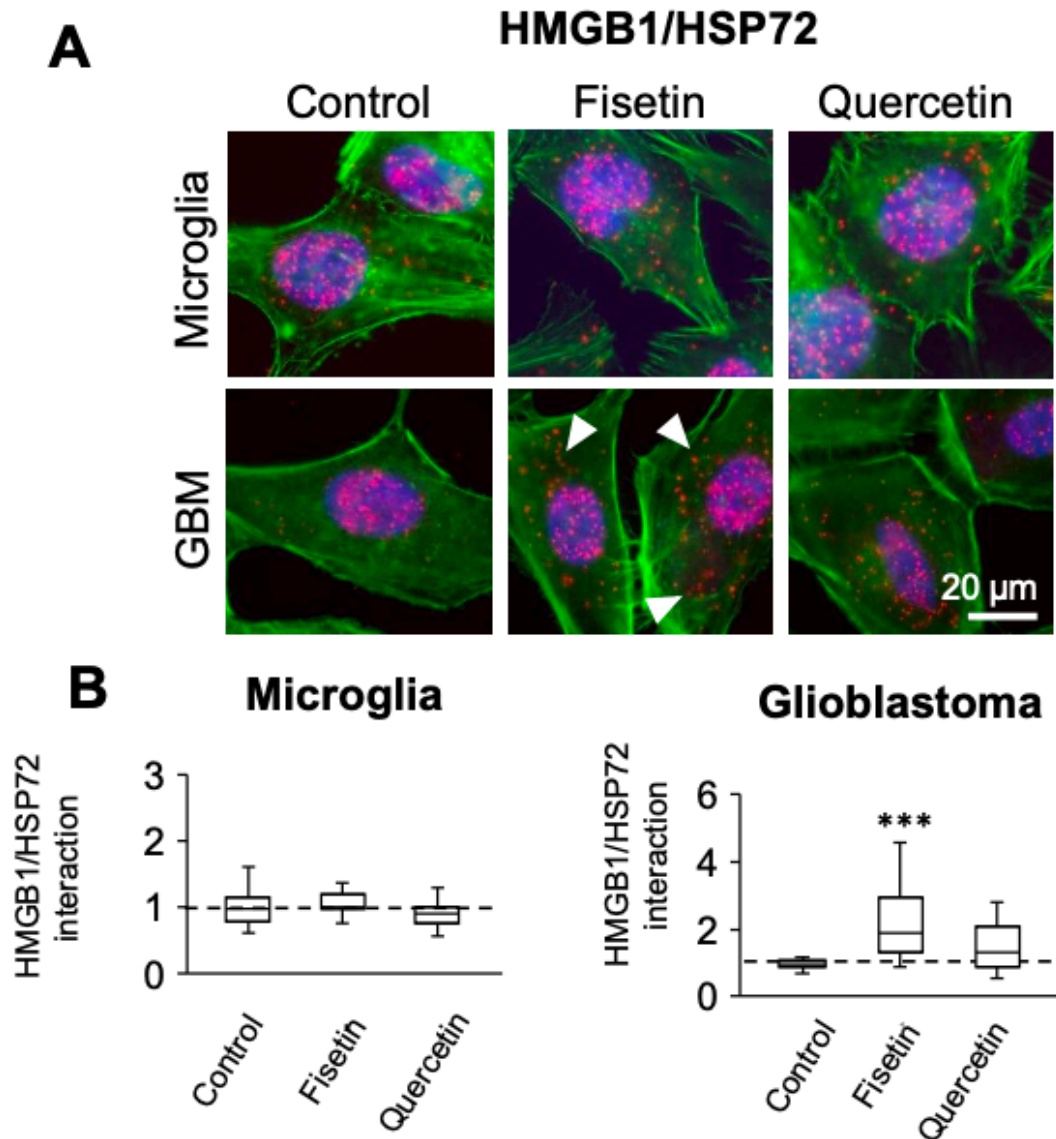


Figure 4.2. Interactions between HMGB1/HSP72 in microglia and glioblastoma treated with fisetin (25 μ M) or quercetin (25 μ M) for 24 h in serum-deprived media. Shown are representative fluorescence micrographs with protein interactions (red dots) in cells labeled for actin (green) and nuclei (blue). The arrowheads indicate protein–protein interactions. Shown are the distribution of the number of interactions per cell as fold change in the untreated control (set to 1), with the minimum value, 25th to 75th percentiles, and maximum values indicated. Box blots show the median, 25–75% quartiles, minimum and maximum values. Dotted line represents the mean of the control normalized to 1. At least 60 cells from three independent experiments were analyzed. (** $p < 0.01$; *** $p < 0.001$). Experiments conducted by Dr. Issan Zhang and figure was adapted from (Joma et al., 2023).

Many natural compounds, such as fisetin, can target multiple molecular pathways, making them valuable candidates for cancer therapy. However, the specific molecular interactions between cellular proteins and neuroprotective polyphenols are not well understood. Previous *in silico* analysis indicated that fisetin binds to biologically relevant sites on key proteins such as KEAP1, HSP72, and HMGB1 (Joma et al., 2023).

Molecular modeling revealed that fisetin has the greatest number of contacting residues with HSP72, deeply embedding into its binding pocket and engaging at least three key residues essential for ATP binding and other molecular interactions (**Figure 4.3**). Given that the HSP72 family responds to cellular stress in both normal and cancerous cells and can interact with other stress-responsive proteins like HMGB1, modulation of the HMGB1-HSP72 pathway by fisetin is clinically significant (D. Tang et al., 2007; K. Zhao et al., 2023). These interactions are particularly relevant for therapeutic strategies, as the HSP70 family has been linked to drug resistance in various cancers (Hermisson et al., 2000; Iglesia et al., 2019; Sha et al., 2023).

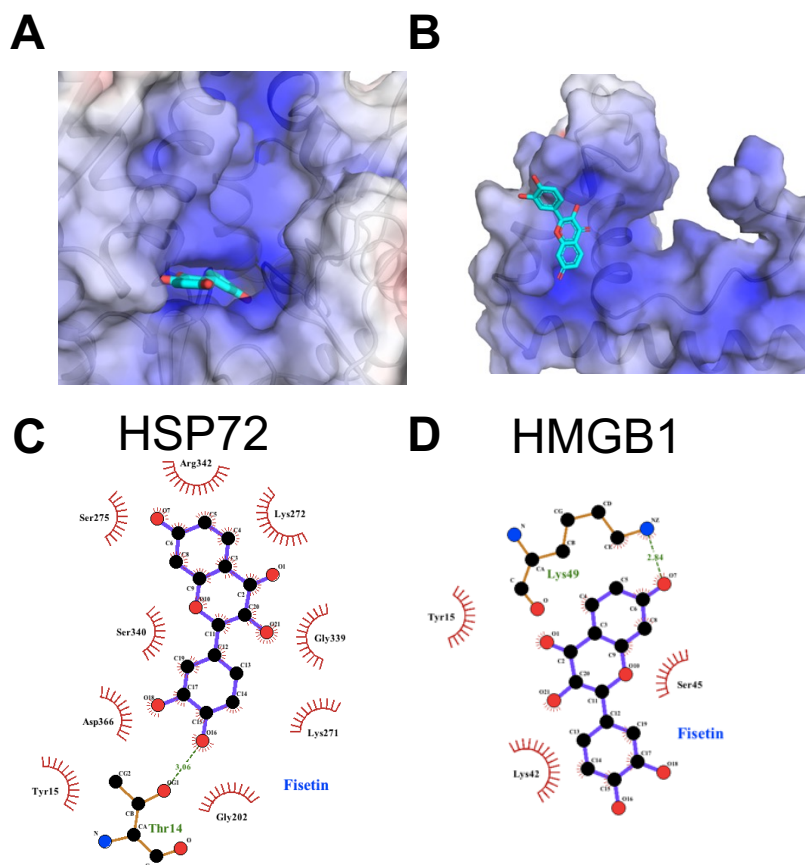


Figure 4.3. Docking analyses of fisetin binding to target proteins. (A-B) 3D representation of fisetin binding to the protein structures of HSP72 (PDB ID: 5BN9) and HMGB1 (PDB ID: 1AAB). Proteins surfaces are colored based on atoms electrostatic potential, shown in a scale of of -10 (red) kT/e to 10 (blue) kT/e . Fisetin is represented as stick and colored in cyan. A cartoon representation of each protein, overlayed with their surface representation, is shown in dark grey. (C-D) 2D representation of the contacting residues and interaction strength of fisetin (purple) interaction with HSP72 and HMGB1. Hydrogen bonds are represented as green dashed lines and connect the ligand to the respective contacting protein residue (orange). Protein residues performing hydrophobic contacts are displayed as red arcs. The crystal structures of HSP72 (PDB ID: 5BN9) and HMGB1 (PDB ID: 1AAB) were used for the binding analysis using LigPlot+. Modeling done by Germanna L. Righetto and figure adapted from (Joma et al., 2023).

4.5 – TFEB: A key regulator in lysosomal function and lipid droplet metabolism

Transcription factor EB (TFEB) serves as a central regulator of autophagy and lysosomal function (Martina & Puertollano, 2016b). Normally, TFEB resides in the cytosol in its phosphorylated form; however, under stress, it undergoes dephosphorylation and translocates to the nucleus. There, it activates gene expression that drives lysosomal biogenesis (Napolitano & Ballabio, 2016). Beyond its role in cellular homeostasis, TFEB is implicated in various pathological conditions, including cancer and inflammatory diseases (Brady et al., 2018; Tan et al., 2022). In lung cancers, TFEB overexpression correlates with increased cell migration and poor prognosis, promoting tumorigenesis, angiogenesis, and metastasis by enhancing lysosomal enzyme activity and the secretion of hydrolases into the extracellular space. Conversely, TFEB depletion hampers cancer cell migration (Magini et al., 2017).

In GBM, TFEB is notably overexpressed in both cell lines and patient samples, where it binds to gene promoters and regulates the expression of lysosomal genes as well as target genes involved in apoptosis and tumorigenesis. Co-treatment with vorinostat and melatonin has been shown to reduce both nuclear localization and oligomerization of TFEB, thereby inhibiting GBM tumorigenesis and tumor-sphere formation by glioma stem cells (GSCs) (Sung et al., 2019).

4.5.1 – Lysosomes

Fisetin induced a transient increase in the nuclear accumulation of TFEB in microglia, though this increase was less pronounced in GBM cells (**Figure 3.5**). This effect could potentially lead to enhanced lysosomal biogenesis and enzyme activity in microglia. To test this model, we measured the abundance of lysosomes by labeling LAMP-2, a marker of lysosomes and late endosomes. Incubation of HMC3 and U251N cells with 25 μ M fisetin resulted in a significant increase in LAMP-2 abundance in both microglia and GBM. However, LAMP-2 immunostaining alone does not reflect the functional state of lysosomes. We further assessed this by measuring the activity of cathepsin B, a lysosomal protease. The fisetin-induced changes in LAMP-2 (**Figure 3.6**) correlated with increased cathepsin B activity in microglia but not in GBM.

Our experiments focused on lysosomes due to their crucial role in cellular homeostasis. Lysosomes are particularly relevant in tumor biology for their ability to degrade damaged proteins and organelles (e.g. lipid droplets) via autophagy (S. Zhang et al., 2022). In the context of GBM and other tumor cells, autophagy can promote tumor growth while its inhibition may induce cancer cell death (Debnath et al., 2023; Kenific & Debnath, 2015; Meena & Jha, 2024; Mulcahy Levy & Thorburn, 2020; T. Tang et al., 2023). The role of autophagy in cancer is still not quite understood as it depends on the type of cancer. For example, fisetin has been shown to trigger autophagy in prostate cancer and melanoma cells (Suh et al., 2010; Syed et al., 2014). Jia et al. showed that a high concentration of fisetin (200 μ M) reduces viability of PANC-1 cells through apoptosis and autophagy, via activating the AMPK/mTOR pathway (Jia et al., 2019).

4.5.2 – Lipid droplets

Lipid droplets (LDs) are versatile organelles that, depending on the cell type, context, and location, can either protect or harm cells, particularly in neurodegenerative diseases (Olzmann & Carvalho, 2019). Peroxidized lipids released from LDs can be especially damaging. In aggressive tumors, such as GBM and breast cancer, LDs not only supply energy to support cancer cell survival but also sequester lipophilic anticancer drugs, thereby enhancing treatment resistance (Xiao et al., 2024; Yee et al., 2020). As previously explored by our group, LDs in GBM sequester lipophilic agents like curcumin, thereby altering their pharmacokinetic and pharmacodynamic profiles (I. Zhang et al., 2016). Findings from that study show that inhibiting LDs enhances the cytotoxic effects of curcumin in GBM. Pyrrolidine-2, an inhibitor of cytoplasmic phospholipase A2 (cPLA2), has been particularly effective as a pharmacological agent, highlighting the essential role of LDs in supporting GBM cell function.

Although GBM cells inherently contain a high number of LDs, fisetin treatment has been observed to unexpectedly increase their quantity (**Figure 3.7**). However, the impact largely depends on the specific types of LDs that are accumulating, which underscores the need for lipidomic analyses to further characterize these lipids. Additionally, lipidomic profiling will be employed to characterize the composition of LDs and determine whether

they contain lipotoxic species that promote ferroptosis or signaling lipids that support tumor survival.

Considering that in the acidic tumor environment, peroxidation of polyunsaturated fatty acids can induce ferroptosis, a form of cell death (Dierge et al., 2021). Neutrophils associated with GBM can contribute to necrosis by inducing tumor cell ferroptosis through the transfer of myeloperoxidase-containing granules (Lu et al., 2024).

Ferroptosis, first described by Stockwell and colleagues (Dixon et al., 2012), is an iron-dependent cell death driven by the accumulation of lipid peroxides (LPOs), making it distinct from apoptosis and other forms of cell death (Stockwell, 2022). Recently, ferroptosis has become increasingly recognized as an important mechanism in the progression of multiple cancers, including GBM (K. Li et al., 2022; X. Li et al., 2024; Sun et al., 2022; Y. Zhang et al., 2021). Understanding how ferroptosis is triggered in GBM cells could provide critical insights for developing effective treatments that target GBM while sparing normal brain cells.

4.6 – Limitations of the study

4.6.1 – Polyphenols have poor aqueous solubility

Flavonoids have shown promising effects against various cancers, but their clinical application is limited by their low solubility, poor absorption, and rapid metabolism. To address these challenges, a wide range of nanocarriers have been designed to improve flavonoids' bioavailability (**Figure 4.4**). Both *in vitro* and *in vivo* studies have demonstrated that flavonoid nanoparticles can effectively target cancer cells such as A549 lung cancer cells, B16F10 melanoma cells, MCF-7 breast cancer cells, HepG2 liver cancer cells, and CT26 colorectal cancer cells (Dobrzynska et al., 2020). Various types of flavonoid nanocarriers are currently employed in cancer therapy, including polymeric nanoparticles (Prabhu et al., 2015), nanocapsules (Kothamasu et al., 2012), metallic nanoparticles such as gold (Jain et al., 2012), and solid lipid nanocarriers (Mu & Holm, 2018).

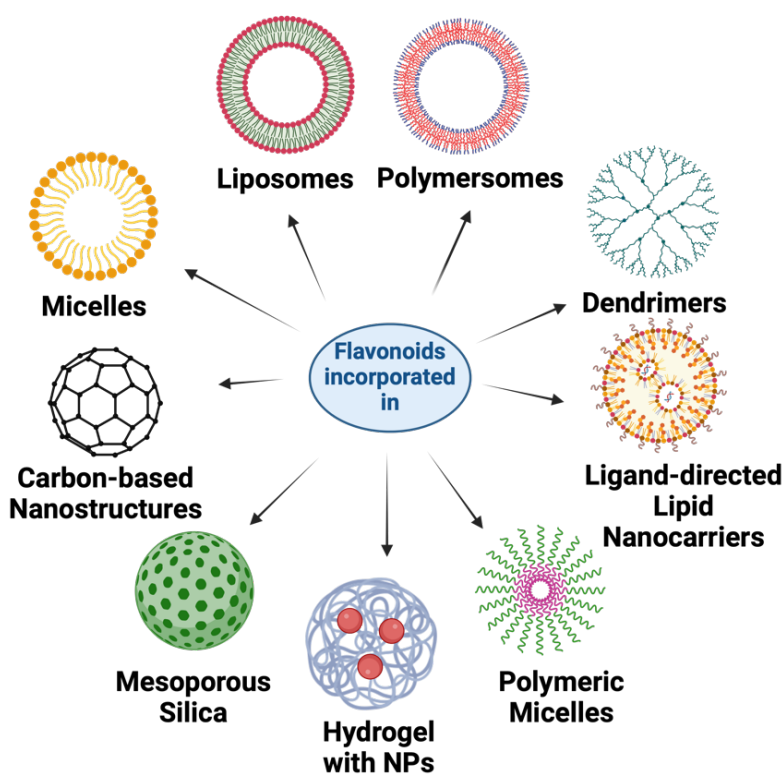
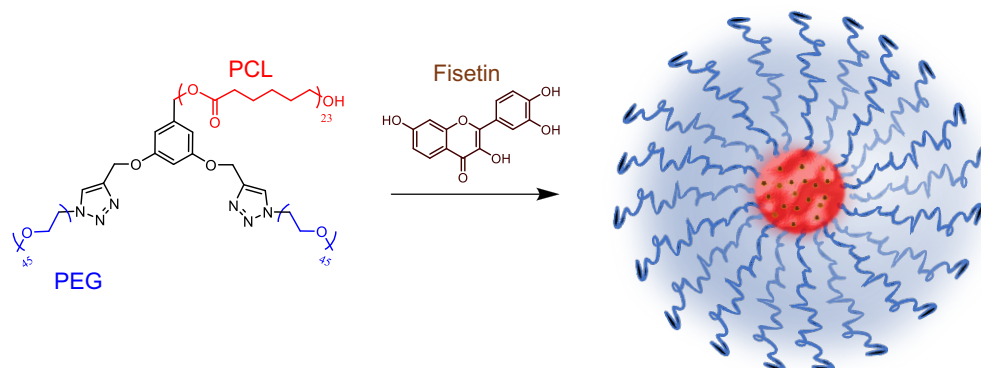


Figure 4.4. Nanocarriers developed for the delivery of flavonoids. Several nanocarriers have been developed for the delivery of natural polyphenols such as resveratrol, fisetin, and quercetin. Created with ©BioRender ([biorender.com](https://www.biorender.com)). Figure made by Patrick-Brian Bielawski and adapted from (Joma et al., 2024).

We proposed incorporating fisetin into polymeric soft nanoparticles with a hydrophobic core and a hydrophilic shell, enhancing the solubility and bioactivity of fisetin. This approach not only extends fisetin's half-life but also ensures a sustained release (**Figure 4.5**), while maintaining its biological activity. This nanodelivery system based on polyethylene glycol (PEG) and polycaprolactone (PCL) micelles is very suitable for incorporation of fisetin since its loading capacity is high, which is not commonly found in such a drug/polymer combination.

A**B**

| Fisetin Loaded Micelles | | | | | |
|--------------------------|-----------------------|------------------------|----------------|------|-------|
| Drug: Polymer Feed Ratio | Diameter ^c | \bar{D} ^d | Zeta Potential | EE | LC |
| 1:10 | 29.2 ± 1.6 nm | 0.174 ± 0.015 | -6.3 mV | 85 % | 7.8 % |

Figure 4.5. Fisetin-loaded nanoparticles. **(A)** Fisetin loading in nanoformulation based on a miktoarm star polymer with AB₂ composition (A = polycaprolactone and B = polyethylene glycol). **(B)** Characterization of fisetin-loaded micelles. EE= encapsulation efficiency; LC = loading capacity. Adapted from (Joma et al., 2023).

4.6.2 – Limitations of GBM and TME models

The U251N cell line, utilized in this thesis, originates from a 75-year-old Caucasian male. This cell line has played a pivotal role in brain tumor research, particularly in elucidating the molecular and cellular mechanisms of malignant gliomas. The HMC3 cell line was established through SV40 immortalization of primary microglia cultures derived from the brains of human male fetuses (Germelli et al., 2021). Patient variables such as sex and age significantly influence treatment responses. Studies indicate that women generally exhibit better responses than men, and younger patients respond better than older ones (Ostrom et al., 2018; Trifiletti et al., 2017; W. Yang et al., 2019). Future glioblastoma research, ranging from *in vitro* studies to clinical trials, should consider sex and age differences in the selection of cell lines and animal models.

Several *in vitro* and *in vivo* preclinical models have been developed to study GBM and the TME. Among these, 2D models are commonly used due to their ease of use and

maintenance. However, these models fall short of representing the three-dimensional complexity of the TME, including cellular components, and they lack a blood-brain barrier (BBB) (Trifiletti et al., 2017). An ideal TME model should not only accurately represent the diverse constituents of the human glioma microenvironment but also exhibit the plasticity and intratumoral heterogeneity of human gliomas. Furthermore, it should replicate the BBB function and facilitate cell-to-cell interactions, both tumor-tumor and tumor-nontumor cells (Osswald et al., 2015).

The complexity of GBM and its microenvironment cannot be studied in the monolayer culture but requires more sophisticated models, such as tumoroids (3D). Even a simple 3D models such as cellular aggregates or neurospheres offer a better representation of glioma and the TME, enabling studies on basic cell-cell interactions. Particularly, patient-derived glioma stem-like cell spheres genetically resemble human tumors more closely than attached cells do. These models allow preliminary studies of tumor cell secretions, responses to changes in nutrients, pH, and oxygen levels, and interactions between tumor and normal cells. However, they still do not fully represent the native TME because they lack a BBB (Chaicharoenaudomrung et al., 2020; Russell et al., 2017), as most organoids do not have a vasculature.

4.7 – Dendrimers as modulators of inflammation

Given the challenges posed by natural polyphenols, such as poor water solubility, the second part of this thesis explores the use of dendrimeric nanostructures. These structures are synthetic with high biocompatibility, potentially overcoming the limitations observed with natural polyphenols.

Dendritic polyglycerol sulfates (dPGS) were synthesized by sulfating dendritic polyglycerols (dPG), initially developed as synthetic alternatives to heparin. While heparin remains widely used as an anticoagulant, its derivation from animal sources raises concerns about pathogen contamination. Despite structural similarities to heparin, dPGS demonstrated significantly reduced anticoagulant effects, and its hydroxylated counterpart, dPG, exhibited none (Türk et al., 2004). dPGS effectively binds to P-selectin

on leukocytes, and studies have highlighted its potential as an anti-inflammatory nanostructure (Dernedde et al., 2010; Rades et al., 2018; Türk et al., 2004).

Our group has confirmed the anti-inflammatory properties of dPGS in various models, including mice and organotypic slice cultures. Notably, dPGS mitigated the increase of cytokines and alarmins such as IL-6, TNF- α , and lipocalin-2 triggered by LPS and amyloid- β . This resulted in diminished impairments in morphological plasticity of hippocampal excitatory neurons and a reduction in the loss of dendritic spines in the hippocampus (Maysinger et al., 2015, 2018, 2019).

4.8 – Dendrimers as drug delivery systems

In addition to its anti-inflammatory and anticoagulant properties, dPGS has been explored as a carrier for anticancer drugs. Studies indicate that dPGS is rapidly taken up by various cell lines, unlike its non-sulfated counterpart, dPG, which exhibits no uptake (Biffi et al., 2013; Gröger et al., 2013; Licha et al., 2011; Paulus et al., 2014). This has positioned dPGS as a promising platform for delivering anticancer drugs. Sousa-Herves et al. conjugated paclitaxel (PTX), a tubulin-binding anticancer drug, to dPGS and assessed the uptake and cytotoxicity in lung and epidermoid cancers (Sousa-Herves et al., 2015). They demonstrated that the dPGS-PTX combination was effectively absorbed by both cell types, resulting in cytotoxic effects from the released PTX. However, the conjugate displayed poor stability in plasma and at physiological pH, leading to premature drug release. This issue was addressed by Ferber et al., who replaced the previous acid-labile ester linkage with a pH-cleavable, more stable hydrazone bond (Ferber et al., 2017). They further evaluated this new conjugate's cell uptake and cytotoxicity in GBM cells, showing that the conjugate could bind to P-selectin, which is highly expressed on tumor cell membranes, facilitating uptake. The hydrazone linkage then allowed for effective PTX release within the GBM environment, significantly inhibiting tumor growth.

Dendrimers, highly branched, monodisperse macromolecules, offer a promising platform for targeted drug delivery in GBM treatment (Gaitsch et al., 2023). The unique architecture of dendrimers allows for the precise functionalization of their surface,

facilitating the controlled delivery of therapeutic agents directly to tumor cells while minimizing off-target effects. For instance, the glycosylation of polyamidoamine (PAMAM) dendrimers has been shown to improve their specificity for tumor-associated macrophages in the GBM microenvironment, thereby increasing therapeutic efficacy while reducing toxicity (R. Sharma et al., 2021). Moreover, dendrimers are carriers for various agents (e.g., chemotherapy, RNA molecules, imaging agents), positioning them as versatile tools in GBM treatment strategies (Knauer et al., 2023; Liu et al., 2022; Sahoo et al., 2022).

One of the critical challenges in treating GBM is the penetration of therapeutic agents through the BBB. Dendrimers, particularly those engineered for nano-scale interactions, have shown potential in crossing this barrier, thereby increasing the concentration of drugs available at the tumor site (Wadhwa et al., 2024). By modifying surface properties or employing multifunctional envelopes, dendrimers can navigate through the BBB more effectively, delivering drugs directly to brain tumors and reducing systemic side effects (Liaw et al., 2021).

4.9 – Dendrimers as therapeutic modulators

In addition to the negatively charged dPGS, we also explored dPG highly functionalized with cationic amine groups (dPGA), with net positively charged surface. Recent findings highlighted dPGA's beneficial role as a substrate in supporting long-term neural cell cultures (I. Zhang et al., 2016). We investigated the effects of both dPGS and dPGA on viability of microglia and GBM cells. Our results showed that dPGS did not impact microglia and GBM viability, while dPGA significantly reduced viability in both cell types (**Figures 3.8 and 3.9**). Notably, GBM cell death was observed at concentrations as low as 1 μ M dPGA, with similar trends noted in microglia. After 72 hours, dPGA was found to be toxic to GBM cells at even lower concentrations, starting from 100 nM. Given the non-specific toxic effects of dPGA on both cancerous and non-cancerous cells, we did not employ concentrations greater than 100 nM.

The differences in lysosomal changes, cathepsin B activity, and nuclear TFEB localization between GBM and microglia underscore the distinct cellular responses to dPGA treatment. Yet, dPGA reduces the viability of both cell lines (**microglia, Figure 3.8; GBM, Figure 3.9**) in a dose-dependent manner. The postulated mechanisms for this toxicity are multifactorial and cell-type dependent (Mukherjee et al., 2010):

1. Cell Membrane Integrity and Charge-Dependent Cytotoxicity:

A significant drawback of highly positively charged dendrimers, such as dPGA, is their inherent cytotoxicity due to disruption of cell membrane integrity. Cationic dendrimers can destabilize lipid bilayers, leading to cell lysis and eventual death. Many transfection agents are highly positively charged, and it has been shown it can also cause cell death (Fox et al., 2018).

2. Selective Cytotoxicity in GBM Cells:

Glioblastoma cells replicate more rapidly than microglia, potentially making them more susceptible to the cytotoxic effects of dPGA. The observed preferential killing of GBM cells at 30% amination levels may be attributed to the higher metabolic and lysosomal activity in these cells. Under these conditions, lysosomal alkalinization and cathepsin B dysregulation likely disrupt essential metabolic pathways, leading to cell death. Additionally, Hellmund et al. (2015) reported that a specific ratio of polyamine to sulfate groups (e.g., 30%) favored GBM cell cytotoxicity. This finding highlights the importance of optimizing dendrimer surface chemistry to achieve targeted therapeutic effects in GBM while minimizing off-target toxicity. This suggests that the ratio of amine to sulfate groups in dPG formulations is a critical determinant of their cytotoxicity profile and selective effects on GBM cells versus microglia.

4.9.1 – Dendrimers modulate lysosomal abundance and activity

Both dPGS and dPGA increased LAMP-2 abundance in GBM, suggesting an enhancement in lysosomal number (**Figure 3.10**). Interestingly, while dPGA increased the activity of cathepsin B, a lysosomal enzyme involved in protein degradation, dPGS reduced its activity (**Figure 3.10**). This contrasting behavior could potentially be linked to their structural differences and charge.

A decrease in a lysosomal biomarker (LysoTracker) was noted in microglia (**Figure 3.13**). However, despite this decrease, we observed an increase in lysosomal activity mediated by dPGS but not by dPGA (**Figure 3.13**). This paradoxical finding suggests that while the overall number of lysosomes may decrease, those that remain become more active, possibly due to enhanced enzyme activities (cathepsins including cathepsin B) or altered trafficking. The observed changes can be partly explained by the increase in TFEB abundance in microglia (**Figure 3.14**). The distinct effects of dPGA and dPGS are summarized in **Figure 4.6**.

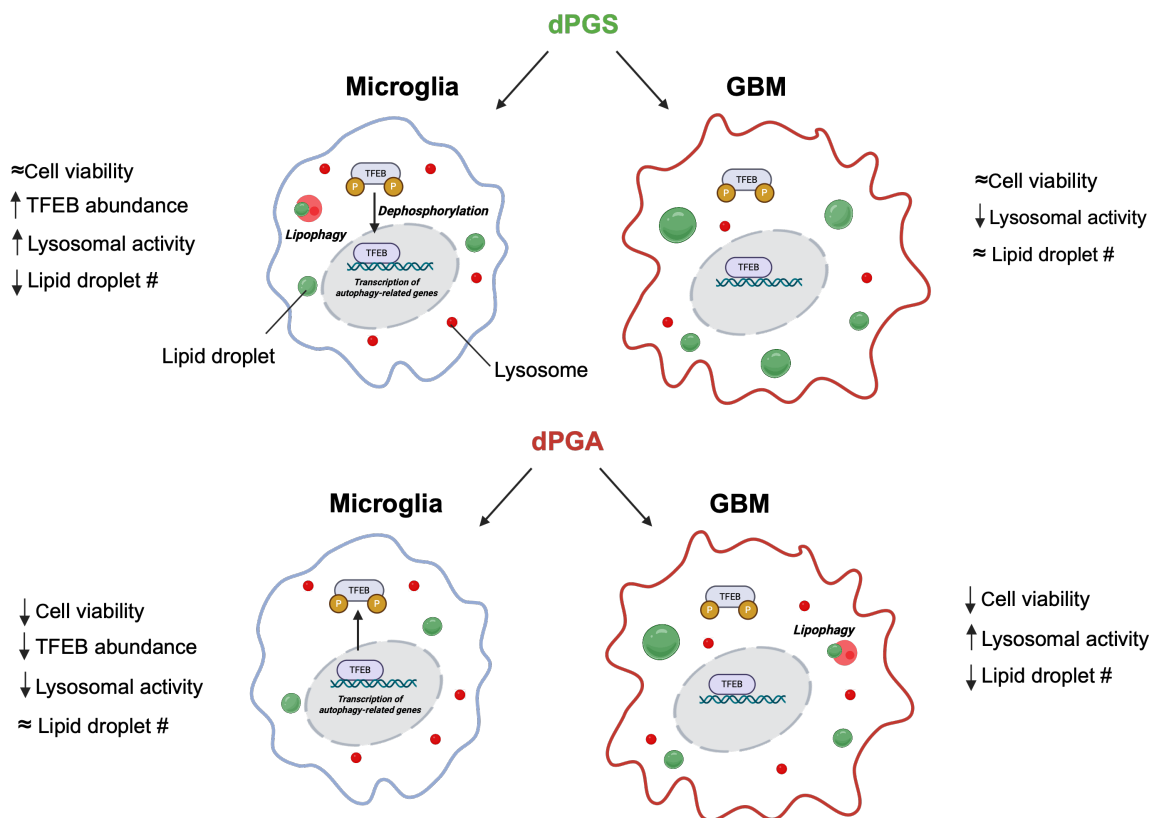


Figure 4.6. Overview of dPGS and dPGA treatments on cell viability, lysosomal activity, and lipid droplet abundance in GBM cells and microglia. Lysosomes are depicted as red circles, and lipid droplets are depicted as green circles. Created with ©BioRender ([biorender.com](https://www.biorender.com)).

4.9.2 – dPGA-induced alkalization of lysosomal pH in GBM

Lysosomal pH, normally maintained at around 5.0 in healthy cells, is often dysregulated in various diseases, including neurodegenerative disorders and cancer (Nixon, 2013). In cancer cells, decreased lysosomal pH can enhance autophagosome activity (Kenific & Debnath, 2015) and contribute to multidrug resistance (Daniel et al., 2013), as well as support the metabolic changes necessary for rapid cell proliferation. Understanding and monitoring lysosomal pH is thus crucial for elucidating their role in disease mechanisms and for the development of precise therapies.

We investigated how dPGA, a nanostructure known to accumulate in lysosomes, can affect pH. Preliminary experiments indicated that dPGA can increase lysosomal pH in GBM, making the internal environment of this organelle more alkaline (**Figure 3.12**). To verify this, we utilized a pH-sensitive fluorescent probe called SNAFL, developed by Laura McKay from the Chemistry department at McGill University, which emits green fluorescence under alkaline conditions. Our observations confirmed an increase in green fluorescence intensity following dPGA treatment, suggesting a rise in lysosomal pH. To ensure that these observations were specific to lysosomes, we co-stained the cells with LysoTracker Red. Significant colocalization of SNAFL with this lysosomal marker was noted post-dPGA treatment. This phenomenon is not limited to GBM cells but is also observed in microglia when using chloroquine, a pharmacological agent known to alkalinize intracellular media. Under such alkalinization conditions, there is a redshift in the emission maxima of SNAFL from 553 nm to 632 nm, which serves as a reliable indicator of increased lysosomal pH (Mordon et al., 1995)

In the context of GBM, this increase in lysosomal pH could have significant implications. It might disrupt the usual acid-dependent processes within cancer cells, potentially affecting their ability to process and recycle materials efficiently. This alteration could lead to a decrease in cellular recycling capabilities, impacting tumor survival and providing a new therapeutic target for disrupting cancer cell homeostasis. In summary, we showed that the charge of dendrimers (–,+) play a critical role in modulating organellar state.

4.10 – Future directions

Traditional GBM therapies predominantly target tumor cells and often overlook the TME. Adjusting this approach to modify the TME components, such as microglia, macrophages, astrocytes, and vasculature, could inhibit tumor growth and resistance, improving the efficacy of existing treatments. Moreover, tumor microtubules contribute significantly to GBM cell proliferation and treatment resistance (Kudruk et al., 2024; X. Wang et al., 2022). Targeting these structures could disrupt the communication and support networks between tumor cells, potentially limiting their ability to resist therapies. Investigating agents or methods that can specifically disrupt or degrade these microtubules could open new therapeutic avenues.

Lipid droplets (LDs) are known to play dual roles in cancer. On the one hand, they act as reservoirs for fatty acids, protecting cells from lipotoxicity and oxidative stress. On the other hand, they can fuel tumor growth by providing energy-rich substrates. In the context of my findings, the accumulation of LDs might reflect a metabolic adaptation to therapy-induced stress. However, the exact role of LDs in this context remains ambiguous, raising important questions about whether they act as protective organelles or contribute to tumor progression (Cruz et al., 2020).

In future work, I plan to conduct the following experiments to address these questions:

1. **Functional Assays:** Use pharmacological inhibitors of lipid droplet formation, such as A922500 (a DGAT inhibitor), to evaluate whether inhibiting LD biogenesis impacts therapy response.
2. **Lipidomic Analysis:** Perform lipidomic profiling to characterize the composition of LDs, identifying whether they contain toxic lipid species or signaling lipids that promote survival or induce cell death.
3. **Time-Resolved Studies:** Conduct time-lapse microscopy to monitor the dynamics of LDs during treatment, assessing whether their accumulation is an early protective mechanism or a response to cellular damage.

Lastly, developing human organoid models that replicate the TME will enhance the testing of new therapies (Jacob et al., 2020; C. Wang et al., 2024; Xu et al., 2023). Techniques such as single-cell and single-nucleus transcriptomics, along with other -OMICS methodologies, provide comprehensive insights into cellular responses and the inherent heterogeneity of GBM. Focusing on these areas could bridge gaps in current therapies and lead to significantly improved patient outcomes.

CHAPTER 5 – CONCLUSION

5.1 – *Flavonoids*

We found that polyphenols exert distinct effects on GBM and microglia cells, impacting GBM cell viability without affecting microglia viability. On a molecular level, flavonoids decrease AcHMGB1 (alarmin) abundance in microglia but not in GBM cells, potentially safeguarding microglia by mitigating excessive inflammation. Due to their role in modulating oxidative stress, using flavonoids alone, without an anticancer drug, is not advisable. Our most effective treatment was the combination between fisetin and TMZ, a standard chemotherapy agent, enhancing its anticancer effects.

5.2 – *Dendrimers*

Our research extended to synthetic nanostructures, specifically dendrimers with varying charges, and their effects on GBM cells and microglia. Given the ongoing search for effective GBM treatments, positively charged nanostructures like dPGA present a promising approach for targeting GBM cells. This nanostructure demonstrates a higher cytotoxic effect on GBM cells compared to microglial cells at nanomolar concentrations, as low as 100 nM. dPGA notably increases lysosomal abundance and cathepsin B activity in GBM cells while simultaneously reducing LD abundance. In contrast, dPGS is non-toxic to both microglial and GBM cells. Its effects are primarily observed at the organellar level, enhancing lysosomal activity in microglial cells but reducing it in GBM cells.

Given the contrasting effects of dPGS and dPGA on GBM and microglial cells, we propose the development of a hybrid nanostructure that incorporates both sulfate and amino groups. By optimizing the ratio of sulfation to amination, we hypothesize that this structure will protect microglial cells with the sulfate groups while eliminating GBM cells with the amino groups.

A significant drawback of highly positively charged dendrimers, such as dPGA, is their inherent cytotoxicity due to disruption of cell membrane integrity. Fischer et al. (2003) reported that cationic dendrimers can destabilize lipid bilayers, leading to cell lysis and

eventual death. To mitigate this, the charge and size of cationic dendrimers can be adjusted to achieve a balance between effective gene delivery and reduced cytotoxicity.

CHAPTER 6 – REFERENCES (ALPHABETICAL)

- Abdel-Hakeem, M. S., Manne, S., Beltra, J.-C., Stelekati, E., Chen, Z., Nzingha, K., Ali, M.-A., Johnson, J. L., Giles, J. R., Mathew, D., Greenplate, A. R., Vahedi, G., & Wherry, E. J. (2021). Epigenetic scarring of exhausted T cells hinders memory differentiation upon eliminating chronic antigenic stimulation. *Nature Immunology*, 22(8), 1008–1019. <https://doi.org/10.1038/s41590-021-00975-5>
- Agrawal, K., Asthana, S., & Kumar, D. (2023). Role of Oxidative Stress in Metabolic Reprogramming of Brain Cancer. *Cancers*, 15(20), 4920. <https://doi.org/10.3390/cancers15204920>
- Akkari, L., Bowman, R. L., Tessier, J., Klemm, F., Handgraaf, S. M., de Groot, M., Quail, D. F., Tillard, L., Gadiot, J., Huse, J. T., Brandsma, D., Westerga, J., Watts, C., & Joyce, J. A. (2020). Dynamic changes in glioma macrophage populations after radiotherapy reveal CSF-1R inhibition as a strategy to overcome resistance. *Science Translational Medicine*, 12(552), eaaw7843. <https://doi.org/10.1126/scitranslmed.aaw7843>
- Anderson, N. M., & Simon, M. C. (2020). The tumor microenvironment. *Current Biology: CB*, 30(16), R921–R925. <https://doi.org/10.1016/j.cub.2020.06.081>
- Andersson, U., & Tracey, K. J. (2011). HMGB1 Is a Therapeutic Target for Sterile Inflammation and Infection. *Annual Review of Immunology*, 29, 139–162. <https://doi.org/10.1146/annurev-immunol-030409-101323>
- Atanasov, A. G., Waltenberger, B., Pferschy-Wenzig, E.-M., Linder, T., Wawrosch, C., Uhrin, P., Temml, V., Wang, L., Schwaiger, S., Heiss, E. H., Rollinger, J. M., Schuster, D., Breuss, J. M., Bochkov, V., Mihovilovic, M. D., Kopp, B., Bauer, R., Dirsch, V. M., & Stuppner, H. (2015). Discovery and resupply of pharmacologically active plant-derived natural products: A review. *Biotechnology Advances*, 33(8), 1582–1614. <https://doi.org/10.1016/j.biotechadv.2015.08.001>
- Balça-Silva, J., Matias, D., Carmo, A. do, Sarmento-Ribeiro, A. B., Lopes, M. C., & Moura-Neto, V. (2019). Cellular and molecular mechanisms of glioblastoma malignancy: Implications in resistance and therapeutic strategies. *Seminars in Cancer Biology*, 58, 130–141. <https://doi.org/10.1016/j.semcancer.2018.09.007>
- Bassi, R., Giussani, P., Anelli, V., Colleoni, T., Pedrazzi, M., Patrone, M., Viani, P., Sparatore, B., Melloni, E., & Riboni, L. (2008). HMGB1 as an autocrine stimulus in human T98G glioblastoma cells: Role in cell growth and migration. *Journal of Neuro-Oncology*, 87(1), 23–33. <https://doi.org/10.1007/s11060-007-9488-y>
- Batra, P., & Sharma, A. K. (2013). Anti-cancer potential of flavonoids: Recent trends and future perspectives. *3 Biotech*, 3(6), 439–459. <https://doi.org/10.1007/s13205-013-0117-5>
- Bielawski, P.-B., Zhang, I., Correa-Paz, C., Campos, F., Migliavacca, M., Polo, E., Del Pino, P., Pelaz, B., Vivien, D., & Maysinger, D. (2024). *Modulation of Abundance and Location of High-Mobility Group Box 1 in Human Microglia and Macrophages under Oxygen–Glucose Deprivation*. <https://doi.org/10.1021/acscptsci.3c00271.s001>
- Biffi, S., Dal Monego, S., Dullin, C., Garrovo, C., Bosnjak, B., Licha, K., Welker, P., Epstein, M. M., & Alves, F. (2013). Dendritic polyglycerolsulfate near infrared fluorescent (NIRF) dye conjugate for non-invasively monitoring of inflammation in

- an allergic asthma mouse model. *PloS One*, 8(2), e57150. <https://doi.org/10.1371/journal.pone.0057150>
- Bleeker, F. E., Molenaar, R. J., & Leenstra, S. (2012). Recent advances in the molecular understanding of glioblastoma. *Journal of Neuro-Oncology*, 108(1), 11–27. <https://doi.org/10.1007/s11060-011-0793-0>
- Butowski, N., Colman, H., De Groot, J. F., Omuro, A. M., Nayak, L., Wen, P. Y., Cloughesy, T. F., Marimuthu, A., Haidar, S., Perry, A., Huse, J., Phillips, J., West, B. L., Nolop, K. B., Hsu, H. H., Ligon, K. L., Molinaro, A. M., & Prados, M. (2016). Orally administered colony stimulating factor 1 receptor inhibitor PLX3397 in recurrent glioblastoma: An Ivy Foundation Early Phase Clinical Trials Consortium phase II study. *Neuro-Oncology*, 18(4), 557–564. <https://doi.org/10.1093/neuonc/nov245>
- Campisi, J., Leem, T. H., & Fleshner, M. (2003). Stress-induced extracellular Hsp72 is a functionally significant danger signal to the immune system. *Cell Stress & Chaperones*, 8(3), 272–286.
- Chaib, S., Tchkonja, T., & Kirkland, J. L. (2022). Cellular senescence and senolytics: The path to the clinic. *Nature Medicine*, 28(8), Article 8. <https://doi.org/10.1038/s41591-022-01923-y>
- Chaicharoenaudomrung, N., Kunhorm, P., Promjantuek, W., Rujanapun, N., Heebkaew, N., Soraksa, N., & Noisa, P. (2020). Transcriptomic Profiling of 3D Glioblastoma Tumoroids for the Identification of Mechanisms Involved in Anticancer Drug Resistance. *In Vivo (Athens, Greece)*, 34(1), 199–211. <https://doi.org/10.21873/invivo.11762>
- Charles, N. A., Holland, E. C., Gilbertson, R., Glass, R., & Kettenmann, H. (2012). The brain tumor microenvironment. *Glia*, 60(3), 502–514. <https://doi.org/10.1002/glia.21264>
- Chen, F., Xiao, M., Hu, S., & Wang, M. (2024). Keap1-Nrf2 pathway: A key mechanism in the occurrence and development of cancer. *Frontiers in Oncology*, 14, 1381467. <https://doi.org/10.3389/fonc.2024.1381467>
- Chen, M., Dai, Y., Liu, S., Fan, Y., Ding, Z., & Li, D. (2021). TFEB Biology and Agonists at a Glance. *Cells*, 10(2), Article 2. <https://doi.org/10.3390/cells10020333>
- Chen, R., Kang, R., & Tang, D. (2022). The mechanism of HMGB1 secretion and release. *Experimental & Molecular Medicine*, 54(2), Article 2. <https://doi.org/10.1038/s12276-022-00736-w>
- Chen, Y., Wu, Q., Song, L., He, T., Li, Y., Li, L., Su, W., Liu, L., Qian, Z., & Gong, C. (2015). Polymeric Micelles Encapsulating Fisetin Improve the Therapeutic Effect in Colon Cancer. *ACS Applied Materials & Interfaces*, 7(1), 534–542. <https://doi.org/10.1021/am5066893>
- Christiansen, A., & Detmar, M. (2011). Lymphangiogenesis and Cancer. *Genes & Cancer*, 2(12), 1146–1158. <https://doi.org/10.1177/1947601911423028>
- Clément, J.-P., Al-Alwan, L., Glasgow, S. D., Stolow, A., Ding, Y., Quevedo Melo, T., Khayachi, A., Liu, Y., Hellmund, M., Haag, R., Milnerwood, A. J., Grütter, P., & Kennedy, T. E. (2022). Dendritic Polyglycerol Amine: An Enhanced Substrate to Support Long-Term Neural Cell Culture. *ASN Neuro*, 14, 17590914211073276. <https://doi.org/10.1177/17590914211073276>

- Corbet, C., & Feron, O. (2017). Tumour acidosis: From the passenger to the driver's seat. *Nature Reviews. Cancer*, 17(10), 577–593. <https://doi.org/10.1038/nrc.2017.77>
- Cruz, A. L. S., Barreto, E. de A., Fazolini, N. P. B., Viola, J. P. B., & Bozza, P. T. (2020). Lipid droplets: Platforms with multiple functions in cancer hallmarks. *Cell Death & Disease*, 11(2), 1–16. <https://doi.org/10.1038/s41419-020-2297-3>
- Daniel, C., Bell, C., Burton, C., Harguindey, S., Reshkin, S. J., & Rauch, C. (2013). The role of proton dynamics in the development and maintenance of multidrug resistance in cancer. *Biochimica et Biophysica Acta (BBA) - Molecular Basis of Disease*, 1832(5), 606–617. <https://doi.org/10.1016/j.bbadis.2013.01.020>
- Davis, M. E. (2016). Glioblastoma: Overview of Disease and Treatment. *Clinical Journal of Oncology Nursing*, 20(5 Suppl), S2-8. <https://doi.org/10.1188/16.CJON.S1.2-8>
- Debnath, J., Gammoh, N., & Ryan, K. M. (2023). Autophagy and autophagy-related pathways in cancer. *Nature Reviews Molecular Cell Biology*, 24(8), 560–575. <https://doi.org/10.1038/s41580-023-00585-z>
- Del Duca, D., Werbowetski, T., & Del Maestro, R. F. (2004). Spheroid Preparation from Hanging Drops: Characterization of a Model of Brain Tumor Invasion. *Journal of Neuro-Oncology*, 67(3), 295–303. <https://doi.org/10.1023/B:NEON.0000024220.07063.70>
- Deng, M., Scott, M. J., Fan, J., & Billiar, T. R. (2019). Location is the key to function: HMGB1 in sepsis and trauma-induced inflammation. *Journal of Leukocyte Biology*, 106(1), 161–169. <https://doi.org/10.1002/JLB.3MIR1218-497R>
- Dernedde, J., Rausch, A., Weinhardt, M., Enders, S., Tauber, R., Licha, K., Schirner, M., Zügel, U., von Bonin, A., & Haag, R. (2010). Dendritic polyglycerol sulfates as multivalent inhibitors of inflammation. *Proceedings of the National Academy of Sciences*, 107(46), 19679–19684. <https://doi.org/10.1073/pnas.1003103107>
- Dierge, E., Debock, E., Guilbaud, C., Corbet, C., Mignolet, E., Mignard, L., Bastien, E., Dessy, C., Larondelle, Y., & Feron, O. (2021). Peroxidation of n-3 and n-6 polyunsaturated fatty acids in the acidic tumor environment leads to ferroptosis-mediated anticancer effects. *Cell Metabolism*, 33(8), 1701-1715.e5. <https://doi.org/10.1016/j.cmet.2021.05.016>
- Dixon, S. J., Lemberg, K. M., Lamprecht, M. R., Skouta, R., Zaitsev, E. M., Gleason, C. E., Patel, D. N., Bauer, A. J., Cantley, A. M., Yang, W. S., Morrison, B., & Stockwell, B. R. (2012). Ferroptosis: An iron-dependent form of nonapoptotic cell death. *Cell*, 149(5), 1060–1072. <https://doi.org/10.1016/j.cell.2012.03.042>
- Dobrzynska, M., Napierala, M., & Florek, E. (2020). Flavonoid Nanoparticles: A Promising Approach for Cancer Therapy. *Biomolecules*, 10(9), 1268. <https://doi.org/10.3390/biom10091268>
- Duraj, T., García-Romero, N., Carrión-Navarro, J., Madurga, R., Mendivil, A. O. de, Prat-Acin, R., Garcia-Cañamaque, L., & Ayuso-Sacido, A. (2021). Beyond the Warburg Effect: Oxidative and Glycolytic Phenotypes Coexist within the Metabolic Heterogeneity of Glioblastoma. *Cells*, 10(2), 202. <https://doi.org/10.3390/cells10020202>
- Estrella, V., Chen, T., Lloyd, M., Wojtkowiak, J., Cornnell, H. H., Ibrahim-Hashim, A., Bailey, K., Balagurunathan, Y., Rothberg, J. M., Sloane, B. F., Johnson, J., Gatenby, R. A., & Gillies, R. J. (2013). Acidity generated by the tumor

- microenvironment drives local invasion. *Cancer Research*, 73(5), 1524–1535. <https://doi.org/10.1158/0008-5472.CAN-12-2796>
- Falchook, G. S., Peeters, M., Rottey, S., Dirix, L. Y., Obermannova, R., Cohen, J. E., Perets, R., Frommer, R. S., Bauer, T. M., Wang, J. S., Carvajal, R. D., Sabari, J., Chapman, S., Zhang, W., Calderon, B., & Peterson, D. A. (2021). A phase 1a/1b trial of CSF-1R inhibitor LY3022855 in combination with durvalumab or tremelimumab in patients with advanced solid tumors. *Investigational New Drugs*, 39(5), 1284–1297. <https://doi.org/10.1007/s10637-021-01088-4>
- Fan, A., Gao, M., Tang, X., Jiao, M., Wang, C., Wei, Y., Gong, Q., & Zhong, J. (2024). HMGB1/RAGE axis in tumor development: Unraveling its significance. *Frontiers in Oncology*, 14. <https://doi.org/10.3389/fonc.2024.1336191>
- Fan, C.-H., Liu, W.-L., Cao, H., Wen, C., Chen, L., & Jiang, G. (2013). O6-methylguanine DNA methyltransferase as a promising target for the treatment of temozolomide-resistant gliomas. *Cell Death & Disease*, 4(10), e876. <https://doi.org/10.1038/cddis.2013.388>
- Fan, Y., Lu, H., Liang, W., Garcia-Barrio, M. T., Guo, Y., Zhang, J., Zhu, T., Hao, Y., Zhang, J., & Chen, Y. E. (2018). Endothelial TFEB (Transcription Factor EB) Positively Regulates Postischemic Angiogenesis. *Circulation Research*, 122(7), 945–957. <https://doi.org/10.1161/CIRCRESAHA.118.312672>
- Ferber, S., Tiram, G., Sousa-Herves, A., Eldar-Boock, A., Krivitsky, A., Scomparin, A., Yeini, E., Ofek, P., Ben-Shushan, D., Vossen, L. I., Licha, K., Grossman, R., Ram, Z., Henkin, J., Ruppin, E., Auslander, N., Haag, R., Calderón, M., & Satchi-Fainaro, R. (2017). Co-targeting the tumor endothelium and P-selectin-expressing glioblastoma cells leads to a remarkable therapeutic outcome. *eLife*, 6, e25281. <https://doi.org/10.7554/eLife.25281>
- Fernandes, C., Costa, A., Osório, L., Lago, R. C., Linhares, P., Carvalho, B., & Caeiro, C. (2017). Current Standards of Care in Glioblastoma Therapy. In S. De Vleeschouwer (Ed.), *Glioblastoma*. Codon Publications. <http://www.ncbi.nlm.nih.gov/books/NBK469987/>
- Forman, H. J., & Zhang, H. (2021). Targeting oxidative stress in disease: Promise and limitations of antioxidant therapy. *Nature Reviews. Drug Discovery*, 20(9), 689–709. <https://doi.org/10.1038/s41573-021-00233-1>
- Fox, L. J., Richardson, R. M., & Briscoe, W. H. (2018). PAMAM dendrimer—Cell membrane interactions. *Advances in Colloid and Interface Science*, 257, 1–18. <https://doi.org/10.1016/j.cis.2018.06.005>
- Frey, H., & Haag, R. (2002). Dendritic polyglycerol: A new versatile biocompatible-material. *Journal of Biotechnology*, 90(3–4), 257–267. [https://doi.org/10.1016/s1389-0352\(01\)00063-0](https://doi.org/10.1016/s1389-0352(01)00063-0)
- Friedman, H. S., Prados, M. D., Wen, P. Y., Mikkelsen, T., Schiff, D., Abrey, L. E., Yung, W. K. A., Paleologos, N., Nicholas, M. K., Jensen, R., Vredenburgh, J., Huang, J., Zheng, M., & Cloughesy, T. (2009). Bevacizumab alone and in combination with irinotecan in recurrent glioblastoma. *Journal of Clinical Oncology: Official Journal of the American Society of Clinical Oncology*, 27(28), 4733–4740. <https://doi.org/10.1200/JCO.2008.19.8721>
- Fujii, K., Idogawa, M., Suzuki, N., Iwatsuki, K., & Kanekura, T. (2021). Functional Depletion of HSP72 by siRNA and Quercetin Enhances Vorinostat-Induced

- Apoptosis in an HSP72-Overexpressing Cutaneous T-Cell Lymphoma Cell Line, Hut78. *International Journal of Molecular Sciences*, 22(20), 11258. <https://doi.org/10.3390/ijms222011258>
- Fukami, A., Adachi, H., Yamagishi, S., Matsui, T., Ueda, S., Nakamura, K., Enomoto, M., Otsuka, M., Kumagae, S., Nanjo, Y., Kumagai, E., Esaki, E., Murayama, K., Hirai, Y., & Imaizumi, T. (2009). Factors associated with serum high mobility group box 1 (HMGB1) levels in a general population. *Metabolism: Clinical and Experimental*, 58(12), 1688–1693. <https://doi.org/10.1016/j.metabol.2009.05.024>
- Gaitsch, H., Hersh, A. M., Alomari, S., & Tyler, B. M. (2023). Dendrimer Technology in Glioma: Functional Design and Potential Applications. *Cancers*, 15(4), 1075. <https://doi.org/10.3390/cancers15041075>
- Galdiero, M. R., Bonavita, E., Barajon, I., Garlanda, C., Mantovani, A., & Jaillon, S. (2013). Tumor associated macrophages and neutrophils in cancer. *Immunobiology*, 218(11), 1402–1410. <https://doi.org/10.1016/j.imbio.2013.06.003>
- Gao, Q., Wang, S., Chen, X., Cheng, S., Zhang, Z., Li, F., Huang, L., Yang, Y., Zhou, B., Yue, D., Wang, D., Cao, L., Maimela, N. R., Zhang, B., Yu, J., Wang, L., & Zhang, Y. (2019). Cancer-cell-secreted CXCL11 promoted CD8⁺ T cells infiltration through docetaxel-induced-release of HMGB1 in NSCLC. *Journal for Immunotherapy of Cancer*, 7(1), 42. <https://doi.org/10.1186/s40425-019-0511-6>
- Gao, X.-Y., Zang, J., Zheng, M.-H., Zhang, Y.-F., Yue, K.-Y., Cao, X.-L., Cao, Y., Li, X.-X., Han, H., Jiang, X.-F., & Liang, L. (2021). Temozolomide Treatment Induces HMGB1 to Promote the Formation of Glioma Stem Cells via the TLR2/NEAT1/Wnt Pathway in Glioblastoma. *Frontiers in Cell and Developmental Biology*, 9, 620883. <https://doi.org/10.3389/fcell.2021.620883>
- Geribaldi-Doldán, N., Fernández-Ponce, C., Quiroz, R. N., Sánchez-Gomar, I., Escorcía, L. G., Velásquez, E. P., & Quiroz, E. N. (2021). The Role of Microglia in Glioblastoma. *Frontiers in Oncology*, 10. <https://www.frontiersin.org/articles/10.3389/fonc.2020.603495>
- Germelli, L., Da Pozzo, E., Giacomelli, C., Tremolanti, C., Marchetti, L., Wetzel, C. H., Barresi, E., Taliani, S., Da Settimo, F., Martini, C., & Costa, B. (2021). De novo Neurosteroidogenesis in Human Microglia: Involvement of the 18 kDa Translocator Protein. *International Journal of Molecular Sciences*, 22(6), 3115. <https://doi.org/10.3390/ijms22063115>
- Ghosh, D., Pryor, B., & Jiang, N. (2024). Cellular signaling in glioblastoma: A molecular and clinical perspective. *International Review of Cell and Molecular Biology*, 386, 1–47. <https://doi.org/10.1016/bs.ircmb.2024.01.007>
- Gorlia, T., Wu, W., Wang, M., Baumert, B. G., Mehta, M., Buckner, J. C., Shaw, E., Brown, P., Stupp, R., Galanis, E., Lacombe, D., & van den Bent, M. J. (2013). New validated prognostic models and prognostic calculators in patients with low-grade gliomas diagnosed by central pathology review: A pooled analysis of EORTC/RTOG/NCCTG phase III clinical trials. *Neuro-Oncology*, 15(11), 1568–1579. <https://doi.org/10.1093/neuonc/not117>
- Gröger, D., Paulus, F., Licha, K., Welker, P., Weinhart, M., Holzhausen, C., Mundhenk, L., Gruber, A. D., Abram, U., & Haag, R. (2013). Synthesis and biological evaluation of radio and dye labeled amino functionalized dendritic polyglycerol

- sulfates as multivalent anti-inflammatory compounds. *Bioconjugate Chemistry*, 24(9), 1507–1514. <https://doi.org/10.1021/bc400047f>
- Gryniewicz, G., & Demchuk, O. M. (2019). New Perspectives for Fisetin. *Frontiers in Chemistry*, 7, 697. <https://doi.org/10.3389/fchem.2019.00697>
- Harvey, A. L., Edrada-Ebel, R., & Quinn, R. J. (2015). The re-emergence of natural products for drug discovery in the genomics era. *Nature Reviews. Drug Discovery*, 14(2), 111–129. <https://doi.org/10.1038/nrd4510>
- Hatoum, A., Mohammed, R., & Zakieh, O. (2019). The unique invasiveness of glioblastoma and possible drug targets on extracellular matrix. *Cancer Management and Research*, 11, 1843–1855. <https://doi.org/10.2147/CMAR.S186142>
- He, R., Wang, M., Zhao, C., Shen, M., Yu, Y., He, L., Zhao, Y., Chen, H., Shi, X., Zhou, M., Pan, S., Liu, Y., Guo, X., Li, X., & Qin, R. (2019). TFEB-driven autophagy potentiates TGF- β induced migration in pancreatic cancer cells. *Journal of Experimental & Clinical Cancer Research: CR*, 38, 340. <https://doi.org/10.1186/s13046-019-1343-4>
- Hermisson, M., Strik, H., Rieger, J., Dichgans, J., Meyermann, R., & Weller, M. (2000). Expression and functional activity of heat shock proteins in human glioblastoma multiforme. *Neurology*, 54(6), 1357–1365. <https://doi.org/10.1212/wnl.54.6.1357>
- Huebener, P., Gwak, G.-Y., Pradere, J.-P., Quinzii, C. M., Friedman, R., Lin, C.-S., Trent, C. M., Mederacke, I., Zhao, E., Dapito, D. H., Lin, Y., Goldberg, I. J., Czaja, M. J., & Schwabe, R. F. (2014). High-mobility group box 1 is dispensable for autophagy, mitochondrial quality control, and organ function in vivo. *Cell Metabolism*, 19(3), 539–547. <https://doi.org/10.1016/j.cmet.2014.01.014>
- Hulikova, A., & Swietach, P. (2014). Rapid CO₂ permeation across biological membranes: Implications for CO₂ venting from tissue. *FASEB Journal: Official Publication of the Federation of American Societies for Experimental Biology*, 28(7), 2762–2774. <https://doi.org/10.1096/fj.13-241752>
- Hussain, S. F., Yang, D., Suki, D., Aldape, K., Grimm, E., & Heimberger, A. B. (2006). The role of human glioma-infiltrating microglia/macrophages in mediating antitumor immune responses. *Neuro-Oncology*, 8(3), 261–279. <https://doi.org/10.1215/15228517-2006-008>
- Iglesia, R. P., Fernandes, C. F. de L., Coelho, B. P., Prado, M. B., Melo Escobar, M. I., Almeida, G. H. D. R., & Lopes, M. H. (2019). Heat Shock Proteins in Glioblastoma Biology: Where Do We Stand? *International Journal of Molecular Sciences*, 20(22), 5794. <https://doi.org/10.3390/ijms20225794>
- Jacob, F., Salinas, R. D., Zhang, D. Y., Nguyen, P. T. T., Schnoll, J. G., Wong, S. Z. H., Thokala, R., Sheikh, S., Saxena, D., Prokop, S., Liu, D., Qian, X., Petrov, D., Lucas, T., Chen, H. I., Dorsey, J. F., Christian, K. M., Binder, Z. A., Nasrallah, M., ... Song, H. (2020). A Patient-Derived Glioblastoma Organoid Model and Biobank Recapitulates Inter- and Intra-tumoral Heterogeneity. *Cell*, 180(1), 188-204.e22. <https://doi.org/10.1016/j.cell.2019.11.036>
- Jain, S., Hirst, D. G., & O'Sullivan, J. M. (2012). Gold nanoparticles as novel agents for cancer therapy. *The British Journal of Radiology*, 85(1010), 101–113. <https://doi.org/10.1259/bjr/59448833>

- Jia, S., Xu, X., Zhou, S., Chen, Y., Ding, G., & Cao, L. (2019). Fisetin induces autophagy in pancreatic cancer cells via endoplasmic reticulum stress- and mitochondrial stress-dependent pathways. *Cell Death & Disease*, 10(2), Article 2. <https://doi.org/10.1038/s41419-019-1366-y>
- Joma, N., Bielawski, P.-B., Saini, A., Kakkar, A., & Maysinger, D. (2024). Nanocarriers for natural polyphenol senotherapeutics. *Aging Cell*, 23(5), e14178. <https://doi.org/10.1111/acer.14178>
- Joma, N., Zhang, I., Righetto, G. L., McKay, L., Gran, E. R., Kakkar, A., & Maysinger, D. (2023). Flavonoids Regulate Redox-Responsive Transcription Factors in Glioblastoma and Microglia. *Cells*, 12(24), 2821. <https://doi.org/10.3390/cells12242821>
- Kanderi, T., & Gupta, V. (2024). Glioblastoma Multiforme. In *StatPearls*. StatPearls Publishing. <http://www.ncbi.nlm.nih.gov/books/NBK558954/>
- Kang, R., Zhang, Q., Zeh, H. J., Lotze, M. T., & Tang, D. (2013). HMGB1 in Cancer: Good, Bad, or Both? *Clinical Cancer Research : An Official Journal of the American Association for Cancer Research*, 19(15), 4046–4057. <https://doi.org/10.1158/1078-0432.CCR-13-0495>
- Kenific, C. M., & Debnath, J. (2015). Cellular and metabolic functions for autophagy in cancer cells. *Trends in Cell Biology*, 25(1), 37–45. <https://doi.org/10.1016/j.tcb.2014.09.001>
- Khan, N., Afaq, F., Syed, D. N., & Mukhtar, H. (2008). Fisetin, a novel dietary flavonoid, causes apoptosis and cell cycle arrest in human prostate cancer LNCaP cells. *Carcinogenesis*, 29(5), 1049–1056. <https://doi.org/10.1093/carcin/bgn078>
- Kim, J. A., Lee, S., Kim, D.-E., Kim, M., Kwon, B.-M., & Han, D. C. (2015). Fisetin, a dietary flavonoid, induces apoptosis of cancer cells by inhibiting HSF1 activity through blocking its binding to the hsp70 promoter. *Carcinogenesis*, 36(6), 696–706. <https://doi.org/10.1093/carcin/bgv045>
- Kim, J. H., Lee, J., Cho, Y.-R., Lee, S.-Y., Sung, G.-J., Shin, D.-M., Choi, K.-C., & Son, J. (2021). TFEB Supports Pancreatic Cancer Growth through the Transcriptional Regulation of Glutaminase. *Cancers*, 13(3), 483. <https://doi.org/10.3390/cancers13030483>
- Kitange, G. J., Carlson, B. L., Schroeder, M. A., Grogan, P. T., Lamont, J. D., Decker, P. A., Wu, W., James, C. D., & Sarkaria, J. N. (2009). Induction of MGMT expression is associated with temozolomide resistance in glioblastoma xenografts. *Neuro-Oncology*, 11(3), 281. <https://doi.org/10.1215/15228517-2008-090>
- Klemm, F., Maas, R. R., Bowman, R. L., Kornete, M., Soukup, K., Nassiri, S., Brouland, J.-P., Iacobuzio-Donahue, C. A., Brennan, C., Tabar, V., Gutin, P. H., Daniel, R. T., Hegi, M. E., & Joyce, J. A. (2020). Interrogation of the Microenvironmental Landscape in Brain Tumors Reveals Disease-Specific Alterations of Immune Cells. *Cell*, 181(7), 1643-1660.e17. <https://doi.org/10.1016/j.cell.2020.05.007>
- Knauer, N., Meschaninova, M., Muhammad, S., Hänggi, D., Majoral, J.-P., Kahlert, U. D., Kozlov, V., & Apartsin, E. K. (2023). Effects of Dendrimer-microRNA Nanoformulations against Glioblastoma Stem Cells. *Pharmaceutics*, 15(3), 968. <https://doi.org/10.3390/pharmaceutics15030968>

- Kothamasu, P., Kanumur, H., Ravur, N., Maddu, C., Parasuramrajam, R., & Thangavel, S. (2012). Nanocapsules: The Weapons for Novel Drug Delivery Systems. *BioImpacts : BI*, 2(2), 71–81. <https://doi.org/10.5681/bi.2012.011>
- Kudruk, S., Forsyth, C. M., Dion, M. Z., Hedlund Orbeck, J. K., Luo, J., Klein, R. S., Kim, A. H., Heimberger, A. B., Mirkin, C. A., Stegh, A. H., & Artzi, N. (2024). Multimodal neuro-nanotechnology: Challenging the existing paradigm in glioblastoma therapy. *Proceedings of the National Academy of Sciences of the United States of America*, 121(8), e2306973121. <https://doi.org/10.1073/pnas.2306973121>
- Kuiper, R. P., Schepens, M., Thijssen, J., van Asseldonk, M., van den Berg, E., Bridge, J., Schuurin, E., Schoenmakers, E. F. P. M., & van Kessel, A. G. (2003). Upregulation of the transcription factor TFEB in t(6;11)(p21;q13)-positive renal cell carcinomas due to promoter substitution. *Human Molecular Genetics*, 12(14), 1661–1669. <https://doi.org/10.1093/hmg/ddg178>
- Kumar, H., Chand, P., Pachal, S., Mallick, S., Jain, R., Madhunapantula, S. V., & Jain, V. (2023). Fisetin-Loaded Nanostructured Lipid Carriers: Formulation and Evaluations against Advanced and Metastatic Melanoma. *Molecular Pharmaceutics*, 20(12), 6035–6055. <https://doi.org/10.1021/acs.molpharmaceut.3c00309>
- Kurdi, M., Baeesa, S., Okal, F., Bamaga, A. K., Faizo, E., Fathaddin, A. A., Alkhotani, A., Karami, M. M., & Bahakeem, B. (2023). Extracranial metastasis of brain glioblastoma outside CNS: Pathogenesis revisited. *Cancer Reports*, 6(12), e1905. <https://doi.org/10.1002/cnr2.1905>
- Lai, W., Li, X., Kong, Q., Chen, H., Li, Y., Xu, L.-H., & Fang, J. (2021). Extracellular HMGB1 interacts with RAGE and promotes chemoresistance in acute leukemia cells. *Cancer Cell International*, 21, 700. <https://doi.org/10.1186/s12935-021-02387-9>
- Le, D. M., Besson, A., Fogg, D. K., Choi, K.-S., Waisman, D. M., Goodyer, C. G., Rewcastle, B., & Yong, V. W. (2003). Exploitation of Astrocytes by Glioma Cells to Facilitate Invasiveness: A Mechanism Involving Matrix Metalloproteinase-2 and the Urokinase-Type Plasminogen Activator–Plasmin Cascade. *The Journal of Neuroscience*, 23(10), 4034–4043. <https://doi.org/10.1523/JNEUROSCI.23-10-04034.2003>
- Li, K., Chen, B., Xu, A., Shen, J., Li, K., Hao, K., Hao, R., Yang, W., Jiang, W., Zheng, Y., Ge, F., & Wang, Z. (2022). TRIM7 modulates NCOA4-mediated ferritinophagy and ferroptosis in glioblastoma cells. *Redox Biology*, 56, 102451. <https://doi.org/10.1016/j.redox.2022.102451>
- Li, X., Zhang, W., Xing, Z., Hu, S., Zhang, G., Wang, T., Wang, T., Fan, Q., Chen, G., Cheng, J., Jiang, X., & Cai, R. (2024). Targeting SIRT3 sensitizes glioblastoma to ferroptosis by promoting mitophagy and inhibiting SLC7A11. *Cell Death & Disease*, 15(2), 1–14. <https://doi.org/10.1038/s41419-024-06558-0>
- Li, Y., Hodge, J., Liu, Q., Wang, J., Wang, Y., Evans, T. D., Altomare, D., Yao, Y., Murphy, E. A., Razani, B., & Fan, D. (2020). TFEB is a master regulator of tumor-associated macrophages in breast cancer. *Journal for Immunotherapy of Cancer*, 8(1), e000543. <https://doi.org/10.1136/jitc-2020-000543>
- Liaw, K., Sharma, R., Sharma, A., Salazar, S., Appiani La Rosa, S., & Kannan, R. M. (2021). Systemic dendrimer delivery of triptolide to tumor-associated

- macrophages improves anti-tumor efficacy and reduces systemic toxicity in glioblastoma. *Journal of Controlled Release: Official Journal of the Controlled Release Society*, 329, 434–444. <https://doi.org/10.1016/j.jconrel.2020.12.003>
- Licha, K., Welker, P., Weinhart, M., Wegner, N., Kern, S., Reichert, S., Gemeinhardt, I., Weissbach, C., Ebert, B., Haag, R., & Schirner, M. (2011). Fluorescence imaging with multifunctional polyglycerol sulfates: Novel polymeric near-IR probes targeting inflammation. *Bioconjugate Chemistry*, 22(12), 2453–2460. <https://doi.org/10.1021/bc2002727>
- Lin, H., Liu, C., Hu, A., Zhang, D., Yang, H., & Mao, Y. (2024). Understanding the immunosuppressive microenvironment of glioma: Mechanistic insights and clinical perspectives. *Journal of Hematology & Oncology*, 17, 31. <https://doi.org/10.1186/s13045-024-01544-7>
- Liu, Z., Ji, X., He, D., Zhang, R., Liu, Q., & Xin, T. (2022). Nanoscale Drug Delivery Systems in Glioblastoma. *Nanoscale Research Letters*, 17(1), 27. <https://doi.org/10.1186/s11671-022-03668-6>
- Lotocki, V., Yazdani, H., Zhang, Q., Gran, E. R., Nyrko, A., Maysinger, D., & Kakkar, A. (2021). Miktoarm Star Polymers with Environment-Selective ROS/GSH Responsive Locations: From Modular Synthesis to Tuned Drug Release through Micellar Partial Corona Shedding and/or Core Disassembly. *Macromolecular Bioscience*, 21(2), e2000305. <https://doi.org/10.1002/mabi.202000305>
- Lu, T., Yee, P. P., Chih, S. Y., Tang, M., Chen, H., Aregawi, D. G., Glantz, M. J., Zacharia, B. E., Wang, H.-G., & Li, W. (2024). LC3-associated phagocytosis of neutrophils triggers tumor ferroptotic cell death in glioblastoma. *The EMBO Journal*, 43(13), 2582–2605. <https://doi.org/10.1038/s44318-024-00130-4>
- Lv, G., Yang, M., Gai, K., Jia, Q., Wang, Z., Wang, B., & Li, X. (2024). Multiple functions of HMGB1 in cancer. *Frontiers in Oncology*, 14. <https://doi.org/10.3389/fonc.2024.1384109>
- Ma, L., Zhang, B., Zhou, C., Li, Y., Li, B., Yu, M., Luo, Y., Gao, L., Zhang, D., Xue, Q., Qiu, Q., Lin, B., Zou, J., & Yang, H. (2018). The comparison genomics analysis with glioblastoma multiforme (GBM) cells under 3D and 2D cell culture conditions. *Colloids and Surfaces. B, Biointerfaces*, 172, 665–673. <https://doi.org/10.1016/j.colsurfb.2018.09.034>
- Mahoney, S. A., Venkatasubramanian, R., Darrah, M. A., Ludwig, K. R., VanDongen, N. S., Greenberg, N. T., Longtine, A. G., Hutton, D. A., Brunt, V. E., Campisi, J., Melov, S., Seals, D. R., Rossman, M. J., & Clayton, Z. S. (2023). Intermittent supplementation with fisetin improves arterial function in old mice by decreasing cellular senescence. *Aging Cell*, e14060. <https://doi.org/10.1111/acer.14060>
- Martina, J. A., & Puertollano, R. (2016a). TFEB and TFE3: The art of multi-tasking under stress conditions. *Transcription*, 8(1), 48–54. <https://doi.org/10.1080/21541264.2016.1264353>
- Martina, J. A., & Puertollano, R. (2016b). TFEB and TFE3: The art of multi-tasking under stress conditions. *Transcription*, 8(1), 48–54. <https://doi.org/10.1080/21541264.2016.1264353>
- Matias, D., Balça-Silva, J., da Graça, G. C., Wanjiru, C. M., Macharia, L. W., Nascimento, C. P., Roque, N. R., Coelho-Aguiar, J. M., Pereira, C. M., Dos Santos, M. F., Pessoa, L. S., Lima, F. R. S., Schanaider, A., Ferrer, V. P., Tania Cristina Leite de

- Sampaio e Spohr, & Moura-Neto, V. (2018). Microglia/Astrocytes–Glioblastoma Crosstalk: Crucial Molecular Mechanisms and Microenvironmental Factors. *Frontiers in Cellular Neuroscience*, 12. <https://www.frontiersin.org/articles/10.3389/fncel.2018.00235>
- Maysinger, D., Gröger, D., Lake, A., Licha, K., Weinhart, M., Chang, P. K.-Y., Mulvey, R., Haag, R., & McKinney, R. A. (2015). Dendritic Polyglycerol Sulfate Inhibits Microglial Activation and Reduces Hippocampal CA1 Dendritic Spine Morphology Deficits. *Biomacromolecules*, 16(9), 3073–3082. <https://doi.org/10.1021/acs.biomac.5b00999>
- Maysinger, D., Ji, J., Moquin, A., Hossain, S., Hancock, M. A., Zhang, I., Chang, P. K. Y., Rigby, M., Anthonisen, M., Grütter, P., Breitner, J., McKinney, R. A., Reimann, S., Haag, R., & Multhaup, G. (2018). Dendritic Polyglycerol Sulfates in the Prevention of Synaptic Loss and Mechanism of Action on Glia. *ACS Chemical Neuroscience*, 9(2), 260–271. <https://doi.org/10.1021/acscchemneuro.7b00301>
- Maysinger, D., Lalancette-Hébert, M., Ji, J., Jabbour, K., Dervede, J., Silberreis, K., Haag, R., & Kriz, J. (2019). Dendritic Polyglycerols Are Modulators of Microglia-Astrocyte Crosstalk. *Future Neurology*, 14(4), FNL31. <https://doi.org/10.2217/fnl-2019-0008>
- Maysinger, D., Zhang, I., Wu, P. Y., Kagelmacher, M., Luo, H. D., Kizhakkedathu, J. N., Dervede, J., Ballauff, M., Haag, R., Shobo, A., Multhaup, G., & McKinney, R. A. (2023). Sulfated Hyperbranched and Linear Polyglycerols Modulate HMGB1 and Morphological Plasticity in Neural Cells. *ACS Chemical Neuroscience*, 14(4), 677–688. <https://doi.org/10.1021/acscchemneuro.2c00558>
- Mbara, K. C., Devnarain, N., & Owira, P. M. O. (2022). Potential Role of Polyphenolic Flavonoids as Senotherapeutic Agents in Degenerative Diseases and Geroprotection. *Pharmaceutical Medicine*, 36(6), 331–352. <https://doi.org/10.1007/s40290-022-00444-w>
- McDuff, S. G. R., Dietrich, J., Atkins, K. M., Oh, K. S., Loeffler, J. S., & Shih, H. A. (2019). Radiation and chemotherapy for high-risk lower grade gliomas: Choosing between temozolomide and PCV. *Cancer Medicine*, 9(1), 3–11. <https://doi.org/10.1002/cam4.2686>
- Meena, D., & Jha, S. (2024). Autophagy in glioblastoma: A mechanistic perspective. *International Journal of Cancer*, 155(4), 605–617. <https://doi.org/10.1002/ijc.34991>
- Mittal, S., Klinger, N. V., Michelhaugh, S. K., Barger, G. R., Pannullo, S. C., & Juhász, C. (2018). Alternating electric tumor treating fields for treatment of glioblastoma: Rationale, preclinical, and clinical studies. *Journal of Neurosurgery*, 128(2), 414–421. <https://doi.org/10.3171/2016.9.JNS16452>
- Mo, F., Pellerino, A., Soffietti, R., & Rudà, R. (2021). Blood–Brain Barrier in Brain Tumors: Biology and Clinical Relevance. *International Journal of Molecular Sciences*, 22(23), 12654. <https://doi.org/10.3390/ijms222312654>
- Mordon, S., Devoisselle, J. M., & Soulié, S. (1995). Fluorescence spectroscopy of pH in vivo using a dual-emission fluorophore (C-SNAFL-1). *Journal of Photochemistry and Photobiology. B, Biology*, 28(1), 19–23. [https://doi.org/10.1016/1011-1344\(94\)07100-3](https://doi.org/10.1016/1011-1344(94)07100-3)

- Mu, H., & Holm, R. (2018). Solid lipid nanocarriers in drug delivery: Characterization and design. *Expert Opinion on Drug Delivery*, 15(8), 771–785. <https://doi.org/10.1080/17425247.2018.1504018>
- Mukherjee, S. P., Lyng, F. M., Garcia, A., Davoren, M., & Byrne, H. J. (2010). Mechanistic studies of in vitro cytotoxicity of poly(amidoamine) dendrimers in mammalian cells. *Toxicology and Applied Pharmacology*, 248(3), 259–268. <https://doi.org/10.1016/j.taap.2010.08.016>
- Mulcahy Levy, J. M., & Thorburn, A. (2020). Autophagy in cancer: Moving from understanding mechanism to improving therapy responses in patients. *Cell Death and Differentiation*, 27(3), 843–857. <https://doi.org/10.1038/s41418-019-0474-7>
- Murtaza, I., Adhami, V. M., Hafeez, B. B., Saleem, M., & Mukhtar, H. (2009). Fisetin, a natural flavonoid, targets chemoresistant human pancreatic cancer AsPC-1 cells through DR3 mediated inhibition of NF- κ B. *International Journal of Cancer. Journal International Du Cancer*, 125(10), 2465–2473. <https://doi.org/10.1002/ijc.24628>
- Muzio, L., Viotti, A., & Martino, G. (2021). Microglia in Neuroinflammation and Neurodegeneration: From Understanding to Therapy. *Frontiers in Neuroscience*, 15, 742065. <https://doi.org/10.3389/fnins.2021.742065>
- Nabizadeh, Z., Nasrollahzadeh, M., Shabani, A. A., Mirmohammadkhani, M., & Nasrabadi, D. (2023). Evaluation of the anti-inflammatory activity of fisetin-loaded nanoparticles in an in vitro model of osteoarthritis. *Scientific Reports*, 13, 15494. <https://doi.org/10.1038/s41598-023-42844-1>
- Napolitano, G., & Ballabio, A. (2016). TFEB at a glance. *Journal of Cell Science*, 129(13), 2475–2481. <https://doi.org/10.1242/jcs.146365>
- Nelson, T. A., & Dietrich, J. (2023). Investigational treatment strategies in glioblastoma: Progress made and barriers to success. *Expert Opinion on Investigational Drugs*, 32(10), 921–930. <https://doi.org/10.1080/13543784.2023.2267982>
- Newman, D. J., & Cragg, G. M. (2020). Natural Products as Sources of New Drugs over the Nearly Four Decades from 01/1981 to 09/2019. *Journal of Natural Products*, 83(3), 770–803. <https://doi.org/10.1021/acs.jnatprod.9b01285>
- Nixon, R. A. (2013). The role of autophagy in neurodegenerative disease. *Nature Medicine*, 19(8), Article 8. <https://doi.org/10.1038/nm.3232>
- Nusraty, S., Boddeti, U., Zaghloul, K. A., & Brown, D. A. (2024). Microglia in Glioblastomas: Molecular Insight and Immunotherapeutic Potential. *Cancers*, 16(11), Article 11. <https://doi.org/10.3390/cancers16111972>
- Olivier, C., Oliver, L., Lalier, L., & Vallette, F. M. (2021). Drug Resistance in Glioblastoma: The Two Faces of Oxidative Stress. *Frontiers in Molecular Biosciences*, 7. <https://www.frontiersin.org/articles/10.3389/fmolb.2020.620677>
- Olzmann, J. A., & Carvalho, P. (2019). Dynamics and functions of lipid droplets. *Nature Reviews Molecular Cell Biology*, 20(3), 137–155. <https://doi.org/10.1038/s41580-018-0085-z>
- Osswald, M., Jung, E., Sahm, F., Solecki, G., Venkataramani, V., Blaes, J., Weil, S., Horstmann, H., Wiestler, B., Syed, M., Huang, L., Ratliff, M., Karimian Jazi, K., Kurz, F. T., Schmenger, T., Lemke, D., Gömmel, M., Pauli, M., Liao, Y., ... Winkler, F. (2015). Brain tumour cells interconnect to a functional and resistant network. *Nature*, 528(7580), 93–98. <https://doi.org/10.1038/nature16071>

- Ostrom, Q. T., Gittleman, H., Truitt, G., Boscia, A., Kruchko, C., & Barnholtz-Sloan, J. S. (2018). CBTRUS Statistical Report: Primary Brain and Other Central Nervous System Tumors Diagnosed in the United States in 2011-2015. *Neuro-Oncology*, 20(suppl_4), iv1–iv86. <https://doi.org/10.1093/neuonc/noy131>
- Pallarés-Moratalla, C., & Bergers, G. (2024). The ins and outs of microglial cells in brain health and disease. *Frontiers in Immunology*, 15, 1305087. <https://doi.org/10.3389/fimmu.2024.1305087>
- Pardridge, W. M. (2005). The Blood-Brain Barrier: Bottleneck in Brain Drug Development. *NeuroRx*, 2(1), 3–14.
- Paudel, Y. N., Angelopoulou, E., Piperi, C., Balasubramaniam, V. R. M. T., Othman, I., & Shaikh, M. F. (2019). Enlightening the role of high mobility group box 1 (HMGB1) in inflammation: Updates on receptor signalling. *European Journal of Pharmacology*, 858, 172487. <https://doi.org/10.1016/j.ejphar.2019.172487>
- Paulus, F., Schulze, R., Steinhilber, D., Zieringer, M., Steinke, I., Welker, P., Licha, K., Wedepohl, S., Dervedde, J., & Haag, R. (2014). The effect of polyglycerol sulfate branching on inflammatory processes. *Macromolecular Bioscience*, 14(5), 643–654. <https://doi.org/10.1002/mabi.201300420>
- Pavlova, N. N., & Thompson, C. B. (2016). The Emerging Hallmarks of Cancer Metabolism. *Cell Metabolism*, 23(1), 27–47. <https://doi.org/10.1016/j.cmet.2015.12.006>
- Perera, R. M., Stoykova, S., Nicolay, B. N., Ross, K. N., Fitamant, J., Boukhali, M., Lengrand, J., Deshpande, V., Selig, M. K., Ferrone, C. R., Settleman, J., Stephanopoulos, G., Dyson, N. J., Zoncu, R., Ramaswamy, S., Haas, W., & Bardeesy, N. (2015). Transcriptional control of autophagy-lysosome function drives pancreatic cancer metabolism. *Nature*, 524(7565), 361–365. <https://doi.org/10.1038/nature14587>
- Perera, R. M., & Zoncu, R. (2016). The Lysosome as a Regulatory Hub. *Annual Review of Cell and Developmental Biology*, 32, 223–253. <https://doi.org/10.1146/annurev-cellbio-111315-125125>
- Prabhu, R. H., Patravale, V. B., & Joshi, M. D. (2015). Polymeric nanoparticles for targeted treatment in oncology: Current insights. *International Journal of Nanomedicine*, 10, 1001–1018. <https://doi.org/10.2147/IJN.S56932>
- Przystal, J. M., Becker, H., Canjuga, D., Tsiami, F., Anderle, N., Keller, A.-L., Pohl, A., Ries, C. H., Schmittnaegel, M., Korinetska, N., Koch, M., Schittenhelm, J., Tatagiba, M., Schmees, C., Beck, S. C., & Tabatabai, G. (2021). Targeting CSF1R Alone or in Combination with PD1 in Experimental Glioma. *Cancers*, 13(10), 2400. <https://doi.org/10.3390/cancers13102400>
- Pyonteck, S. M., Akkari, L., Schuhmacher, A. J., Bowman, R. L., Sevenich, L., Quail, D. F., Olson, O. C., Quick, M. L., Huse, J. T., Teijeiro, V., Setty, M., Leslie, C. S., Oei, Y., Pedraza, A., Zhang, J., Brennan, C. W., Sutton, J. C., Holland, E. C., Daniel, D., & Joyce, J. A. (2013). CSF-1R inhibition alters macrophage polarization and blocks glioma progression. *Nature Medicine*, 19(10), 1264–1272. <https://doi.org/10.1038/nm.3337>
- Qian, F., Xiao, J., Gai, L., & Zhu, J. (2019). HMGB1-RAGE signaling facilitates Ras-dependent Yap1 expression to drive colorectal cancer stemness and

- development. *Molecular Carcinogenesis*, 58(4), 500–510. <https://doi.org/10.1002/mc.22944>
- Quail, D. F., & Joyce, J. A. (2017). Molecular Pathways: Deciphering Mechanisms of Resistance to Macrophage-Targeted Therapies. *Clinical Cancer Research: An Official Journal of the American Association for Cancer Research*, 23(4), 876–884. <https://doi.org/10.1158/1078-0432.CCR-16-0133>
- Rao, R., Han, R., Ogurek, S., Xue, C., Wu, L. M., Zhang, L., Zhang, L., Hu, J., Phoenix, T. N., Waggoner, S. N., & Lu, Q. R. (2022). Glioblastoma genetic drivers dictate the function of tumor-associated macrophages/microglia and responses to CSF1R inhibition. *Neuro-Oncology*, 24(4), 584–597. <https://doi.org/10.1093/neuonc/noab228>
- Rider, P., Kaplanov, I., Romzova, M., Bernardis, L., Braiman, A., Voronov, E., & Apte, R. N. (2012). The transcription of the alarmin cytokine interleukin-1 alpha is controlled by hypoxia inducible factors 1 and 2 alpha in hypoxic cells. *Frontiers in Immunology*, 3, 290. <https://doi.org/10.3389/fimmu.2012.00290>
- Riemann, A., Schneider, B., Gündel, D., Stock, C., Gekle, M., & Thews, O. (2016). Acidosis Promotes Metastasis Formation by Enhancing Tumor Cell Motility. *Advances in Experimental Medicine and Biology*, 876, 215–220. https://doi.org/10.1007/978-1-4939-3023-4_27
- Rivera Vargas, T., & Apetoh, L. (2017). Danger signals: Chemotherapy enhancers? *Immunological Reviews*, 280(1), 175–193. <https://doi.org/10.1111/imr.12581>
- Rodríguez-Camacho, A., Flores-Vázquez, J. G., Moscardini-Martelli, J., Torres-Ríos, J. A., Olmos-Guzmán, A., Ortiz-Arce, C. S., Cid-Sánchez, D. R., Pérez, S. R., Macías-González, M. D. S., Hernández-Sánchez, L. C., Heredia-Gutiérrez, J. C., Contreras-Palafox, G. A., Suárez-Campos, J. de J. E., Celis-López, M. Á., Gutiérrez-Aceves, G. A., & Moreno-Jiménez, S. (2022). Glioblastoma Treatment: State-of-the-Art and Future Perspectives. *International Journal of Molecular Sciences*, 23(13), 7207. <https://doi.org/10.3390/ijms23137207>
- Rudrapal, M., Khairnar, S. J., Khan, J., Dukhyil, A. B., Ansari, M. A., Alomary, M. N., Alshabrm, F. M., Palai, S., Deb, P. K., & Devi, R. (2022). Dietary Polyphenols and Their Role in Oxidative Stress-Induced Human Diseases: Insights Into Protective Effects, Antioxidant Potentials and Mechanism(s) of Action. *Frontiers in Pharmacology*, 13, 806470. <https://doi.org/10.3389/fphar.2022.806470>
- Russell, S., Wojtkowiak, J., Neilson, A., & Gillies, R. J. (2017). Metabolic Profiling of healthy and cancerous tissues in 2D and 3D. *Scientific Reports*, 7(1), 15285. <https://doi.org/10.1038/s41598-017-15325-5>
- Russo, M. A., Sansone, L., Carnevale, I., Limana, F., Runci, A., Polletta, L., Perrone, G. A., De Santis, E., & Tafani, M. (2015). One Special Question to Start with: Can HIF/NFkB be a Target in Inflammation? *Endocrine, Metabolic & Immune Disorders Drug Targets*, 15(3), 171–185. <https://doi.org/10.2174/1871530315666150316120112>
- Sahoo, R. K., Gupta, T., Batheja, S., Goyal, A. K., & Gupta, U. (2022). Surface Engineered Dendrimers: A Potential Nanocarrier for the Effective Management of Glioblastoma Multiforme. *Current Drug Metabolism*, 23(9), 708–722. <https://doi.org/10.2174/1389200223666220616125524>

- Sandireddy, R., Yerra, V. G., Komirishetti, P., Areti, A., & Kumar, A. (2016). Fisetin Imparts Neuroprotection in Experimental Diabetic Neuropathy by Modulating Nrf2 and NF- κ B Pathways. *Cellular and Molecular Neurobiology*, 36(6), 883–892. <https://doi.org/10.1007/s10571-015-0272-9>
- Sardiello, M., Palmieri, M., di Ronza, A., Medina, D. L., Valenza, M., Gennarino, V. A., Di Malta, C., Donaudo, F., Embrione, V., Polishchuk, R. S., Banfi, S., Parenti, G., Cattaneo, E., & Ballabio, A. (2009). A gene network regulating lysosomal biogenesis and function. *Science (New York, N.Y.)*, 325(5939), 473–477. <https://doi.org/10.1126/science.1174447>
- Sha, G., Jiang, Z., Zhang, W., Jiang, C., Wang, D., & Tang, D. (2023). The multifunction of HSP70 in cancer: Guardian or traitor to the survival of tumor cells and the next potential therapeutic target. *International Immunopharmacology*, 122, 110492. <https://doi.org/10.1016/j.intimp.2023.110492>
- Sharifi-Rad, J., Seidel, V., Izabela, M., Monserrat-Mequida, M., Sureda, A., Ormazabal, V., Zuniga, F. A., Mangalpady, S. S., Pezzani, R., Ydyrys, A., Tussupbekova, G., Martorell, M., Calina, D., & Cho, W. C. (2023). Phenolic compounds as Nrf2 inhibitors: Potential applications in cancer therapy. *Cell Communication and Signaling*, 21(1), 89. <https://doi.org/10.1186/s12964-023-01109-0>
- Sharma, P., Aaroe, A., Liang, J., & Puduvalli, V. K. (2023). Tumor microenvironment in glioblastoma: Current and emerging concepts. *Neuro-Oncology Advances*, 5(1), vdad009. <https://doi.org/10.1093/noajnl/vdad009>
- Sharma, R., Liaw, K., Sharma, A., Jimenez, A., Chang, M., Salazar, S., Amlani, I., Kannan, S., & Kannan, R. M. (2021). Glycosylation of PAMAM dendrimers significantly improves tumor macrophage targeting and specificity in glioblastoma. *Journal of Controlled Release: Official Journal of the Controlled Release Society*, 337, 179–192. <https://doi.org/10.1016/j.jconrel.2021.07.018>
- Shikalov, A., Koman, I., & Kogan, N. M. (2024). Targeted Glioma Therapy-Clinical Trials and Future Directions. *Pharmaceutics*, 16(1), 100. <https://doi.org/10.3390/pharmaceutics16010100>
- Silberreis, K., Niesler, N., Rades, N., Haag, R., & Dornedde, J. (2019). Sulfated Dendritic Polyglycerol Is a Potent Complement Inhibitor. *Biomacromolecules*, 20(10), 3809–3818. <https://doi.org/10.1021/acs.biomac.9b00889>
- Singh, N., Miner, A., Hennis, L., & Mittal, S. (2021). Mechanisms of temozolomide resistance in glioblastoma—A comprehensive review. *Cancer Drug Resistance*, 4(1), 17–43. <https://doi.org/10.20517/cdr.2020.79>
- Smolarska, A., Pruszyńska, I., Wasylko, W., Godlewska, K., Markowska, M., Rybak, A., Botther, J., Kucharzewska, P., Nowakowska, J., Szeliga, J., Kubiak, M., Gorczak, M., & Krol, M. (2023). Targeted therapies for glioblastoma treatment. *Journal of Physiology and Pharmacology: An Official Journal of the Polish Physiological Society*, 74(3). <https://doi.org/10.26402/jpp.2023.3.01>
- Soliman, G. M., Sharma, R., Choi, A. O., Varshney, S. K., Winnik, F. M., Kakkar, A. K., & Maysinger, D. (2010). Tailoring the efficacy of nimodipine drug delivery using nanocarriers based on A2B miktoarm star polymers. *Biomaterials*, 31(32), 8382–8392. <https://doi.org/10.1016/j.biomaterials.2010.07.039>
- Sousa-Herves, A., Würfel, P., Wegner, N., Khandare, J., Licha, K., Haag, R., Welker, P., & Calderón, M. (2015). Dendritic polyglycerol sulfate as a novel platform for

- paclitaxel delivery: Pitfalls of ester linkage. *Nanoscale*, 7(9), 3923–3932. <https://doi.org/10.1039/C4NR04428B>
- Stockwell, B. R. (2022). Ferroptosis turns 10: Emerging mechanisms, physiological functions, and therapeutic applications. *Cell*, 185(14), 2401–2421. <https://doi.org/10.1016/j.cell.2022.06.003>
- Stros, M. (2010). HMGB proteins: Interactions with DNA and chromatin. *Biochimica Et Biophysica Acta*, 1799(1–2), 101–113. <https://doi.org/10.1016/j.bbagr.2009.09.008>
- Stupp, R., Hegi, M. E., Mason, W. P., van den Bent, M. J., Taphoorn, M. J. B., Janzer, R. C., Ludwin, S. K., Allgeier, A., Fisher, B., Belanger, K., Hau, P., Brandes, A. A., Gijtenbeek, J., Marosi, C., Vecht, C. J., Mokhtari, K., Wesseling, P., Villa, S., Eisenhauer, E., ... National Cancer Institute of Canada Clinical Trials Group. (2009). Effects of radiotherapy with concomitant and adjuvant temozolomide versus radiotherapy alone on survival in glioblastoma in a randomised phase III study: 5-year analysis of the EORTC-NCIC trial. *The Lancet. Oncology*, 10(5), 459–466. [https://doi.org/10.1016/S1470-2045\(09\)70025-7](https://doi.org/10.1016/S1470-2045(09)70025-7)
- Stupp, R., Taillibert, S., Kanner, A. A., Kesari, S., Steinberg, D. M., Toms, S. A., Taylor, L. P., Lieberman, F., Silvani, A., Fink, K. L., Barnett, G. H., Zhu, J.-J., Henson, J. W., Engelhard, H. H., Chen, T. C., Tran, D. D., Sroubek, J., Tran, N. D., Hottinger, A. F., ... Ram, Z. (2015). Maintenance Therapy With Tumor-Treating Fields Plus Temozolomide vs Temozolomide Alone for Glioblastoma: A Randomized Clinical Trial. *JAMA*, 314(23), 2535–2543. <https://doi.org/10.1001/jama.2015.16669>
- Suh, Y., Afaq, F., Khan, N., Johnson, J. J., Khusro, F. H., & Mukhtar, H. (2010). Fisetin induces autophagic cell death through suppression of mTOR signaling pathway in prostate cancer cells. *Carcinogenesis*, 31(8), 1424–1433. <https://doi.org/10.1093/carcin/bgq115>
- Sun, S., Gao, T., Pang, B., Su, X., Guo, C., Zhang, R., & Pang, Q. (2022). RNA binding protein NKAP protects glioblastoma cells from ferroptosis by promoting SLC7A11 mRNA splicing in an m6A-dependent manner. *Cell Death & Disease*, 13(1), 1–14. <https://doi.org/10.1038/s41419-022-04524-2>
- Syed, D. N., Lall, R. K., Chamcheu, J. C., Haidar, O., & Mukhtar, H. (2014). Involvement of ER stress and activation of apoptotic pathways in fisetin induced cytotoxicity in human melanoma. *Archives of Biochemistry and Biophysics*, 563, 108–117. <https://doi.org/10.1016/j.abb.2014.06.034>
- Szatrowski, T. P., & Nathan, C. F. (1991). Production of large amounts of hydrogen peroxide by human tumor cells. *Cancer Research*, 51(3), 794–798.
- Taal, W., Oosterkamp, H. M., Walenkamp, A. M. E., Dubbink, H. J., Beerepoot, L. V., Hanse, M. C. J., Buter, J., Honkoop, A. H., Boerman, D., de Vos, F. Y. F., Dinjens, W. N. M., Enting, R. H., Taphoorn, M. J. B., van den Berkmortel, F. W. P. J., Jansen, R. L. H., Brandsma, D., Bromberg, J. E. C., van Heuvel, I., Vernhout, R. M., ... van den Bent, M. J. (2014). Single-agent bevacizumab or lomustine versus a combination of bevacizumab plus lomustine in patients with recurrent glioblastoma (BELOB trial): A randomised controlled phase 2 trial. *The Lancet. Oncology*, 15(9), 943–953. [https://doi.org/10.1016/S1470-2045\(14\)70314-6](https://doi.org/10.1016/S1470-2045(14)70314-6)
- Tafani, M., Di Vito, M., Frati, A., Pellegrini, L., De Santis, E., Sette, G., Eramo, A., Sale, P., Mari, E., Santoro, A., Raco, A., Salvati, M., De Maria, R., & Russo, M. A. (2011).

- Pro-inflammatory gene expression in solid glioblastoma microenvironment and in hypoxic stem cells from human glioblastoma. *Journal of Neuroinflammation*, 8, 32. <https://doi.org/10.1186/1742-2094-8-32>
- Tamimi, A. F., & Juweid, M. (2017). Epidemiology and Outcome of Glioblastoma. In S. De Vleeschouwer (Ed.), *Glioblastoma*. Codon Publications. <http://www.ncbi.nlm.nih.gov/books/NBK470003/>
- Tanaka, F., Irie, K., Fukui, N., Horii, R., Imamura, H., Hirabatake, M., Ikesue, H., Muroi, N., Fukushima, S., Sakai, N., & Hashida, T. (2023). Pharmacokinetics of Temozolomide in a Patient With Glioblastoma Undergoing Hemodialysis: A Short Communication. *Therapeutic Drug Monitoring*, 45(6), 823–826. <https://doi.org/10.1097/FTD.0000000000001125>
- Tang, D., Kang, R., Xiao, W., Jiang, L., Liu, M., Shi, Y., Wang, K., Wang, H., & Xiao, X. (2007). Nuclear Heat Shock Protein 72 as a Negative Regulator of Oxidative Stress (Hydrogen Peroxide)-Induced HMGB1 Cytoplasmic Translocation and Release. *Journal of Immunology (Baltimore, Md. : 1950)*, 178(11), 7376–7384.
- Tang, T., Liang, H., Wei, W., Han, Y., Cao, L., Cong, Z., Luo, S., Wang, H., & Zhou, M.-L. (2023). Alopentine targets lysosomes to inhibit late autophagy and induces cell death through apoptosis and paraptosis in glioblastoma. *Molecular Biomedicine*, 4(1), 42. <https://doi.org/10.1186/s43556-023-00155-x>
- Tang, Y., Zhao, X., Antoine, D., Xiao, X., Wang, H., Andersson, U., Billiar, T. R., Tracey, K. J., & Lu, B. (2016). Regulation of Posttranslational Modifications of HMGB1 During Immune Responses. *Antioxidants & Redox Signaling*, 24(12), 620–634. <https://doi.org/10.1089/ars.2015.6409>
- Tatla, A. S., Justin, A. W., Watts, C., & Markaki, A. E. (2021). A vascularized tumoroid model for human glioblastoma angiogenesis. *Scientific Reports*, 11(1), 19550. <https://doi.org/10.1038/s41598-021-98911-y>
- Teraiya, M., Perreault, H., & Chen, V. C. (2023). An overview of glioblastoma multiforme and temozolomide resistance: Can LC-MS-based proteomics reveal the fundamental mechanism of temozolomide resistance? *Frontiers in Oncology*, 13. <https://doi.org/10.3389/fonc.2023.1166207>
- Thomsen, M. S., Routhe, L. J., & Moos, T. (2017). The vascular basement membrane in the healthy and pathological brain. *Journal of Cerebral Blood Flow & Metabolism*, 37(10), 3300–3317. <https://doi.org/10.1177/0271678X17722436>
- Tosoni, A., Franceschi, E., Poggi, R., & Brandes, A. A. (2016). Relapsed Glioblastoma: Treatment Strategies for Initial and Subsequent Recurrences. *Current Treatment Options in Oncology*, 17(9), 49. <https://doi.org/10.1007/s11864-016-0422-4>
- Trifiletti, D. M., Sturz, V. N., Showalter, T. N., & Lobo, J. M. (2017). Towards decision-making using individualized risk estimates for personalized medicine: A systematic review of genomic classifiers of solid tumors. *PLOS ONE*, 12(5), e0176388. <https://doi.org/10.1371/journal.pone.0176388>
- Türk, H., Haag, R., & Alban, S. (2004). Dendritic polyglycerol sulfates as new heparin analogues and potent inhibitors of the complement system. *Bioconjugate Chemistry*, 15(1), 162–167. <https://doi.org/10.1021/bc034044j>
- Valerius, A. R., Webb, L. M., & Sener, U. (2024). Novel Clinical Trials and Approaches in the Management of Glioblastoma. *Current Oncology Reports*, 26(5), 439–465. <https://doi.org/10.1007/s11912-024-01519-4>

- Vaupel, P., & Mayer, A. (2014). Hypoxia in tumors: Pathogenesis-related classification, characterization of hypoxia subtypes, and associated biological and clinical implications. *Advances in Experimental Medicine and Biology*, 812, 19–24. https://doi.org/10.1007/978-1-4939-0620-8_3
- Wadhwa, K., Chauhan, P., Kumar, S., Pahwa, R., Verma, R., Goyal, R., Singh, G., Sharma, A., Rao, N., & Kaushik, D. (2024). Targeting brain tumors with innovative nanocarriers: Bridging the gap through the blood-brain barrier. *Oncology Research*, 32(5), 877–897. <https://doi.org/10.32604/or.2024.047278>
- Wang, C., Sun, M., Shao, C., Schlicker, L., Zhuo, Y., Harim, Y., Peng, T., Tian, W., Stöfler, N., Schneider, M., Helm, D., Chu, Y., Fu, B., Jin, X., Mallm, J.-P., Mall, M., Wu, Y., Schulze, A., & Liu, H.-K. (2024). A multidimensional atlas of human glioblastoma-like organoids reveals highly coordinated molecular networks and effective drugs. *Npj Precision Oncology*, 8(1), 1–21. <https://doi.org/10.1038/s41698-024-00500-5>
- Wang, G., Zhong, K., Wang, Z., Zhang, Z., Tang, X., Tong, A., & Zhou, L. (2022). Tumor-associated microglia and macrophages in glioblastoma: From basic insights to therapeutic opportunities. *Frontiers in Immunology*, 13. <https://doi.org/10.3389/fimmu.2022.964898>
- Wang, H., Bloom, O., Zhang, M., Vishnubhakat, J. M., Ombrellino, M., Che, J., Frazier, A., Yang, H., Ivanova, S., Borovikova, L., Manogue, K. R., Faist, E., Abraham, E., Andersson, J., Andersson, U., Molina, P. E., Abumrad, N. N., Sama, A., & Tracey, K. J. (1999). HMG-1 as a late mediator of endotoxin lethality in mice. *Science (New York, N.Y.)*, 285(5425), 248–251. <https://doi.org/10.1126/science.285.5425.248>
- Wang, S., & Zhang, Y. (2020). HMGB1 in inflammation and cancer. *Journal of Hematology & Oncology*, 13(1), 116. <https://doi.org/10.1186/s13045-020-00950-x>
- Wang, W., Zhang, Y., Jian, Y., He, S., Liu, J., Cheng, Y., Zheng, S., Qian, Z., Gao, X., & Wang, X. (2024). Sensitizing chemotherapy for glioma with fisetin mediated by a microenvironment-responsive nano-drug delivery system. *Nanoscale*, 16(1), 97–109. <https://doi.org/10.1039/D3NR05195A>
- Wang, X., Liang, J., & Sun, H. (2022). The Network of Tumor Microtubes: An Improperly Reactivated Neural Cell Network With Stemness Feature for Resistance and Recurrence in Gliomas. *Frontiers in Oncology*, 12, 921975. <https://doi.org/10.3389/fonc.2022.921975>
- Wang, X., Sun, Y., Zhang, D. Y., Ming, G., & Song, H. (2023). Glioblastoma modeling with 3D organoids: Progress and challenges. *Oxford Open Neuroscience*, 2, kvad008. <https://doi.org/10.1093/oons/kvad008>
- Webb, B. A., Aloisio, F. M., Charafeddine, R. A., Cook, J., Wittmann, T., & Barber, D. L. (2021). pHLARE: A new biosensor reveals decreased lysosome pH in cancer cells. *Molecular Biology of the Cell*, 32(2), 131–142. <https://doi.org/10.1091/mbc.E20-06-0383>
- Weiss, S. A., Djureinovic, D., Jessel, S., Krykbaeva, I., Zhang, L., Jilaveanu, L., Ralabate, A., Johnson, B., Levit, N. S., Anderson, G., Zelterman, D., Wei, W., Mahajan, A., Trifan, O., Bosenberg, M., Kaech, S. M., Perry, C. J., Damsky, W., Gettinger, S., ... Kluger, H. M. (2021). A Phase I Study of APX005M and Cabiralizumab with or without Nivolumab in Patients with Melanoma, Kidney Cancer, or Non-Small Cell Lung Cancer Resistant to Anti-PD-1/PD-L1. *Clinical Cancer Research: An Official*

- Journal of the American Association for Cancer Research*, 27(17), 4757–4767. <https://doi.org/10.1158/1078-0432.CCR-21-0903>
- Wiedmann, R. M., von Schwarzenberg, K., Palamidessi, A., Schreiner, L., Kubisch, R., Liebl, J., Schempp, C., Trauner, D., Vereb, G., Zahler, S., Wagner, E., Müller, R., Scita, G., & Vollmar, A. M. (2012). The V-ATPase-inhibitor archazolid abrogates tumor metastasis via inhibition of endocytic activation of the Rho-GTPase Rac1. *Cancer Research*, 72(22), 5976–5987. <https://doi.org/10.1158/0008-5472.CAN-12-1772>
- Xiao, L., Xian, M., Zhang, C., Guo, Q., & Yi, Q. (2024). Lipid peroxidation of immune cells in cancer. *Frontiers in Immunology*, 14. <https://doi.org/10.3389/fimmu.2023.1322746>
- Xu, C., Yuan, X., Hou, P., Li, Z., Wang, C., Fang, C., & Tan, Y. (2023). Development of glioblastoma organoids and their applications in personalized therapy. *Cancer Biology & Medicine*, 20(5), 353–368. <https://doi.org/10.20892/j.issn.2095-3941.2023.0061>
- Yalamarty, S. S. K., Filipczak, N., Li, X., Subhan, M. A., Parveen, F., Ataide, J. A., Rajmalani, B. A., & Torchilin, V. P. (2023). Mechanisms of Resistance and Current Treatment Options for Glioblastoma Multiforme (GBM). *Cancers*, 15(7), 2116. <https://doi.org/10.3390/cancers15072116>
- Yan, D., Kowal, J., Akkari, L., Schuhmacher, A. J., Huse, J. T., West, B. L., & Joyce, J. A. (2017). Inhibition of colony stimulating factor-1 receptor abrogates microenvironment-mediated therapeutic resistance in gliomas. *Oncogene*, 36(43), 6049–6058. <https://doi.org/10.1038/onc.2017.261>
- Yang, W., Warrington, N. M., Taylor, S. J., Whitmire, P., Carrasco, E., Singleton, K. W., Wu, N., Lathia, J. D., Berens, M. E., Kim, A. H., Barnholtz-Sloan, J. S., Swanson, K. R., Luo, J., & Rubin, J. B. (2019). Sex differences in GBM revealed by analysis of patient imaging, transcriptome, and survival data. *Science Translational Medicine*, 11(473), eaao5253. <https://doi.org/10.1126/scitranslmed.aao5253>
- Yang, Y., Schubert, M. C., Kuner, T., Wick, W., Winkler, F., & Venkataramani, V. (2022). Brain Tumor Networks in Diffuse Glioma. *Neurotherapeutics*, 19(6), 1832–1843. <https://doi.org/10.1007/s13311-022-01320-w>
- Ye, C., Li, H., Li, Y., Zhang, Y., Liu, G., Mi, H., Li, H., Xiao, Q., Niu, L., & Yu, X. (2022). Hypoxia-induced HMGB1 promotes glioma stem cells self-renewal and tumorigenicity via RAGE. *iScience*, 25(9), 104872. <https://doi.org/10.1016/j.isci.2022.104872>
- Yee, P. P., Wei, Y., Kim, S.-Y., Lu, T., Chih, S. Y., Lawson, C., Tang, M., Liu, Z., Anderson, B., Thamburaj, K., Young, M. M., Aregawi, D. G., Glantz, M. J., Zacharia, B. E., Specht, C. S., Wang, H.-G., & Li, W. (2020). Neutrophil-induced ferroptosis promotes tumor necrosis in glioblastoma progression. *Nature Communications*, 11(1), 5424. <https://doi.org/10.1038/s41467-020-19193-y>
- Zhang, I., Beus, M., Stochaj, U., Le, P. U., Zorc, B., Rajić, Z., Petrecca, K., & Maysinger, D. (2018). Inhibition of glioblastoma cell proliferation, invasion, and mechanism of action of a novel hydroxamic acid hybrid molecule. *Cell Death Discovery*, 4, 41. <https://doi.org/10.1038/s41420-018-0103-0>
- Zhang, I., Cui, Y., Amiri, A., Ding, Y., Campbell, R. E., & Maysinger, D. (2016). Pharmacological inhibition of lipid droplet formation enhances the effectiveness of

- curcumin in glioblastoma. *European Journal of Pharmaceutics and Biopharmaceutics: Official Journal of Arbeitsgemeinschaft Fur Pharmazeutische Verfahrenstechnik e.V.*, 100, 66–76. <https://doi.org/10.1016/j.ejpb.2015.12.008>
- Zhang, I. Y., Zhou, H., Liu, H., Zhang, L., Gao, H., Liu, S., Song, Y., Alizadeh, D., Yin, H. H., Pillai, R., & Badie, B. (2020). Local and Systemic Immune Dysregulation Alters Glioma Growth in Hyperglycemic Mice. *Clinical Cancer Research: An Official Journal of the American Association for Cancer Research*, 26(11), 2740–2753. <https://doi.org/10.1158/1078-0432.CCR-19-2520>
- Zhang, L., Shi, H., Chen, H., Gong, A., Liu, Y., Song, L., Xu, X., You, T., Fan, X., Wang, D., Cheng, F., & Zhu, H. (2019). Dedifferentiation process driven by radiotherapy-induced HMGB1/TLR2/YAP/HIF-1 α signaling enhances pancreatic cancer stemness. *Cell Death & Disease*, 10(10), 724. <https://doi.org/10.1038/s41419-019-1956-8>
- Zhang, S., Peng, X., Yang, S., Li, X., Huang, M., Wei, S., Liu, J., He, G., Zheng, H., Yang, L., Li, H., & Fan, Q. (2022). The regulation, function, and role of lipophagy, a form of selective autophagy, in metabolic disorders. *Cell Death & Disease*, 13(2), 1–11. <https://doi.org/10.1038/s41419-022-04593-3>
- Zhang, Y., Kong, Y., Ma, Y., Ni, S., Wikerholmen, T., Xi, K., Zhao, F., Zhao, Z., Wang, J., Huang, B., Chen, A., Yao, Z., Han, M., Feng, Z., Hu, Y., Thorsen, F., Wang, J., & Li, X. (2021). Loss of COPZ1 induces NCOA4 mediated autophagy and ferroptosis in glioblastoma cell lines. *Oncogene*, 40(8), 1425–1439. <https://doi.org/10.1038/s41388-020-01622-3>
- Zhao, K., Zhou, G., Liu, Y., Zhang, J., Chen, Y., Liu, L., & Zhang, G. (2023). HSP70 Family in Cancer: Signaling Mechanisms and Therapeutic Advances. *Biomolecules*, 13(4), Article 4. <https://doi.org/10.3390/biom13040601>
- Zhao, L., Au, J. L.-S., & Wientjes, M. G. (2010). Comparison of methods for evaluating drug-drug interaction. *Frontiers in Bioscience (Elite Edition)*, 2, 241–249.
- Zhao, X.-L., Lin, Y., Jiang, J., Tang, Z., Yang, S., Lu, L., Liang, Y., Liu, X., Tan, J., Hu, X.-G., Niu, Q., Fu, W.-J., Yan, Z.-X., Guo, D.-Y., Ping, Y.-F., Wang, J. M., Zhang, X., Kung, H.-F., Bian, X.-W., & Yao, X.-H. (2017). High-mobility group box 1 released by autophagic cancer-associated fibroblasts maintains the stemness of luminal breast cancer cells. *The Journal of Pathology*, 243(3), 376–389. <https://doi.org/10.1002/path.4958>
- Zhou, Y., Zhou, X., Huang, X., Hong, T., Zhang, K., Qi, W., Guo, M., & Nie, S. (2021). Lysosome-Mediated Cytotoxic Autophagy Contributes to Tea Polysaccharide-Induced Colon Cancer Cell Death via mTOR-TFEB Signaling. *Journal of Agricultural and Food Chemistry*, 69(2), 686–697. <https://doi.org/10.1021/acs.jafc.0c07166>